Holocene reconstruction of vegetation and fire history at South Lake Futululu, northern KwaZulu-Natal

By

Salona Sathaiaseelen Reddy

Submitted in fulfillment of the academic requirements for the degree of Master of Science in the School of Agricultural, Earth and Environmental Sciences

University of KwaZulu-Natal

Pietermaritzburg

July 2022

ABSTRACT

This study investigated a Holocene palaeoenvironmental record from South Lake Futululu, a blocked valley lake in the Mfolozi-Msunduze catchment, northern KwaZulu-Natal. A multi-proxy approach was applied, combining accelerator mass spectrometry (AMS) radiocarbon and optically stimulated luminescence (OSL) dating, with fossil pollen and charcoal analysis to investigate Holocene climate and vegetation change. The record commenced ca. 7600 yr BP with a dominance in pollen from local reed sedge wetland taxa with the presence of prominent grasses and low abundance of tree taxa. This early phase was followed by a pollen preservation hiatus from ca. 6600-5900 yr BP. The Mid Holocene (ca. 5900-4900 yr BP) saw an environmental transition with the appearance of key coastal forest taxa like *Podocarpus*, *Celtis* and *Trema* and swamp forest taxa like *Barringtonia*, *Ficus*, *Morella* and *Syzygium*, high in abundance, which lasted well into the Mid Holocene inferring wet conditions. This was followed by a coastal forest retreat during the latter part of the Mid Holocene transitioning to the Late Holocene (ca. 1200-300 yr BP). This period inferred an interesting linkage with the charcoal data indicating a clear shift from grassy (W/L: <0.5) to woody (W/L:>0.5) fuel type. The Late Holocene presents a clear indication of a retreat in forest taxa and a shift to coastal grassland thicket inferring dry conditions during last ca. 300 yr BP. The charcoal record provided insight into past fire regimes and fuel types, reflecting the interplay between changes in available fuel within the landscape, and shifts between natural fires and anthropogenic burning. The South Lake Futululu record falls under the understudied Mfolozi-Msunduze catchment hence extending the existing knowledge of palaeoenvironments in the subregion.

PREFACE

The experimental work described in this dissertation was carried out in the School of Agriculture, Earth and Environmental Science, University of KwaZulu-Natal, Pietermaritzburg, from February 2015 to July 2022, under the supervision of Dr J.M. Finch.

The studies represent the original work of the author and have not otherwise been submitted in any form of degree or diploma to any University. Where use has been made of the work of others, it is duly acknowledged in the text.

Student name _Salona Reddy_____ 

Dr J.M. Finch __  _____

Acknowledgments

I would like to deeply express my gratitude and appreciation to my supervisor **Dr. Jemma Finch** for never giving up on me, even when I gave up on myself. Only you will understand each challenge I faced, and I thank you for your continuous support. Your love for research is contagious, I thank you for igniting mine once more.

To **Dr. Michael Grenfell** thank you for allowing me the opportunity to onboard the Lake Futululu project and your continuous guidance throughout my research.

Jamie Wood, thank you for allowing me access to your data to help support my own and for availing yourself to address my endless emails.

To the **Pollen Lab Team** my journey was a long one and meeting you all has been for a short while however I am so grateful for all your support and our constructive Monday meetings.

My research was funded through an **NRF Scare Skills Masters Scholarship**, **UKZN Postgrad Scholarship for Further Studies** and **Dr. Jemma Finch** for radiocarbon dating and laboratory processing apparatus.

To my mother **Nareena Reddy**, thank you for giving me those extra hard pushes when I lost my way.

To my sisters **Shanay** and **Sancha Reddy** thank you for supporting me throughout my journey, for making me late night snacks and bottomless teas to keep me going through the nights.

To **Jacolette Adam**, your late night ‘pep talks’ days off, financial and continuous support never went unnoticed you are appreciated.

To the rest of my family and friends I am ever so grateful to have you in my corner, thank you for remaining ready to help me no matter the task.

Table of Contents

ABSTRACT i

PREFACE ii

List of Figures viii

List of Tables x

List of Plates x

List of Appendices x

1. CHAPTER ONE: INTRODUCTION 1

1.1. Aim and Objectives 2

1.2. Thesis outline 3

2. CHAPTER TWO: LITERATURE REVIEW 4

2.1. Climatic drivers 4

2.1.1. Orbital Forcing and Milankovitch Cycle 4

2.1.2. Sea Surface Temperature 5

2.1.3. Greenhouse Gasses 6

2.2. Holocene records in South Africa 7

2.2.1. Early Holocene 10

2.2.2. Mid and Late Holocene 12

2.2.3. Late Holocene 14

2.2.4. Human impacts 16

3. CHAPTER THREE: THEORETICAL METHODOLOGY 19

3.1. Introduction 19

3.2. Pollen Analysis 19

3.2.1. Background 19

3.2.2. Advantages 19

3.2.3. Limitations 20

3.3. Field Techniques 20
3.3.1. Site Selection 20
3.3.2. Core Extraction 20
3.4. Core description 21
3.5. Laboratory techniques 22
3.5.1. Subsampling and standard laboratory process 22
3.5.2. Reference material 22
3.5.3. Pollen counts and identification 23
3.5.4. Data Presentation 23
3.5.5. Pollen Zonation 24
3.6. Interpretation 25
3.6.1. Indicator species 25
3.6.2. Assemblage Approach 26
3.6.3. Modern Analogue technique 26
3.7. Sediment archives 26
3.8. Chronologies 27
3.8.1. Radiocarbon dating 28
3.9. Sedimentary charcoal 31
3.9.1. Wildfire charcoal 32
3.9.2. Macroscopic methods 33
3.10. Conclusion 34
4. CHAPTER FOUR: MATERIALS AND METHODS 35
4.1. Introduction 35
4.2. Study Area 35
4.2.1. Site description 35
4.2.2. Geology- Sedimentology 37
4.2.3. Climate 39

4.3. Contemporary vegetation 39
4.3.1. Biomes 39
4.3.2. Anthropogenic Impacts 43
4.4. Methodology of the Study Site 45
4.4.1. Field Techniques 45
4.4.2. Chronology 47
4.4.3. Loss of Ignition (LOI) 48
4.4.4. Pollen analysis 48
4.4.5. Macroscopic charcoal analysis 49
5. CHAPTER FIVE: RESULTS 51
5.1. Stratigraphy 51
5.2. Chronology 52
5.3. Zonation 55
5.4. Pollen and Charcoal analysis 56
5.4.1. Zone S-1 (470-290 cm; ca. 7600-4900 yr BP) 61
5.4.2. Zone S-2 (290-120 cm; ca. 4900-1200 yr BP) 63
5.4.3. Zone S-3 (120-50 cm; ca. 1100-280 yr BP) 65
5.4.4. Zone S-4 (50-0 cm; ca. 60 yr BP - present) 66
5.5. Summary 67
6. CHAPTER SIX: DISCUSSION 69
6.1. Holocene palaeoenvironmental reconstruction for the Mfolozi Floodplain 69
6.1.1. Early reed sedge wetland phase (470-390 cm; ca. 7600 – 6600 yr BP) 69
6.1.2. Mid Holocene Transition phase (380-290cm; ca. 5900-4900 yr BP) 72
6.1.3. Mid to Late Holocene (280-120 cm; 4900-1200 yr BP) 73
6.1.4. Coastal Forest retreat phase (110-50 cm; 1200-300 yr BP) 76
6.1.5. Late Holocene Phase (40-0 cm; 300 yr BP -present) 78
6.2. Limitations 83

7. Conclusion 85
7.1. Key Findings 85
7.1.1. Aims and Objectives Review 86
7.1.2. Future research directions 88
8. References 89
Appendix A: Chronologies 111
Appendix B: Grain and Particle size description 114
Appendix C: Procedure for sub sampling 118
Appendix D: Procedure for preparing fossil pollen samples 119
Appendix E: Preparation procedure for reference collection pollen 122
Appendix F: LacCore Microsphere Pollen Spike 124
Appendix H: Bayesian Model Calibrated Ages 126
Appendix H: Data Sheets 141

List of Figures

Figure 2.1 Map of sites mentioned in text. Codes correspond with the sites presented in Table 2.1.....10
Figure 4.1 Location of south Lake Futululu in relation to Lake Eteza, Lake Futululu and Lake St Lucia. 36
Figure 4.2 Vegetation within south Lake Futululu and the surrounding area (*Source: Mucina et al., 2006; Scott-Shaw and Escott, 2011*).....42
Figure 4.3 Location of the 4.78 cm sediment core extracted from South Lake Futululu...46
Figure 4.4 (a) Using a vibracorer to extract a sediment core (b) from South Lake Futululu (*Source: Jamie Wood*).....47
Figure 5.1. Profile stratigraphy description of the South Lake Futululu core *(Source: Jamie Wood)*.....52
Figure 5.2 Bayesian age-depth model for South Lake Futululu with OSL (green wider error bars) and Radiocarbon dates (blues horter error bars). 55
Figure 5.3 Pollen diagram plotted against a dual age-depth axis indicating the main sum and dendrogram with associated Troels Smith lithology. The age axis is based on the age-depth model presented in Fig. 5.1 based on both OSL and AMS ages of which their position are indicated on the diagram. The grey area on the diagram indicates the position of a low pollen preservation hiatus from 400-350 cm. 58
Figure 5.4 Pollen diagram excluding rare taxa (<1%) plotted against a dual age-depth axis indicating the main sum and dendrogram with associated Troels Smith lithology. The age axis is based on the age-depth model presented in Fig. 5.1 based on both OSL and AMS ages of which their position are indicated on the diagram. The grey area on the diagram indicates the position of a low pollen preservation hiatus from 400-350 cm. 59
Figure 5.5 Summary diagram of organic content, pollen ecological groupings and macroscopic charcoal which includes $CHAR_n$, length and W/L plotted against a dual age-depth with associated Troels Smith lithology.. The age axis is based on the age-depth model presented in Fig. 5.1 is based on both OSL and AMS ages of which their position are indicated on the diagram. The grey area on the diagram indicates the position of a low pollen

preservation hiatus from 400-350 cm. The dashed line represents the W/L cut off between predominantly woody (>0.5) and grassy (<0.5) fuel types. 60
Figure 8.1. Grain particle size along the South Lake profile plotted against depth (Source: Jamie Wood) 114
Figure 8.2. Moisture and organic content profiles of core south Lake Futululu plotted against their depth scales along zonations based on pollen data (Source: Jamie Wood) 116

List of Tables

Table 2.1 Selected Holocene-aged records from the SRZ. 8
Table 5.1 AMS and OSL results for South Lake Futululu core. AMS results are calibrated using SHCal 20 (Hogg *et al*., 2013). 52
Table 5.2 Average sediment accumulation rates for South Lake Futululu. 54
Table 5.3 Classification of pollen taxa according to regional (Coastal Grassland Thicket Mosaic, Coastal Forest, Swamp Forest and Reed Sedge wetlands) (*indicates rare taxa with total counts of <1%, L= Local pollen taxa). 57
Table 6.1 Summary of vegetation history and inferred palaeoenvironmental changes at south Lake Futululu. 79

List of Plates

Plate 6.1 Descriptive images of the four phases within the South Futululu Record. 82

List of Appendices

Appendix A: Chronologies 111
Appendix B: Grain and Particle size description 114
Appendix C: Procedure for sub sampling 118
Appendix D: Procedure for preparing fossil pollen samples 119
Appendix E: Preparation procedure for reference collection pollen 122
Appendix F: LacCore Microsphere Pollen Spike 124
Appendix G: Macrocharcoal extraction (Stevenson and Haberle, 2005) 125
Appendix H: Bayesian Model Calibrated Ages 126

CHAPTER ONE: INTRODUCTION

Wetlands are one of the most valuable ecosystems on the planet and are identified as the kidneys of the Earth due to their function as downstream receivers of waste from both natural and human sources (Mitsch et al., 2015; Slagter et al., 2020). These important ecosystems are also facing serious threats of loss and degradation due to changes in land use by transformation, pollution, mining, hydrologic cut-offs by means of damming, lack of protection, mining and climate change (Owens, 2004; Gardner et al., 2015; Xu et al., 2019; Adeeyo *et al*., 2022). Wetlands provide a range of key ecosystem services, including acting as carbon sinks (Kayranli *et al*., 2010), and on the contrary are known as the largest terrestrial biological carbon pool (Chmura et al., 2003). In contrast, and particularly when degraded or mismanaged, wetlands can also act as a significant source of the greenhouse gas methane, thereby contributing to climate change (Kayranli *et al*., 2010; Mitsch *et al*., 2013). It is therefore critical to understand long-term wetland processes and functioning in the context of global change, both from a conservation and from an ecosystem service point of view. Wetlands in South Africa are regarded as an important ecosystem due to their physical and economic benefits however are grossly threatened by anthropogenic pollution, developmental activities, invasive plants, sedimentation, nutrient and chemical pollution (Van Deventer *et al.*, 2019, Adeeyo *et al*., 2022).

Wetland sediments accumulate steadily over time and thereby act as archives of long-term environmental change (Owens, 2020). Through the use of proxy evidence preserved in these sediments, such as plant and animal remains, geochemical signatures, and physical sediment characteristics, it is possible to reconstruct past climates and environments. In South Africa, wetland sediments have been widely used to produce a framework of past climatic changes (Neumann *et al*., 2008; Finch and Hill, 2008; Neumann *et al*., 2010; Scott *et al*., 2012; Norström et al., 2022). Paleoenvironmental records can contribute to conservation in four areas. These areas include the determination of the rate at which rates and nature of biodiversity respond to climate change, the climate processes responsible for ecological thresholds, the identification of ecological resilience to climate change and lastly the management of novel ecosystems (Willis *et al*., 2010).

South Africa is a water scarce country, not conducive to the accumulation of wetland deposits with high organic content (Scott, 1987). However, in the eastern summer rainfall zone wetlands are relatively abundant, with two RAMSAR designated areas, the Drakensberg and the iSimangaliso Wetland Park which is also a UNESCO World Heritage Site (Mbatha, 2022). The Maputaland Coastal Plain, on the north coast of KwaZulu-Natal, is host to extensive peat wetland deposits (Grundling and Grobler, 2016), providing an ideal opportunity for reconstructing climate and environmental change and understanding long-term wetland dynamics. Peatlands are presented in a variety of sizes varying between a few hectares and 278 ha where 20% of South Africa's peat resources are located in the southern Maputaland and North and South Coast areas (Grundling *et al*., 2000). Peatlands in South Africa are a threatened resource as they experience anthropogenic pressures by urban and industrialization, commercial sugar cane cultivation and afforestation (Grundling *et al*., 2000). It was noted that afforestation is considered the primary threat which leads to wetland degradation, particularly in Maputaland (Grundling *et al*., 2000). This research investigates the peat deposits of South Lake Futululu on the Mfolozi Floodplain in Maputaland to understand ecosystem response to past environmental and climate change, and management strategies, particularly for this threatened natural resource.

1.1. Aim and Objectives

i. To investigate Holocene palaeoenvironmental change through fossil pollen and charcoal analysis of a sediment core from South Lake Futululu to infer past environmental conditions in Maputaland during the Holocene period.

Specific objectives are:

ii. To produce an age-depth model for the sedimentary sequence based on a combination of accelerator mass spectrometry (AMS) radiocarbon and optically stimulated luminescence (OSL) ages.

iii. To conduct relative fossil pollen counts along the length of the core with the aim of reconstructing the Holocene vegetation history for the area; and

iv. To conduct macroscopic charcoal counts along the length of the core, such that fire history may be reconstructed for the area.

1.2. Thesis outline

The Introduction justifies the study and outlines the study aims and objectives of this study. Chapter Two presents a literature review of palaeoenvironmental research in South Africa. Chapter Three is a theoretical methodology and provides a theoretical background to the methods used in this study, describing methods such as pollen, charcoal, optically stimulated luminescence and radiocarbon analysis. Chapter Four is a Methodology chapter and describes the methods employed in this study. The Results chapter describes the findings of the study. The Discussion chapter presents a reconstruction of the palaeoenvironmental conditions at South Lake Futululu. In the final chapter, a synthesis of the palaeoenvironmental changes at South Lake Futululu is provided.

CHAPTER TWO: LITERATURE REVIEW

The chapter provides an overview of Holocene palaeoenvironmental records from the summer rainfall zone of South Africa, including some examples from Lesotho. Before delving into the past environmental changes that occurred in the region, an overview of key drivers of climate change is provided.

The frequency, intensity and duration of extreme weather events (droughts, wildfires, terrestrial and marine heatwaves, cyclones and flooding) will increase because of human-induced climate change, which impacts human and natural systems (IPCC, 2022; Yi-Lun et al., 2022). Globally the environment has observed the effects of climate change in the form of glaciers shrinking resulting in an accelerated rise in sea levels, ice on rivers and lakes breaking earlier, and the ranges of plants and animals shifting and trees which flower sooner (Goudie, 2018). These extremes expose millions of people to acute food insecurity, with the largest impacts observed in developing regions such as southern Africa (IPCC, 2022; Yi-Lun *et al*., 2022)

Against the backdrop of recent climate changes, southern Africa has undergone a range of long-term environmental changes linked to natural ecological processes. For example, the marked changes associated with Quaternary climate shifts have shaped the environment observed today (Nash and Meadows, 2012). These changes include climatic changes; sea level changes; shifts in various vegetation belts; animal and human populations; and soils and landforms (Rojas-Downing *et al*., 2017). There are many theories and ideas surrounding the reasons for climate change, including changes in solar radiation, atmospheric transparency, ocean level changes, the changes in the landscape and the geometry of the earth which includes the orbital forcing and Milankovitch Cycles and Greenhouse Gasses such as atmospheric carbon dioxide (CO_2) and carbon monoxide (CH_4) (Nash and Meadows, 2012). These are described in detail in the following section.

2.1. Climatic drivers

2.1.1. Orbital Forcing and Milankovitch Cycle

The theory of astronomical fluctuations of palaeoclimates attempts to explain the climatic variations that occurred between tens of hundreds of thousands of years. These variations are

recorded in media such as deep-sea sediments, ice sheets and continental archives (Berger & Loutre, 2004). The theory of astronomical fluctuations is also known as the Milankovitch Cycle, explained by the gravitational interactions of the moon and other planets which influence the Earth's orbit around the sun (Bennett, 1990). This cycle is known for its correlation with records that interpret variations of ice volumes and/or palaeotemperatures and which are continuous and well-dated (Chappell, 1973). This theory uses the variations in aspects of the earth's orbit and integrates the effect of changes in the following parameters: changes in eccentricity (100,000 year cycle), obliquity (41,000 year cycle) and precession of the equinoxes (19-23,000 year cycle) (Berger, 1981; Cole-Dai, 2010).

The amount of solar radiation received by the earth and the latitudinal and seasonal distribution of the radiation varies in accordance with these Milankovitch Cycles (Bennett, 1990; Berger, 1978). This influences temperature, precipitation and other atmospheric environmental aspects (Bennett, 1990). When the amount of incoming insolation varies due to the combination of the aforementioned parameters, glacial and interglacial cycles arise, causing ice sheet volumes to fluctuate (Calov *et al*., 2005).

Incoming insolation can be reduced because of atmospheric compositions that are caused by volcanic dust and backscattering. Al-Ghussain (2019) explains that this can be caused by natural events, including volcanic eruptions which eject sulphuric gases and ash into the upper atmosphere, causing the formation of clouds that block solar radiation (Cole-Dai, 2010). This can reduce global temperature for about three years (Al-Ghussain, 2019). The volcanic dust in the atmosphere results in the formation of ice crystals where the atmospheric conditions are below freezing and where the conditions are saturated sulphur dioxide and the water droplets already present may promote acid rain which results in insolation (Chakraborty *et al*., 2021). The influence of volcanic ashes are short term while aerosols are long term on atmospheric circulation, sea ice and ocean current (Chakraborty *et al*., 2021). The effects of a volcanic eruption result in more shortwave radiation reflected hence creating a negative balance in the atmosphere coming in from the sun to space (Chakraborty *et al*., 2021). These effects also cause more absorption of infrared radiation emitted from the earth which results in an increase in stratospheric temperature (Gerstell et al, 1995).

2.1.2. Sea Surface Temperature

According to Kim *et* al. (2003) the ocean absorbs heat and results in an increase in Sea Surface Temperature (SST). The increase in SST changes the circulation patterns which help

distribute heat around the globe. The ocean directly interacts with the atmosphere affecting the global climate because of changes in SSTs.

Sherwood *et al*. (2018) described water vapour as the most abundant and powerful greenhouse gas (GHG) that is emitted by human activities. Although the ocean contributes to the majority of the atmospheric water vapour the water vapour emitted from irrigation, power plant, cooling, aviation and domestic use increases atmospheric humidity and the water vapour greenhouse effect (Sherwood *et* al., 2018). The water vapour emitted from these anthropogenic activities are far greater than any other GHG including CO_2 (Sherwood *et* al., 2018).

According to the IPCC (2022), an increase in atmospheric water vapour over the ocean is expected with the increase in SSTs which led to an increase in GHG in the atmosphere and increased warm conditions. The increase in atmospheric water vapour feeds the weather systems that are responsible for producing precipitation such as heavy rain and snow (Paeth and Pollinger, 2020). The increase in SST can cause a shift in storm tracks causing drought in various areas (Paeth and Pollinger, 2020; IPCC, 2013). This brings to light the phenomenon of the El Niño Southern Oscillation (ENSO) and SST which are linked. Brook *et al*. (2010) indicated that the increase in SST is linked to the presence of ENSO (dry) events. The ENSO events are determined by a calculation whereby the monthly SST for the area, 4°N-4°S and 90°-150°W, anomalies are +0.5°C or more for at least six months (Wang, 2019).

2.1.3. Greenhouse Gasses

When considering GHGs such as CO_2 and CH_4 it is important to remember that these gases are considered drivers of climate change as they tend to enhance the effects of insolation (Cao *et al*., 2019). These gases trap the outgoing radiation so that the radiation cannot escape into the atmosphere which results in an increase in temperature (Cao *et al*., 2019). For example, Cao *et al*. (2019) indicated that a decrease in GHG concentration would reduce insolation and increase the presence of ice sheets which is directly affected by the lowering of the sea level. This is also evident in the records of ice cores that trapped bubbles of CO_2 which indicated low levels of CO_2 and resulted in climatic cooling (Anderson et al., 2007). It is understood that CO_2 levels are enhanced by anthropogenic activities this has been seen in Broecker *et al*. (2006) during the Holocene. A similar trend is observed in levels of CH_4 where an increase is observed during the LGM and the Holocene (Harder *et al*., 2007; Chappellaz *et al*., 1993).

Considering the above climate drivers no one factor can be directly responsible for driving climate change. Rather incorporating minor environmental changes from the land, sea, atmosphere and ice sheets will have an enhanced effect on climatic changes (Anderson et al., 2007). This can be described as the feedback mechanism or the forcing mechanism (Berger and Yin, 2011). This mechanism explains that climate drivers are interrelated. For example, the absorption of insolation is dependent on the earth's surface during that period (Berger and Yin, 2011). Another example is an increase in CO_2 can enhance the effects of insolation. Understanding the impact of global climate drivers and how these drivers have performed in the past will better enable the understanding of possible challenges that may be faced in the future of climate change (Vellend *et al*., 2013). The Holocene presented an interesting perspective to the records as it coincides with the late and post-stone age history of humankind with the most dramatic changes with regard to climate change and sea level changes (Dreibrodt *et al*., 2021).

2.2. Holocene records in South Africa

The Holocene in South Africa provides many variations to the climate for both warming and cooling events for precipitation amount and seasonality. Here we focus on Holocene-aged records from the summer rainfall zone of South Africa (Table 2.1; Figure 2.1), which receives >66% of its mean annual precipitation between October and March (Chase & Meadows, 2007). It must be noted that due to the aridity of much of the country poor preservation of fossil proxies poses a critical challenge (Fitchett, 2017). Multi proxy studies in recent years have progressed in various disciplines and are advancing with time. These include fossil leaves, boreholes, pollen grains, dinoflagellate cysts, lake and ocean sediments (Birks & Birks, 2006). This review includes palaeoenvironmental records such as dendrochronology and speleothems. With the ever-growing body of datasets, it is important to compare studies to determine trends and conclusions particularly those that are similar to the South Lake Futululu regional context.

Table 2.1 Selected Holocene-aged records from the SRZ.

Code	Site	Country	Longitude	Latitude	Altitude (above sea level)	Age (cal yr BP)	Type	Authors
BH	Braamhoek	South Africa	28°14'S	29°35'E	1700	0-*ca*. 16, 000	Wetland	(Scott *et al*., 2012; Norström *et al*., 2009; Norström *et al*., 2014)
CL	Clarens	South Africa	28°30'S	28°24'E	1735, 1800, 1880	*0-ca*. 23, 000	Swamp deposit	(Scott, 1989a)
CP	Cathedral Peak	South Africa	28°59'S	29°15'E	1899	0-*ca*. 15, 500	Peat deposit	(Lodder, 2010)
DB	Drakensberg	South Africa	28°56'S	29°12' E	1630	*0- ca*. 4835	Swamp	(Finch *et al*., 2021)
LB	Ladybird	Lesotho	29°35'S	29°15'E	2890	*0- ca.* 1200	Wetland	(Norström et al., 2018a)
LE	Lake Eteza	South Africa	28°31'S	32°8'E	14	0- ca. 10, 200	Lake	(Scott *et al*., 2012; Neumann *et al*., 2010)
LM	Lake Muzi	South Africa	27°38'S	32°25' E	22	*0- ca.* 5759	Lake	(Humphries *et al*., 2019)
LS	Lake Sibaya	South Africa	27°21'S	32°37'E	14.5	0-*ca*. 7700	Lake	(Neumann *et al*., 2008; Stager *et al*., 2013)
MA	Mafadi	Lesotho	29°11'S	29°21'E	3 390	*0- ca.* 8140	Wetland	(Fitchett *et al*., 2016a)
MF	Mfabeni	South Africa	28°9'S	32°31'E	11	0-*ca.* 44, 000	Peatland	(Finch and Hill, 2008; Baker *et al*., 2014; Baker et al 2016a; Baker et al 2016b; Baker et al 2017, Baker et al 2018; Miller et al., 2019)
ML	Maputaland	South Africa	27°06'S	32°49'E	15	0-*ca*. 6080	Peat deposit	(Mazus, 2000; Grundling et al 1998; Patrick and Ellery, 2007)
MP	Makapansgat	South Africa	24°8'S	29°10' E	1399	*0- ca.* 21, 777	Cave	(Holmgren, 2003)
MS	Mdlanzi Swamp	South Africa	27°36'S	32°28'E	40	0-*ca.* 1500	swamp	(Turner and Plater, 2004)
MW	Mahwaqa	South Africa	29°47'S	29°43' E	1858	*0- ca*. 11, 880	Wetland	(Neumann, 2014)
RE	Rietvlei	South Africa	25°50'S	28°20'E	1480	0-*ca*. 15, 500	Peat deposit	(Tusenius, 1989; Scott, 1993; 1999; Scott and Vogel, 1983)
SL	St Lucia	South Africa	28°00'S	32°28'E	0	*0- ca.* 9500	Lake	(Green et al 2022; Humphries et al 2015)
SK	Sekhokong	Lesotho	29°36'S	29°15'E	2 920	*0- ca.* 17, 000	Wetland	(Fitchett *et al*., 2016a; Fitchett *et al*., 2016b; Fitchett

								et al., 2017)
TC	Tswaing Crater	South Africa	25°24’S	28°4’E	1045	0-*ca*. 44, 998	Crater	(Scott, 2016; Scott 1999; Kristen et al., 2007; Metwally *et al*., 2014)
TV	Tate Vondo	South Africa	22°52’S	30°19’E	1100	0-*ca*. 10, 200	swamp	(Scott, 1993; 1999; 1987)
UZ	Umzimvubu	South Africa	31°42’S	29°38’E	0	*0- ca. 5550*	Marine sediment	(Hahn *et al*., 2021)
WC	Wonderwerk Cave	South Africa	27°59’S	23°24’E	1480	0-*ca*. 10, 000	Cave (Stalagmite)	(Scott *et al*., 2012; Brook et al., 2010; Tusenius, 1989)
WK	Wonderkrater	South Africa	24°25’S	28°44’E	1110	0-*ca*. 34, 500	Spring peat site	(Scott, 1982a; Scott and Vogel, 1983; Scott, 1993; 1999; Tyson *et al*., 2000; Scott, 2002; Truc *et al*., 2013; Horwitz et al., 2015; Bamford, 2015; House et al., 2020; Bamford, 2021;)

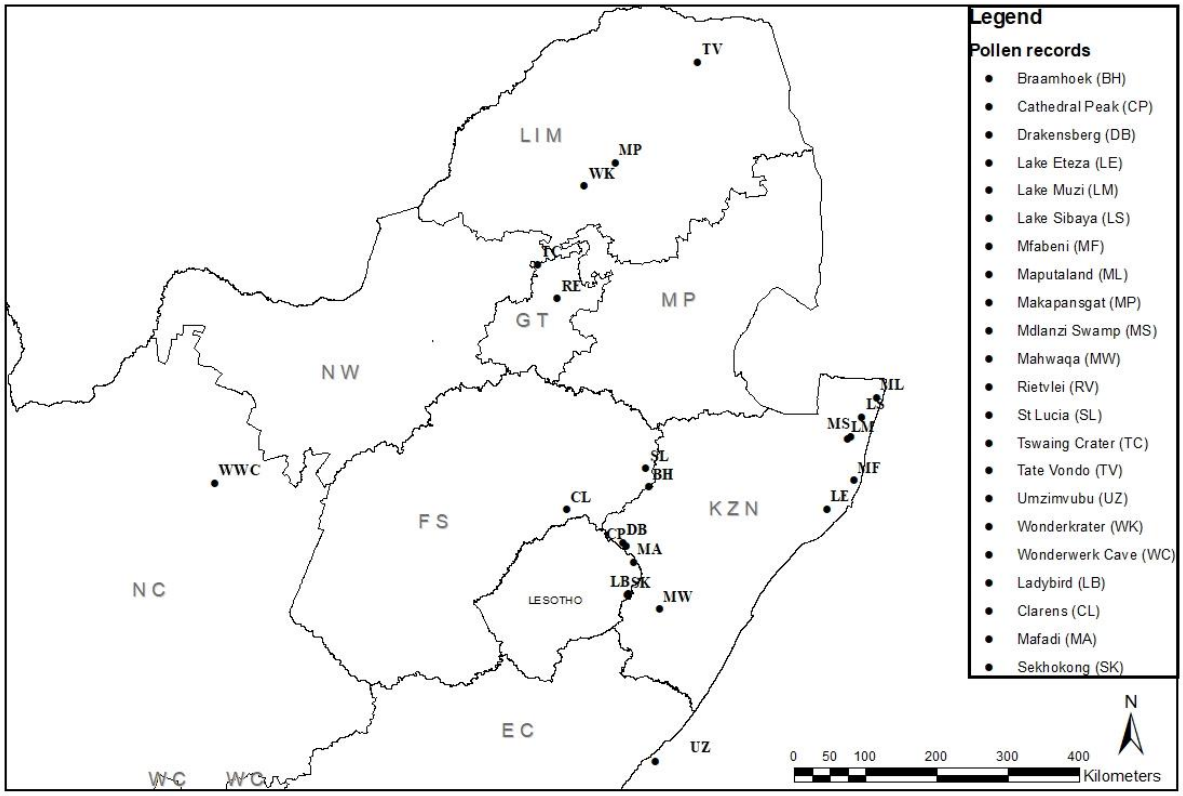

Figure 2.1 Map of sites mentioned in text. Codes correspond with the sites presented in Table 2.1.

The Holocene refers to the last 11,700 cal yr BP and is divided into two periods namely the Early Holocene (*ca.* 11,700 to 6000 cal yr BP)[1] and the Late Holocene (*ca.* 6000 to present) (Feurdean *et al*., 2012).

2.2.1. Early Holocene

The early Holocene is described by Scott (1990) as a period when warm and dry conditions were experienced, together with moist woodlands during the Pleistocene which resulted in the expansion of warm and semi-arid savannah type areas (Scott, 1982). The Sekhokong record in Lesotho, different from the records located at the coast, particularly because of the higher altitude, inferred a shift from drier conditions which slowly transition to warmer wetter conditions between ca. 14,150 to 8560 cal yr BP (Fitchett et al., 2016a). Between ca. 12,500 to 6500 yr BP in the Wonderwerk record, Asteraceae presented a dominant vegetation resemblance to that of the dry Nama Karoo Biome indicative of arid conditions (Brook et al., 2010). High evaporative conditions are indicated in the Wonderkrater between 12,000 and 10,000 230Th/234U yr BP inferring a dry warm environment (before 2000 AD) (Holmgren et

[1] Chronologies are standardised by converting all radiocarbon ages to calibrated years before present (cal yr BP) using SHCal20 (Hogg *et al.*, 2020).

al., 2003). Three key records among the many mentioned in Table 2.1 that help interpret the Holocene include the Makapansgat/Cold Air Cave speleothem (Holmgren, 2003), Braamhoek biomarker (Scott *et al*., 2012; Norström *et al*., 2009; Norström *et al*., 2014) and the Mfabeni stable carbon record (Finch and Hill, 2008; Baker *et al*., 2014; Baker et al 2016a; Baker et al 2016b; Baker et al 2017, Baker et al 2018; Miller et al., 2019) all described as moisture proxies. It should be noted that different proxies yield contradictory results. The Makapansgat record is important as it is an independent climate proxy and permits comparison with other similar well dated records (Holmgren, 2003). The Makapansgat record indicated low rainfall conditions during *ca*. 12,000 to 10,000 yr BP (Holmgren, 2003; Scott 1982). The Mfabeni biomarker record indicated a rise in precipitation which began during the Antarctic Cold reversal and continued to the early and mid Holocene where two major wet phases were reached (*ca.* 12,000 cal yr BP to 5 000 cal yr BP) (Miller *et al*., 2019). This record also indicated low and stable aeolian sediment flux during this period inferring a moist climate (Miller et al., 2019). The Mfabeni stable carbon record displayed a similar trend to Braamhoek, by inferring the expansion of arboreal taxa at *ca*. 12,000 yr BP (Finch and Hill, 2008) and the establishment of swamp forest vegetation during the early Holocene (Miller *et al.,* 2019). The Mfabeni record in Grundling *et al*. (2013) contradicts the results yielded in Miller *et al*. (2019).

The Mahwaqa record indicated dry conditions at ca. 11,700 cal yr BP with the presence of Mohria caffrorum (Neumann et al., 2014). Coastal lake records such as Lake Eteza, Lake Sibaya, Lake Muzi and St Lucia are important in the reconstruction of the Holocene period particularly in southeast Africa (Norström et al., 2022). The early to mid Holocene in the Summer Rainfall Zone was generally characterized by an increase in wetness between *ca.* 11500 to 8000 yr BP (Norström *et al*., 2022). The Braamhoek biomarker record indicated similar wetter conditions during the early Holocene (*ca*. 11,000 -10,200 yr BP) which lasted until *ca*. 8500 yr BP (Norström *et al*., 2014). During the beginning of the Holocene between ca. 10,200 and 6800 cal yr BP, the Lake Eteza record depicted a vegetation shift from wet woodlands to a dry grassier environment which coincides with the rising SST in the Mozambiquan Channel (Neumann et al., 2010). The Makapansgat and Braamhoek records were both in agreement during ca. 10,000 to 6000 yr BP where the δ18O stalagmite inferred generally warm conditions (Holmgren, 2003). The Braamhoek moisture proxy suggests a shift to an increase in dryness from *ca*. 8500 yr BP contradicting the Makapansgat record (Norström *et al*., 2014). Norström *et al.* (2022) indicated warming conditions during *ca*. 8000

to 5500 yr BP. During the early to mid Holocene (between *ca.* 8000-4000 yr BP) South Africa experienced variable climatic patterns with some of the warmest conditions observed (Chase and Meadows, 2007).

The opposite was inferred in the higher altitude record of Mafadi in Lesotho which indicated cold wet conditions at around *ca*. 8140 to 7580 cal yr BP (Fitchett *et al*., 2016b). Lake Eteza indicated a drier environment between *ca.* 8000-7000 cal yr BP which coincides with the low SST in the Mozambiquan Channel recorded at this time (Neumann *et al*., 2010). During this time the onset of high Chenopodiaceae and Amaranthaceae (Cheno/Ams or CHENO-AM-type undiff.) and Poaceae percentages was indicated in the Lake Eteza record inferring drier conditions (Neumann *et al.,* 2010). The Mafadi in Lesotho record indicated and warmer conditions between *ca*. 7520 and 6680 cal yr BP and *ca*. 6160 and 5700 cal yr BP (Fitchett *et al*., 2016b).

2.2.2. Mid and Late Holocene

Unlike the coast, the Sekhokong record in Lesotho inferred warm dry conditions between *ca*. 8560 to 7430 cal yr BP which was later followed by wet conditions between *ca*. 7280 to 6560 cal yr BP (Fitchett *et al*., 2016a). During the mid Holocene (between *ca.* 7100-6750 cal yr BP) Lake Sibaya indicated a forest composition that was observed to be the highest in the pollen record whereas Poaceae and other herbs were scarce (Neumann, 2008). Arid conditions are particularly evident in the southern records namely: Braamhoek and Lakes Eteza and Mfabeni which all experienced arid environments during ca. 7000-5000 cal yr BP (Chevalier Chase, 2015). Whereas the northern records namely: Wonderkrater, Tswaing Crater, Rietvlei Dam and Tate Vondo all experienced an increase in rainfall during this period (Chevalier Chase, 2015). The Cold Air Cave record inferred wetter conditions during the mid Holocene coinciding with the northern records (Holmgren *et al*., 2003). Between *ca.* 6800 and 3600 cal yr BP both the Eteza and Wonderkrater records appeared to be more humid than present day (Scott *et al*., 2012). The higher altitude Sekhokong range record inferred a warmer period between *ca*. 6560 to 3640 cal yr BP (Fitchett *et al*., 2016a). The Mfabeni record indicated the expansion of forests after *ca.* 6300 cal yr BP (5600 ^{14}C yr BP) (Finch & Hill, 2008). Scott *et al*. (2012) described a shift in the mid-Holocene from warmer conditions to cool conditions between *ca.* 6000-1500 cal yr BP in the Wonderwerk cave record. The presence of *Burkea* and Combretaceae and less *Acacia* pollen in the Tswaing Crater record inferred a wetter climate during *ca*. 6400-3500 cal yr BP (Scott, 1999). The Makapansgat stalagmite and Wonderkrater records indicated cooling during the mid-

Holocene (6000-3000 cal yr BP) (Holmgren *et al*., 2003). Between *ca.* 6000 to 1000 yr BP the $\delta^{13}C_{wax}$ values from the Mfabeni record indicated mostly C_4 type vegetation inferring arid conditions of which the most obvious arid event occurred during *ca*. 2800 yr BP (Miller *et al*., 2019). A mid Holocene cooling was described by the Makapansgat record between *ca.* 6000 to 3000 yr BP shifting from a warm to a cooler environment (Holmgren, 2003; Scott, 1982). During the Mid to Late Holocene, the Braamhoek record suggested a shift to warmer conditions with pronounced summer rainfalls as compared to the early Holocene opposite to the Makapansgat record (Norström *et al*., 2014). The Wonderwerk record indicated a transition to grassy veld suggesting a change from drier to wetter conditions which peaked at *ca.* 5600 and 4500 cal yr BP (Scott, 1987; Scott & Thackeray, 2015). Between *ca*. 5000 and present day the Mfabeni record indicated multiple shifts. One major shift was that of C_3 to more C_4 type vegetation moving to present day (Miller *et al*., 2019). The Mafadi record infrared fluctuations between cold and wet conditions during *ca*. 5500 and 1100 cal yr BP (Fitchett *et al*., 2016b). Hahn *et al*., 2021 indicated arid conditions between *ca.* 5500 to 1500 cal yr BP in the Mpondoland record and further north the inorganic proxy record of the Mkhuze delta swamp from 4600 cal yr BP (Norström *et al*., 2022).

Neumann *et al*. (2010) indicated a similar trend in the Lake Eteza record during *ca.* 5500 cal yr BP with an increase in forest pollen. Whereas after the mid Holocene, around ca. 5500 cal yr BP Mfabeni record indicated more open vegetation or secondary forests due to either disturbance or fire with evidence of *M. serrata* and *Acacia* (Finch & Hill, 2008). This was contradicted by the study conducted by Grunndling et al. (2013) in Mfabeni during the Middle Holocene (5280+/- 50 yr BP) which represented wetter conditions with the indication of open sedge fern. Both Nhlangu (Mazus, 1996) and Lake Eteza records (Scott & Steenkamp, 1996) indicated regional deforestation during this time.

Norström *et al*. (2021) however indicated a wet phase during the mid-Holocene (5500 cal yr BP) in the Drakensberg record. Lake Muzi displayed a similar trend to the Mpondoland record which indicated severe arid and drought conditions during 4600-4200, 3700-2600, 2100-1400 and 850-550 cal yr BP, with short periods in-between of relative wetness (Humphries *et al.*, 2019). The Mfabeni record indicated a similar trend to that of Wonderwerk which recorded an increase in arboreal pollen resulting in cool wet conditions during *ca.* 4400 cal yr BP (4000 ^{14}C yr BP) (Finch *et al*., 2008). Lake Mkhuze presented similar severe drought episodes between 4700 to 4200 cal yr BP and 3700 to 2600 cal yr BP

(Norström *et al*., 2022). The Wonderwerk record indicated a very variable climate with alternating wet and dry conditions during *ca.* 4000 cal yr BP (Brook *et al*., 2010).

The Mfabeni record indicated a decrease in forest pollen after *ca.* 3700 cal yr BP (Finch & Hill, 2008) which infers drier conditions. Lake Eteza indicated humid conditions at around *ca.* 3600 cal yr BP and gradual drying between *ca.* 3600-1500 cal yr BP and another moist spell at *ca.* 800 yr BP (Scott *et al*., 2012). Neumann *et al*. (2010) indicated from the Lake Eteza record an elevated percentages of Poaceae and Asteraceae and lower arboreal pollen which is indicative of grassy environments between *ca.* 3601 and 2000 cal yr BP setting the stance for the drought onset with a shift to drier conditions

It must be noted however that the decrease in forest pollen may be attributed to human disturbance rather than climate change (Scott *et al*., 2012). At the end of the Holocene the Tswaing Crater record inferred slightly wetter conditions with the increase in Cyperaceae indicating local swamp characteristics (Scott, 1999).

2.2.3. Late Holocene

The Late Holocene presented the onset of drier conditions within the coastal records. The montane records indicated relatively stable moist and warm conditions (Norström *et al*., 2022).

During *ca.* 3500-1000 cal yr BP the presence of *Acacia* pollen was indicated in the Tswaing Crater record which is indicative of deep soils and shallow water (Scott *et al*., 2003). The higher altitude, Sekhokong record inferred cool wet conditions during *ca*. 3400 to 1200 cal yr BP (Fitchett *et al*., 2016a). During *ca.* 3100 cal yr BP (3000 ^{14}C yr BP) the Tswaing record indicated low temperatures and dry conditions similar to that of the coastal records (Scott *et al*., 2003). During *ca.* 3000 to 2000 yr BP Makapansgat and Wonderkrater coincide which indicated high grass and Asteraceae counts which inferred cool grassy environments (Holmgren, 2003; Scott, 1982). The Cold Air Cave record indicated a warming during *ca*. 2900-2100 cal yr BP (Holmgren *et al*., 2001). The Makapansgat record later indicated a shift to moist conditions during *ca.* 2900-2100 cal yr BP (Holmgren *et al*., 2003). A similar trend was observed in Lake Sibaya diatom records (Stager *et al*., 2013) and the C_4 vegetation of the Cango Caves (Holmgren *et al*., 1999). The pollen data recorded from the alpine Ladybird site indicated cool winter rainfall conditions during the Late Holocene (Norström *et al*., 2022). The Braamhoek (Norström *et al*., 2014) and Mahwaqa (Neumann *et al*., 2014) records indicated stable moist and warm conditions between 2000 cal yr BP to present day (Norström

et al., 2022). During the last 2000 years, the Mfabeni record inferred dryness and a highly fluctuating hydroclimate at the coast (Norström *et al*., 2022). During *ca.* 2000 cal yr BP the Wonderwerk record contradicted the Mfabeni and Braamhoek record indicating an increase in $\delta^{18}O$ and $\delta^{13}C$ values which are indicative of drier conditions (Brook *et al*., 2010).

During *ca.* 1500-1250 cal yr BP Lake Sibaya indicated a decrease in *Podocarpus* pollen and an increase in wheat and other type of Poaceae which is indicative of human presence (Neumann et al., 2008). Braamhoek's record indicated relatively wet or less evaporative conditions during *ca.* 1500 cal yr BP-present day (Norström *et al*., 2009). The Lake Eteza record indicated an increase in Poaceae and a decrease in arboreal and shrub taxa resulting in a shift to drier conditions and an obvious retreat of forests (Neumann *et al*., 2010). Understanding the changes described by Neumann *et al*. (2010) may be indicative of evidence of Iron Age farming and crop cultivation which began at *ca.* 1400 cal yr BP (1600 ^{14}C BP). During the colonial period Finch *et al*., (2021) indicated that pollen changes are directly linked to human activity. For example, the decrease in *Podocarpus* numbers and various forest pollen taxa is directly correlated to local deforestation during this period (Finch *et al*., 2021). The charcoal record supports the pollen record indicating altered fire regimes (Finch *et al*., 2021). During *ca*. 1200-600 cal yr BP the Wonderkrater charcoal record indicated low charcoal concentrations however charcoal concentrations of Tswaing Crater were frequently peaking (Scott, 2002). The peak in charcoal concentrations in the Tswaing Crater record occurred during ca. 1000 cal yr BP which coincides with the Middle and Later Stone Age along with the increase in Chenopodiaceae which represents an increase in disturbance in the area (Scott, 2002). The Makapansgat and Wonderkrater from *ca*. 1200 to 600 yr BP indicated warm wet conditions were described with a bushy environment (Holmgren, 2003; Scott, 1982). During the last 1200 years of the Holocene various records indicated wet conditions. These records include the Makapansgat (during 1200-600 cal yr BP) (Norström *et al*., 2009). During the Iron Age charcoal concentrations indicate an increase in fire activity which coincides with human activity in the Lake Sibaya record (Neumann *et al*., 2008). Between 1200-400 cal yr BP Neumann *et al*. (2008) indicated a decrease in charcoal concentrations which may be attributed to the reduced fuel load because of overgrazing and extreme erosion rates due to human activities. Together reduced fire frequencies and the decreased charcoal concentrations led to better management in both Lake Sibaya and the Greater St. Lucia Wetland Park. A final indication of human activity is mentioned in the Lake Eteza (Neumann *et al*., 2008) and the Mdlanzi Swamp record (Turner & Plater, 2004) where *Zea mays*, *Pinus*, *Casuarina* and *Eucalyptus* were located in recent

sediments of their respective profiles indicating exotic plantations and increased human activities.

Both the high altitude records in Lesotho inferred colder dry conditions from *ca*. 1100 cal yr BP to present day (Fitchett *et al*., 2016a, Fitchett *et al*., 2016b). From *ca.* 860 cal yr BP to present day the Mfabeni record indicated higher Poaceae percentages and lower arboreal and Cyperaceae percentages between *ca.* 860 cal yr BP to present (Finch and Hill, 2008). The conditions described in the Cold Air Cave indicated humid conditions at *ca.* 690 cal yr BP (800 ^{14}C yr BP) and later shifted to dry cool conditions during *ca.* 570 cal yr BP (800 ^{14}C yr BP) (Repinski et al., 1999).

The Medieval period is poorly represented in most of South African records which may be because of poor resolution found in the records. This time period indicated an increase in temperature at around *ca*. 567-596 cal yr BP, up to 3-4°C higher than that of present day (Tyson *et al*., 2000). The Umzimvubu River catchment record however inferred high precipitation changes that took place during the period of the Medieval Climate Anomaly and Little Ice Age (Hahn *et al*., 2021). Following the Medieval period is the Little Ice Age which occurred at around *ca*. 615-150 cal yr BP (Tyson *et al*., 2000). During the Little Ice Age, the Makapansgat record indicated a cool, arid period between *ca.* 486-502 (Holmgren *et al*., 1999). Lake Eteza indicated an increase in *Pinus* from ca. 300 cal yr BP whereas a decrease in *Podocarpus, Isoglossa* and *Celtis* which all indicate an increase in human disturbance (Neumann *et al*., 2008).

This record recorded the lowest temperature at *ca*. 250 cal yr BP which is 1.4°C cooler than today (Holmgren *et al*., 1999). The Makapansgat record *ca*. 150 cal yr BP which coincides with the northern hemisphere Little Ice Age (Holmgren *et al*., 1999). During the Little Ice Age, the Lake Eteza record indicated a decrease in charcoal concentrations together with a decrease in moisture which resulted in a reduced fuel load (Neumann *et al*., 2010). A contradiction was noted by Meadows *et al*. (1996) who indicated that winter rainfall zones recorded an increase in rainfall during the Little Ice Age. Interestingly the Ladybird record indicated higher moisture during the Little Ice Age because of the decrease in evaporated water loss due to the cooler climate and a shift in precipitation patterns which resulted in precipitation during the winter season (Norström *et al*., 2018).

2.2.4. Human impacts

The late Holocene is characterised by the increase in anthropogenic impacts on vegetation in South Africa. These impacts provide evidence in the form of physical (heavy metals, organic

compounds, fly ash, black carbon, microplastics), ecological (pollen, diatoms, ostracods, foraminifera, invasive species, domestic species, extinctions) and human markers (sediment and erosion, mines, refuse/landfills, building and infrastructure, urbanisation and agriculture) (Rose *et al*., 2021). Human activities have also influenced the change in landscape by means of open patches in degraded pastures, reduction of grass cover and the removal of vegetation (Tabares *et al*., 2019). At around 2000 cal yr BP the introduction of large-scale human influences was apparent on the landscape. Neumann *et al.* (2008) referred to Iron Age herders who arrived *ca*. 2000 yr BP. This anthropogenic evidence of the climate signal is apparent in the landscape (Norström *et al*., 2022). The Umzimvubu River indicated human activity with the presence of soil erosion rates and vegetation changes during *ca*. 1500 cal yr BP indicating the arrival of Iron Age Settlers (Hahn *et al*., 2021). The Mdlanzi Swamp indicated at around 1450 cal yr BP evidence of the Early Iron Age by the formation of reed-sedge wetland in the valley (Turner and Plater, 2004).

Feely and Bell (2019) described the absence of trees as an indication of early farmers who utilized timber for settlement construction, food preparation and iron smelting. The Mdlanzi Swamp record indicated evidence of charcoal increase occurrence in the catchment at the wetland which is most likely a result of the Iron Age agriculturalists. The increase in charcoal from these agriculturalists presented evidence that fire was used to clear local woodlands for cultivation and grazing (Turner and Plater, 2004). The Wonderkrater record provided evidence of the Middle and Later Stone Age cultures during *ca.* 1000 cal yr BP by observing the increase in charcoal and Chenopodiaceae pollen which indicates disturbance during this time (Scott, 2002). Hahn *et al*. (2021) indicated that at around *ca*. 300 cal yr BP the arrival of European settlers is evident in the region. The evidence was resented by the presence of neophytic trees which include Pinus, *Cupressus*, and *Eucalyptus*, and neophytic weeds which include Ambrosia and Parietaria as well as Helianthus (Hahn *et al*., 2021). The Princess vlei record indicated a similar trend at *ca*. 300 cal yr BP which presented anthropogenic disturbances by the presence of Pinus and *Zea mays* and a peak in charcoal indicating an increase in fuel load during this time with the arrival of the European settlers (Neumann *et al*., 2011). Lake Sibaya presented similar evidence of the presence of Pinus and algae at around *ca*. 300 cal yr BP and the decrease in *Podocarpus*, *Isoglossa* and *Celtis* which indicated the presence of human disturbance (Neumann *et al*., 2008). The evidence of the increase in charcoal recorded by Neumann *et al*. (2008) indicated the presence of the Iron Age by means of increased human activity and fire activities *ca.*1500-1300 yr BP. Neumann

et al. (2008) indicated that the conditions during this time did not support the presence of natural fire occurrences hence pointing to evidence of increased human activity resulting in an increase in fire frequencies and intensities over the past 2000 years in KwaZulu-Natal. Neumann *et al*. (2008) indicated a decline in charcoal within the Lake Sibaya record at around *ca*. 1200-400 cal yr BP attributed to the already changed landscape which may have presented a reduction in the available fuel load because of erosion and overgrazing due to the increased anthropogenic activities. The Lake Eteza record indicated an increase in the presence of *Zea Mays*, *Pinus* and *Casuarina* (Thamm *et al*., 1996) described in the Majiji, Nhlangu, Mgobezeleni and Mfabeni mires, the presence of *Pinus* between depths 0 and 50 cm. It is important to note that Tabares *et al*. (2019) explained that the macrocharcoal record suggested a decrease in fire activities when associated with the intensification of farming particularly because of the suppression of wildfires and the control of fires to preserve pastures for livestock.

2.3. Conclusion

A number of sites have provided an understanding of environmental drivers and changes that have taken place and several sites during the Holocene in South Africa. During the Holocene various high-resolution records are available for comparison so that a clear regional image of environmental changes occur. A review of historic climatic changes in South Africa has provided a reliable palaeoenvironmental background for this study. The Holocene presented the associated shift in the climate along with the presence of anthropogenic activities. These anthropogenic activities have been inferred by the presence of *Pinus, Zea Mays* and *Casuarina* together with the decrease in natural vegetation and charcoal influx.

CHAPTER THREE: THEORETICAL METHODOLOGY

3.1. Introduction

This chapter will include the theoretical background of the palaeoenvironmental techniques applied in this research. This will include the key proxy methods of pollen analysis for reconstructing past vegetation and charcoal analysis for reconstructing fire history. The chapter will further review the palaeodating techniques that are applied in this research, viz., radiocarbon analysis and Optically Stimulated Luminescence (OSL) dating.

3.2. Pollen Analysis

3.2.1. Background

The study of palynology, or pollen analysis, was first introduced by the Swedish botanist von Post, who was the first to publish a quantitative pollen diagram in 1916 (Birks and Berglund, 2017). The technique makes use of the naturally occurring fallout of pollen grains, the male gametophyte of a flowering plant, gymnosperms and spores in lower plants, originating from the local and regional surrounding vegetation which are dispersed through the air and are later deposited in the sediment (Ellison, 2008). These pollen grains and spores contain an exine, an outer wall that is highly resistant to decay, and results in an abundance of pollen being found in peat and lake sediments (Loader and Hemming, 2004; Ellison, 2008). Palynology aims to interpret or predict vegetation changes that may be a result of climatic, edaphic, biotic, or human factors by relying on the preservation, recovery and identification of pollen in sequence (Davis, 1963).

3.2.2. Advantages

Pollen grains are produced in large quantities and tend to be well distributed when compared with other macrofossils, which makes this type of proxy statistically suitable for analysis (Faegri and Iverson, 1989; Walker, 2005). Pollen grains are extracted by using appropriate chemicals to disperse sediment so that they may be viewed and identified under a high magnification microscope. Pollen grains vary in size and range from 20-40 μm in diameter. Pollen assemblages or spectra provide detailed information on the composition of vegetation at a given point in time and can be used to determine vegetation change over a period of time.

Pollen grains possess morphological diversity such as size, symmetry or structure making them unique to the plant species (Dunker, 2021).

3.2.3. Limitations

Pollen analysis assumes that there is a relationship between the pollen that is deposited into the sediment and the vegetation that produced it. Pollen identification is limited in taxonomic resolution and several ecologically important taxa have indistinguishable pollen grains (Seppä and Bennet, 2003). Pollen is often unidentifiable to a species level where many ecosystems cannot be characterized by an indicator species approach (Gosling et al., 2003). Pollen analysis has to account for the complex composition of pollen rain. There are different proportions of taxa some of which produce small amounts of locally dispersed pollen whereas other species produce large quantities of wind-dispersed pollen (Birks et al., 2000).

Arid environments have a limited number of identified pollen taxa and the numbers of good climate indicators are rare. This makes it difficult to conduct an objective climate reconstruction (Herzschuh et al., 2004). Within temperate forests, pollen analysis is used to determine evidence of major palaeoecological changes. In areas that lack trees such as alpine and arctic areas the local pollen production is low. This means that distant pollen rain becomes important but may become overrepresented in floristic and vegetation reconstructions leading to misleading interpretations (Birks et al., 2000). These issues can be overcome by means of effective modeling. Hill et al. (2021) utilized statistical modeling in the Drakensberg to demonstrate the effectiveness of modeling to overcome the assumption of dispersion.

3.3. Field Techniques

3.3.1. Site Selection

Several types of sediments are not uniform in their stratigraphic features (Moore and Webb, 1978). To determine the optimum location for recovering a sample for detailed analysis there are two important guiding principles of site selection understanding the sediment and successional history of the site. This is done in the field before the removal of the core which is used for pollen analysis.

3.3.2. Core Extraction

Where there are no exposed sections of a deposit, available cores should be extracted from the surface of the site. The collection of samples from peat sites are simpler than from lake

sites, because the equipment can be operated from the peat surface where on lake sites it cannot. Lake coring is done by using two small boats which are roped together with a sampling platform between them (Patterson et al., 2018). Sediment sequences are studied by sampling top down using a coring device. Since different coring equipment are devised to suit different situations and types of sediment three different, popular samplers will be explained in more detail (Glew et al., 2002).

The Hiller Sampler is a chamber sampler with an angular head which allows it to be twisted as it penetrates the sediment. This allows for the potential to penetrate stiff or fibrous materials (Thomas, 1964). The sample is obtained by twisting in the opposite direction when the inner rotating flanged chamber opens and scours a sample from the adjacent sediment (Thomas, 1964; Shotyk and Noernberg, 2020).

The Russian Sampler was designed by Russian research workers and the sampler was generally designed for peat stratigraphic work because of its clean action and its speed of operation and cleaning (Shotyk and Noernberg, 2020). The sampler lacks an auger head and therefore is required to be pushed vertically into the sediment (Moore and Webb, 1978; Shotyk and Noernberg, 2020). This limits the Russian sampler to soft materials but has a great advantage that the sediment through which it passes is not disturbed by the churning action (Moore and Webb, 1978; Shotyk and Noernberg, 2020). When the sampler is withdrawn and the fin rotated 180° the entire sample intact in the chamber is revealed intact and clean.

A vibratory corer, commonly known as a vibracorer, is used to obtain samples in various sediment deposit (lacustrine, offshore marine and coastal) environments (Fisher, 2004). A vibracorer is made up of three components, a frame, a coring tube or barrel and a drive head with a vibrator (Fisher, 2004). The frame can either be a quadruped or a tripod where the legs are connected to a vertical beam. An advantage to this method is this beam supports the core barrel and vibrator mechanism which allows the corer to be free-standing on the land (Fisher, 2004).

3.4. Core description

After the extraction of the sediment core and the stratigraphy is examined, thereafter divided along their length into subsamples which are then further analysed for a variety of proxy data (Slayton, 2010). Initially, the sediment core is described in the colour changes and physical appearances and further analysed along the length for bulk density, moisture content and

organic content which is accomplished through loss of ignition (Slayton, 2010). There are further sub samples that are extracted for radiocarbon dating for the determination of sediment rates (Anderson et al., 2007). The inorganic material is used to determine the particle size distribution of changes in proportions of clay, silt, sand and gravel. These are essential in providing information on the source of material that contributes to fluvial sediments and explain the transportation and competence of the flow that carried the sediment before the deposition (Wen et al., 2010). When considering fluvial sediments particle size information can infer past levels of discharge into the stream systems which indicates the past climatic conditions which affected the hydrological cycle and the past changes in the drainage basin system (Slayton, 2010).

3.5. Laboratory techniques

3.5.1. Subsampling and standard laboratory process

When dealing with unstratified material, subsampling can be done randomly. Usually, palaeoecological material is stratified in a temporal sequence and the sampling process is designed to show changes in sediment pollen over time (Green et al., 1988). Depth is closely linked with this method. The intervals of subsampling are dependent on the rate of growth of the deposit which can only be determined after the samples have been dated. The degree of precision with which the sample will detect changes and the time that the researcher has for the project (Chevalier et al., 2020). A common approach to subsampling is to begin at wide intervals (20 or 10 cm) and later fill in the gaps to provide greater detail (Chevalier et al., 2020).

The subsampling is done where the core surface is first carefully cleaned with a sharp scalpel and all cuts are made horizontally (sideward) to the axis of the core. A 1cm sample is cut out with a scalpel and placed in a known volume of water using the displacement method (Chevalier et al., 2020).

Various chemical processes have been developed for the treatment of pollen samples that relate to different matrix materials in which they are embedded.

3.5.2. Reference material

Reference materials are usually obtained in the form of fresh samples from the site (Moore *et al*., 1991). Identification guides, atlases and databases such as the European Pollen Database

(EPD, 2013) and the African Pollen Database (APD, 2013) are often utilized in the identification process. Other guides included the UKZN and East African pollen references.

3.5.3. Pollen counts and identification

Being familiar with the identification of majority pollen types counting and identification becomes simpler. Scanning at a magnification of x20 in prepared slides for pollen is ideal as there is a larger field of view. A x40 objective lens is appropriate for the counting and identification of slides with reasonable pollen densities (Birks and Birks, 1980). Oil immersion microscopy at x100 is used for grains when a clearer view is required for smaller grains (Birks and Birks, 1980). This magnification is not ideal for scanning as it provides a very small field of view. When counting it is important to avoid counting only the center of the coverslip or only at the edges as there is evidence that larger grains migrate to the center and smaller grains to the edges (Faegri and Iverson, 1989). This pattern is overcome by sampling the slide by means of linear traverses by passing from one edge to another. This operation demands the use of a mechanical stage on the microscope which needs to be graduated so that the coordinates for any particular reference can be recorded (Faegri and Iverson, 1989). The slide should always be moved in one direction rather than reversing the direction every time a new transverse begins (Faegri and Iverson, 1989).

3.5.4. Data Presentation

The data is usually displayed graphically in the form of a pollen diagram. There are a range of diagrams that the data can be presented in namely: Arrangement, stratigraphy, pollen curves, pollen abundance scales, order of taxa, other data, diversity and a summary diagram

The data is presented in a diagram where the vertical axis represents the depth and the horizontal axis is the abundance of the pollen taxon in absolute terms (Faegri and Iverson, 1989). The alignment of the diagram is always logical as it represents a vertical core which also relates to time which means that a greater depth equals a greater age (Faegri and Iverson, 1989). Stratigraphy is the sequence of sediment types that is represented in a diagram with a vertical column on the left hand side (Faegri and Iverson, 1989). This is an important part of the diagram which provides essential information for the interpretation of the fluctuating pollen curves. The most commonly used system is the Troels-Smith (1955) which has been modified from the Aaby and Berglund (1986). Pollen curves are represented where the proportions of pollen types are indicated at each level of sampling by either a bar or histogram or a point on a continuous curve (Aaby and Berglund, 1986).

The order of taxa is represented conventionally where the pollen diagrams are arranged into groups of taxa with a set order (arboreal, shrubs, dwarf shrubs, dryland herbs, aquatics and finally spores) (Moore et al., 1991). The summary diagram is to be incorporated into a pollen diagram which displays graphically how the total pollen sum is divided into tree, shrub, dwarf shrub and herbaceous components at each level (Moore et al., 1991). This allows the reader at one glance to identify major shifts for example in arboreal and non-arboreal pollen ratios which may be important in the zonation and interpretation of pollen diagrams (Moore et al., 1991).

3.5.5. Pollen Zonation

Pollen diagrams are divided into a series of zones based on their pollen content. The diagram is divided using horizontal lines which are drawn across the diagram which divide it into a sequence of units or pollen zones (Gordon and Birks, 1972). These units are divided according to the criteria of pollen components and without reference to timescale, sediment stratigraphy, inferences concerning past climate, vegetation, archaeology etc. The pollen zone should be a biostratigraphic unit which is a unit defined purely on its pollen content (Gordon and Birks, 1972). The main aim of zonation is to divide the pollen diagram into a series of convenient units where each is internally homogenous and displays pollen characteristics that may be different from adjacent zones (Gordon and Birks, 1972). The zone boundaries will be placed at points where the changes between pollen spectra are most obvious.

Numerical methods are most often used to establish diagram zonation, including two major techniques: agglomerative and the other divisive. The agglomerative method is (CONSLINK) which compares samples with their stratigraphic methods and pairs the most similar samples according to their total pollen assemblages (Gordon and Birks, 1972). It is a measurement of dissimilarity and the fused pairs are those with the lowest dissimilarity coefficients (Gordon and Birks, 1972). The repeated pairing of the most similar adjacent samples results in the establishment of a hierarchy of clusters. This means that the higher order clusters will form a basis for the zones (Gordon and Birks, 1972).

CONISS is a method that carries out stratigraphically constrained cluster analysis with the use of an incremental sum of squares (Grimm, 1987). It is known to work best for datasets that are stratigraphic or linear data that are ordered such as vegetation zones along a natural gradient like pollen frequency data (Grimm, 1987). CONISS is fundamentally based on cluster analysis. This is based on the idea that clusters are derived by hierarchal

agglomeration. The Constrained Incremental Sum of Squares (CONISS) cluster technique was used to define boundaries between the most distinguishable pollen zones. The CONISS algorithm was applied to the regional pollen data to produce a dendrogram (Bennett, 2005). These zones are primarily used for descriptive purposes to identify zones of homogenous pollen and charcoal content (Grimm, 1987). This is illustrated in the form of a dendrogram which indicates the hierarchical relationship of clusters defined by the analysis (Fig. 5.3). The purpose of the zonation is to provide a sequence of smaller units to simplify the description, the discussion, interpretation, and comparison along with the correlation in time of the sequences (Gordon and Birks, 1972). Together with identifying zones of homogenous pollen content (Grimm, 1987).

3.6. Interpretation

The interpretation of pollen diagrams lies in the understanding of the pollen grain distinctive structure with the identification, their abundance and wide properties of dispersal in nature, the quantities of pollen grains produced which may differ according to species and distances vary not only between taxa but the position of release and geographical location (Moore et al., 1991). Pollen stratigraphy provides a record of the past changing vegetation in terms of land use and climate history (Moore and Webb, 1978). Three main approaches are used in environmental reconstruction from fossil pollen such as the Indicator Species approach, the Assemblage Approach (Transfer Function) and the Modern Analogue Technique.

3.6.1. Indicator species

Certain individual taxa provide information because they have specific environmental conditions these are known as indicator species (Moore et al., 1991). These species provide definitive statements of past conditions just by their presence. The assumption of this approach is that the physiological requirements of the taxon have not changed during the time that has passed since it was deposited and that it has a similar physiological race of the taxon is being dealt with (Moore et al., 1991; Birks et al., 2010). The relationship that is displayed between the assemblage and the environment can be reduced to a numerical function known as a transfer function. This is done by means of multiple linear regressions (Moore et al., 1991; Birks et al., 2010). Transfer functions are essential in providing detailed climate reconstructions but require high quality datasets (Moore et al., 1991; Birks et al., 2010).

3.6.2. Assemblage Approach

This is the use of the entire assemblage. This approach provides the argument that the full spectrum of vegetation is a better reflection of environmental conditions (climate, land use). The approach also emphasizes that a full pollen assemblage should provide a better guide to past environmental conditions than any individual species that are taken in isolation (Moore et al., 1991).

3.6.3. Modern Analogue technique

This technique involves the comparison between fossil pollen assemblages with modern pollen assemblages which are obtained from surface samples (Birks and Birks, 1980). This involves the use of statistical and numerical tools to help assign quantitative estimates of the similarity and dissimilarity between fossil and modern pollen assemblages. This allows for known environmental elements to be allocated to fossil pollen spectra which enables past conditions to be inferred (Birks and Birks, 1980).

3.7. Sediment archives

Sedimentary archives allow for the reconstruction of past environments including lakes, peatlands and fluvial deposits (Moore et al., 1991). At times lake sediments are the only viable strategic sequence of microfossils or chemical materials relating to palaeoclimates in many terrestrial environments (Wright, 1991). Continuous deposits are important to determine past environmental changes and depositional rates which provide insight into mode and rate of sedimentation and landscape at different time periods (Moore et al., 1991). In a fluvial environment, channel migration may lead to changes in sedimentation and post depositional reworking making the interpretation of fluvial records complicated (Anderson et al., 2007).

Lake sediments are composed of materials that originate from organisms within the lake and materials being washed into the lake from surrounding drainage basins and catchment areas (Anderson *et al*., 2007). The sediments that are derived from peatlands are studied for their chemical and physical characteristics of the sediment and for the biological remains that it contains (Anderson et al., 2007). Water retention, yield coefficient and the ability to be hydraulic conductive make up the physical importance of peat materials as these three factors determine the hydraulic features of organic soils (Boelter, 1968).

The extraction of one core is a representative of the entire basin this is the reason for stratigraphic studies to replicate the study by the extraction and analysis of many cores unless

the aim of the study is looking at finer details of the basin sedimentary evolution (Ellison, 2008). Sediment sequences are studied by sampling top down using a coring device. Initially, the sediment core is described in colour changes and physical appearances and further analysed along the length for bulk density, moisture content and organic content which is accomplished through loss of ignition (Anderson *et al*., 2007). Inorganic material is used to determine particle size distribution as the changes in their proportions of clay, silt, sand and gravel are essential in providing information on the source of the material that contributes to fluvial sediments which explains the transportation and competence of the flow which carried the sediment before the deposition (Anderson *et al*., 2007). When considering fluvial sediments particle size information can infer past levels of discharge into the stream systems which indicates the past climatic conditions that affects the hydrological cycle and the past changes in the drainage basin system (Anderson *et al*., 2007).

3.8. Chronologies

Constructing chronologies are essential in determining the sequence of events and timing of past changes that are inferred from the proxy evidence (Birks, 2006). It is essential to correlate different proxy records so that it is possible to test the different causes and linkages to environmental change (Blaauw *et al*., 2007). The better the chronology the more rigorous the testing in environmental systems particularly the rates of change and identifying the leads, lags and feedback (Birks, 2006). The ability to reconstruct palaeoenvironments and understanding of various mechanisms that govern the processes of climate change has been a goal for present day research (Brown, 1992). The chronologies of cores are obtained by the use of radiocarbon measurements on the total organic carbon on the bulk sediment (Brown *et al*., 1989). These chronologies allow a correlation between the variations that are observed within the core from different sites and for relating changes that are preserved in fossil pollen records to those that are found in other proxy climate records (Brown, 1992).

Age-depth models form the back-bone of any palaeoenvironmental study. They are built to estimate the calendar ages of the depths in a core from a deposit (Blaauw, 2010). This is based on a limited number of dated depths and on the assumption as to how the deposit has accumulated between the dated depths. It was noted that very few studies provide details of their calibration like the type of calibration curve and software that was applied in their procedures of C_{14} dates (Blaauw, 2010). Fewer give information if point estimates, the software that was used to determine the age-depth curves, the indication of age-depth uncertainties that were calculated and the specification of the age-depth model that was

applied (Blaauw, 2010). Most use Bayesian age-depth modelling and the others use a classical-age depth model which includes liner interpolation or liner/polynomial regression (Blaauw, 2010).

Constructing age-depth models with the use of radiocarbon dating and other forms of chronological control to various sediment types forms a temporal correlation between climatic shifts (Blaauw, 2010). There are techniques to determine past hydrological changes that are potentially climatically driven can be derived from peat sequences (Blaauw, 2010).

3.8.1. Radiocarbon dating

Radiocarbon dating is relatively affordable and has become popular in dating methods. This dating method has contributed to the understanding of Earth's history but is limited where in most circumstances is useful from only a few hundred years to 60 000 years (Lian and Roberts, 2006). This method requires fossil vegetation which is often broken. Radiocarbon ages need to be compared to calendar years which will provide us with knowledge of the variations of past carbon concentrations that occurred in the atmosphere (Lian and Roberts, 2006).

Radiocarbon dating is the dominant technique that is used to establish chronologies for Late Pleistocene and Holocene pollen records which are taken from lake sediments and peat deposits (Brown, 1992). Radiocarbon measurements are taken from the total decay counting organic carbon of bulk lake sediments or peat deposits. The reason for using total organic carbon of bulk samples is that it requires a specific sample size for the decay counting method (Brown, 1992).

Some of the most commonly used techniques are isotopic dating techniques, especially radiocarbon, uranium series and potassium-argon. Radio carbon has the isotope ^{14}C and the half-life (years) is 5730±40 and the range (years) is 0-75000 materials that can be used for this technique is peat, wood, shell, charcoal, organic muds, algae, tufa, soil carbonate and coral (Gillespie, 1991). Accelerator Mass Spectrometry radiocarbon dating allows a chronology from samples where there is a limited amount of material which is available and the ability to perform pretreatments to remove contaminants (Gillespie, 1991). In the past large amounts of samples were to be sent for dating but with the progression of this method Accelerator Mass Spectrometry method of radiocarbon dating directly measures the $^{14}C/^{12}C$ ratio of a sample which eliminates the problem of a large sample size. AMS dating is able to date leaves, seeds and pollen grains (Gillespie, 1991).

The majority of the ^{14}C is absorbed in oceans as dissolved carbonate which means that the organisms which live in the ocean also take up ^{14}C in their lifetime (Gillespie, 1991). Even though the ^{14}C in terrestrial biosphere and the ocean is constantly decaying it is also constantly replenished from the atmosphere (Gillespie, 1991). Hence the ocean which is known as the global carbon reservoir and the amount of ^{14}C in animal and plant tissue remains fairly constant through time (Gillespie, 1991).

When an organism dies it does not take up ^{14}C anymore and becomes isolated there is no further replenishment of ^{14}C and hence radioactive decay takes place (Boreux et al., 1997). To infer the age of death of an organism the amount of ^{14}C in a fossil sample can be measured and compared to a modern sample (Wood, 2015). Using this method allows for several variables for instance determining the decay rate of ^{14}C (Gillespie, 1991). Several experimental studies indicate that the occurrence of decay takes place at 1% every 83 years hence meaning that after 8300 years the residual activity will have halted within the sample (Gillespie, 1991).

Residual activity ^{14}C activity can be measured in two approaches first in materials mentioned by Lian and Roberts (2006) which include: inter alia, wood, peat, organic lake sediment, plant remains, charcoal, shell and coral. One approach is called beta counting and the second is accelerator mass spectrometry (AMS). The difference between the two is that radiometric dating tools can detect beta particles within the decay of the ^{14}C atoms whereas AMS counts the ^{14}C isotope ratio in the decaying sample (Lian and Roberts, 2006). This is accomplished by accelerating ions to high kinetic energies which separates small ^{14}C signals from other isotopes. The relativeness of these stable isotopes (12C and 13C) isotopes are then counted (Lian and Roberts, 2006). The AMS age is then determined by the comparison of the ratio to that of a known ^{14}C isotope (Lian and Roberts, 2006).

3.8.1.1. Limitations

The contamination of samples may occur which could cause a varying difference between the bulk sediment of the radiocarbon dating and that of the proxy climate indicator (Brown et al., 1989). Humic acids, organic decay products and calcium carbonate may be carried downwards and could contaminate the underlying sediment (Brown et al., 1989). With the fluctuations in atmospheric ^{14}C it is important to note that radiocarbon dating may be precise and at the same time a single radiocarbon date may represent a range of possible calendar

dates (Brown et al., 1989). It is important to understand that radiocarbon dates cannot be directly compared to calendar years (Anderson et al., 2007).

3.8.1.2. Assumptions

The contamination of samples may occur which could cause a varying difference between the bulk sediment of the radiocarbon dating and that of the proxy climate indicator (Brown et al., 1989). Humic acids, organic decay products and calcium carbonate may be carried downwards and could contaminate the underlying sediment (Anderson et al., 2007). With the fluctuations in atmospheric ^{14}C it is important to note that radiocarbon dating may hinder precision and a single radiocarbon date may represent a range of possible calendar dates (Anderson et al., 2007). It is important to understand that radiocarbon dates cannot be directly compared to calendar years (Anderson et al., 2007).

3.8.1.3. Sources of Error

These include contamination which is the addition of older or younger carbon to the sample material and if unquantified this will result in the dates being aberrant (Pessendra et al., 2001). Contamination could occur prior to field sampling in the case where in peat or solid profile the downward penetration of roots or the infiltration of younger humic acids dissolved in water can introduce younger material to older horizons resulting in younger ages (Pessendra et al., 2001). Bioturbation is another way in a lake or a pond where contamination may occur where the disturbance of the sediment is caused by the organisms on the lake bed and causes a downward movement of younger sediments (Pessendra et al., 2001). Contamination can occur during field sampling or in the laboratory where fungal growth may occur during sample storage or modern contamination by dust or skin (Pessendra et al., 2001). The laboratory procedure in the radiocarbon laboratories employs physical or chemical pretreatments to remove these contaminants so an error is kept to a minimum (Pessendra et al., 2001). Other sources of error include isotopic fractionation where carbon occurs in ^{12}C, ^{13}C and ^{14}C Marine reservoir effects and long-term variations in ^{14}C production (Pessendra et al., 2001).

3.8.1.4. Application of pollen for ^{14}C

The study by Long et al 1992, used pollen which is known to be the most abundant plant fossil which is adequately preserved. As typical pollen grains range from 0.01 to 0.2 $\times 10^{-6}$ g at least 10^2 to 10^3 grains depending on their species can be used for an acceptable AMS ^{14}C date (Long et al 1992). But with the development of AMS technology the amount of carbon

needed has decreased to 100-200µg without compromising the precision of the date hence the practicality of using manual pollen isolation was tested (Long et al 1992). The study concluded that macrofossils like wood fragments, pinecones, or even charcoal is not always present in core material but microfossils like pollen grains are present and in a quantity sufficient for AMS dating (Long et al 1992). Hence pure pollen has the potential to provide a valuable approach to presenting high confidence dates to botanical changes which can be observed from pollen analysis (Long et al 1992).

3.9. Sedimentary charcoal

Iversen (1941) was the first to quantify charcoal fragments found in pollen preservations and concluded the fire history of various sites relating to vegetation history and human settlement. The first time possibility of using charcoal analysis as a palaeoecological discipline was first recognized by Santa in 1961 whilst working in North Africa where new observation methods using reflected microscopy allowed for the development of charcoal analysis (Figueiral and Mosbrugger, 2000). Only after the 60's others decide to follow Iversen which led to Waddington (1969) who developed how particle area within size classes is measured. Swain (1973) went on to provide evidence that explains that the charcoal preserved within sediments resembles fire history and has the potential to be reconstructed. This evidence paved the way for other studies (Clark, 1984). At present, there are two domains of research approaches that are developed with respect to the source of material. The source of the material can stem from archaeological horizons or soil profiles. Archaeological charcoal fragments are identified with the purpose of studying historical ecosystems and assessing the temporal variations and anthropogenic effects within these ecosystems (Figueiral and Mosbrugger, 2000). Charcoal is resistant to oxidation and microbial activity which makes it persistent on a geological time scale (Mooney and Tinner, 2011). Charcoal records are preserved in sedimentary records (water logged peat) as a proxy for past fire activity over long timescales (Mooney and Tinner. 2011). Charcoal can float for a period of time (hours, days, or weeks) before becoming waterlogged and can be transported vast distances within this time before being deposited and incorporated into the sediment which could be terrestrial, non-marine, near shore, shallow marine and deeper marine shelf sediments. Charcoal transportation is assumed that larger particles derive from a local source within a catchment and smaller particles are transported over longer distances (Finsinger and Tinner, 2005). This provides evidence that micro-charcoal fragments, which are not taxonomically

identifiable, may be windblown and found in terrestrial deep ocean deposits where a record of wildfire may have occurred (Scott, 2010).

Charcoal analysis may also be used to study the effects of fire on ecosystems by the reconstruction of forest fire occurrences (Finsinger and Tinner, 2005). Two fundamental characteristics of charcoal are essential in the identification of these fragments. The anatomy of the plant is preserved in the fragment which is a little bigger than a few microns in size and the fragment is relatively inert and easily preserved within a fossil record (Scott, 2010). The awareness of fire history has become apparent and the role of fire on the Holocene vegetation development and the importance of the carbon cycle in its relationship to climate change (Sarmaja-Korjonen, 1991; Carcaillet, 2001; Finsinger and Tinner, 2005). Fire history is the interpretation of charcoal and reconstructions are based on these measurements from lake sediment, peats or dune sediments from about 1000 sites globally (Carcaillet, 2001; Mooney and Tinner, 2011).

3.9.1. Wildfire charcoal

Charcoal produced from wildfires within vegetation are dependent on various factors. Micro charcoal which is a product of combustion of various types of living vegetation and litter may be lifted into the atmosphere by wind (Scott et al., 2010). Microscopic charcoal distribution is understood and is used to assess for history in the Quaternary and Recent(Scott et al., 2000). This is key to understanding the relationship between fire and climate change and the impact that man has on the environment. Macro charcoal (>1mm) charcoal production and dispersal is more complex (Whitlock and Larsen, 2001).

Source is an important principle in determining if charcoal is macroscopic or microscopic. When considering scrub, heathland or grassland much of the charcoal is produced from the incomplete combustion of dead vegetation and does not have a large build-up of surface fuels (Whitlock and Larsen, 2001). Grasslands are an example of a frequently burnt medium that provides little microscopic charcoal (Scott et al., 2010). In contrast, heathlands produce a large number of charcoal fragments generated from living vegetation (Scott et al., 2010). When compared to forests where crown fires often occur, large amounts of microcharcoal are produced in the smoke with very little macroscopic charcoal (Scott et al., 2010). The litter layer of forests presents surface fires that produce large amounts of charcoal and may be transported away from the fire site by means of water and some finer fractions may be windblown (Scott et al., 2010). Such transportation may result in taphonomic bias to final

charcoal assemblages. Charcoal may also occur in in peat forming systems where both living vegetation and peat have the potential in a fire to become charred, however, charred peat is recognized petrographically.

3.9.2. Macroscopic methods

Understanding the source (human or natural) fires, material (wood, leaves, grasses) and lastly transport (wind, water, distance) will allow for the use of macroscopic and microscopic charcoal for palaeoenvironmental reconstruction (Peters and Higuera 2007). Macroscopic charcoal is known to have a high density hence shortening travel distance to approximately 100 m (Carcaillet 2007; Peters and Higuera 2007). Microscopic charcoal on the contrary is known to travel a distance of over 100 km (Duffin *et al.,* 2008); Conedera *et al.,* 2009). Macrocharcoal is therefore a representative of local fire events and microcharocal is a representative of regional fire events (Duffin *et al.,* 2008); Conedera *et al.,* 2009).

3.9.2.1. Subsampling and processing

The intervals of subsampling are dependent on the rate of growth of the deposit, the degree of precision with which the sample will detect changes and the time that the researcher has for the project (Chevalier et al., 2020). Samples are sampled evenly across the sediment core at 1 cm layers. Subsamples are analysed in 1 cm^3 volume when the core is sufficiently solid (Aleman et al., 2013). The macroscopic charcoal was quantified with the use of a wet sieve (Finch et al., 2021). The method used to extract charcoal is the hydrochloric digestion described by Aleman et al. (2013). This method uses sodium hypochlorite (NaOCl) (digest cellulose) (Ekblom and Gillson 2010) and sodium hexametaphosphate (NaPO3)6 (facilitate deflocculation) remove organic material from the fragments and minimize fragmentation (Oris et al., 2014, Reddad et al. 2013).

3.9.2.2. Charcoal counts

Charcoal counts are conducted under a stereomicroscope. This is often associated with a digital camera which is attached to the microscope. The camera aids in image analysis software to easily calculate the area, length and width of each particle. According to Carcaillet (2007) and Ali et al., (2009) macroscopic charcoal is defined as particles that are ≥150μm in diameter. Particles > 100 μm will be located closer to the fire source and particles < 100 μm will be located further from the fire source as understood by the Gaussian plume model by Whitlock and Larsen (2001). It should however be noted that different studies utilized different size categories.

3.9.2.3. Data representation

Macroscopic charcoal has been widely utilized by researchers such as Ekblom and Gillson (2010), Oris et al., (2014), Reddad et al., (2013). The data can be represented by Width Length Ratio (W/L), Charcoal estimation or fragment number and influx of charcoal (CHAR) (Aleman et al., 2013).

3.9.2.4. Width to Length ratio (W/L)

The Width to Length ratio is an important tool in charcoal analysis. This ratio indicates the biomass type in the sample, either woody or grassy (Aleman et al., 2013). If there is an increase in the ratio the representation will mean that the biomass is woody and if the ratio is low the biomass will be represented as grassy (Umbanhowar and McGrath 1998). The fuel type of a fire is also determined by the W/L ratio. If the W/L ratio is >0.5 the fuel type will be represented as woody and if the W/L ratio is <0.5 then the ratio will be represented as grassy (Umbanhowar and McGrath 1998; Aleman et al., 2013). The more blocky or square the charcoal fragment the more woody it appears and the more elongated and sharp the more grassy the fragment (Aleman et al., 2013).

3.9.2.5. Charcoal accumulation rate (CHAR)

The influx of charcoal is calculated by the number of charcoal fragments (CHARn, particles/cm^2/yr) and by the average surface area (CHARa mm^2/cm^2/yr) Aleman et al., 2013). The changes in charcoal influx, area or number of charcoal fragments will ultimately affect the CHAR values (Aleman et al., 2013).

CHAR was used by Higuera et al., (2009), Brossier et al., (2014) and Oris et al., (2014) to determine fire peak. The sedimentation rate presents a level of bias which is initially removed by means of interpolation. The CHAR value was reduced to CHAR interpolation which was later decomposed. This method is used to eliminate low frequency background signals. The CHAR background id subtracted from the CHAR interpolation to determine the CHAR peak (Higuera et al., 2009), Brossier et al., 2014) and Oris et al., 2014).

3.10. Conclusion

This chapter provides a background to the palaeotechniques used in this research. Both pollen and charcoal analysis have been discussed with regard to their advantages, limitations, methodology, data analysis and interpretation. Both OSL and AMS radiocarbon dating have been discussed to link chronology to these techniques.

CHAPTER FOUR: MATERIALS AND METHODS

4.1. Introduction

This chapter will include the research site and the receiving environment, which includes the description of the geology, catchment and land use. The vegetation indigenous to South Africa such as forests and grassland biomes are discussed with a particular focus on the Ocean Coastal belt biome and Subtropical Alluvial Forest subregion.

4.2. Study Area

4.2.1. Site description

Due to the lack of information available on South Lake Futululu, the information presented in this study is drawn primarily from Lake Futululu and Lake Eteza. South Lake Futululu (28°29'55.30"S, 32°13'17.70"E, 9 m a.m.s.l.) is one of several wetlands located on the southeastern periphery of the Mfolozi-Msunduze River floodplain and the eastern seaboard of South Africa, approximately 200 km north of Durban, KwaZulu-Natal. The three large lakes that occur on the Mfolozi floodplain periphery include Lake Eteza (southwest), Lake Futululu (north) and Lake St Lucia (northeast) (Figure 4.1) (Grenfell *et al.*,2009; Garden, 2008). Lake Futululu as described in Grenfell *et al*. (2010) presented historic imagery since 1937 which indicated areas of open water. South Lake Futululu is located 9 km from Lake Futululu which is a major blocked valley lake located in the Mfolozi catchment. The Mfolozi catchment is described as a steep hinterland whose headwaters originate in the Drakensberg Mountains at an altitude of 3000 m (Grenfell *et al*., 2009). There are two major tributaries that make up the Mfolozi River, namely the Black Mfolozi in the north (1500 m a.m.s.l.) and the White Mfolozi in the south (1620 m a.m.s.l.) (Grenfell *et al*. 2010). The two tributaries converge approximately 50 km west of the mouth of the Mfolozi River (Grenfell & Ellery, 2009). Lake Futululu owes its origin to a minor tributary of the northern Mfolozi floodplain boundary (Garden, 2008). The southern margin of the Futululu Valley is located on the Mfolozi floodplain, draining around 1.1 x 10^{-3} ha of the catchment (Grenfell *et al*., 2010). The Mfolozi is one of South Africa's largest floodplains, extending approximately 30 km from its head through to the foothills of the Lebombo Mountains and finally to its entry into the Indian Ocean south of Lake St Lucia.

The Mfolozi River flows eastward along the northern area of the floodplain a second river known as the Msunduze River flows along the southern margin which joins the Mfolozi River near its mouth (Grenfell *et al*., 2009). South Lake Futululu is approximately 18 km away from the east coast and is located directly on the floodplain of the Msunduze River which is a tributary of the Mfolozi River (Neumann *et al*., 2010). South Lake Futululu has a smaller tributary called the Mavuya River flowing through the most southern portion of the delineated wetland. The connectivity of the Mfolozi and the Msunduze River is predominantly due to the common mouth that both these rivers share. The Mfolozi catchment is estimated at between 9918 and 10 700 km^2 (Ngqulana *et al*., 2009). The Msunduze catchment is much smaller and is estimated to be 559 km^2 (Ngqulana *et al*., 2009). The Mfolozi has a history of severe flooding which tends to overflow across its floodplain directly into the Msunduze River depositing silt on land between the two rivers (Ngqulana *et al*., 2009). When the Mfolozi overflows the water pushes back up the Msunduze which flows into both South Lake Futululu and Lake Eteza (Neumann, *et al*., 2010).

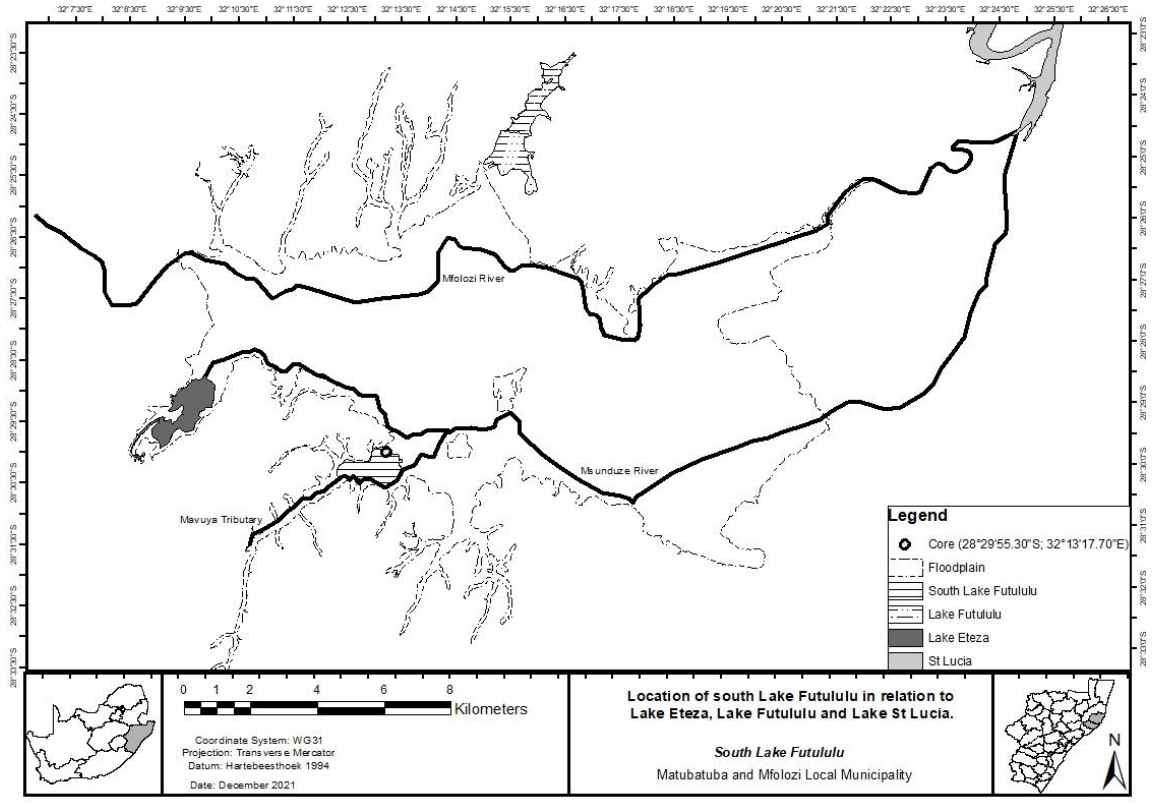

Figure 4.1 Location of south Lake Futululu in relation to Lake Eteza, Lake Futululu and Lake St Lucia.

Therefore the description of Lake Futululu and Lake Eteza will be utilized as supporting information when describing South Lake Futululu. Grenfell *et al*. (2010) classified Lake Futululu as a blocked valley lake. Blocked valley lakes are formed when tributaries are impounded by rapid deposition because of a large river and its associated floodplain (Grenfell *et al*., 2010). The barriers which hold back the water in Lake Futululu show evidence of floods that extended to an elevation of 17 m above sea level (amsl) (Grenfell *et al.,* 2010). South Lake Futululu is located 10 km from Lake Futululu and falls within the Msunduze flood zone. The formation of South Lake Futululu is likely due to the overflowing of the Mfolozi River pushing back into the Msunduze River which in turn pushes into the Mavuya River similarly observed in Lake Eteza.

The South Lake Futululu vegetation is described according to Mucina *et al.* (2006) as the Maputaland coastal plain ecoregion and includes the Mfolozi Floodplain. The Maputaland coastal plain of northern KwaZulu-Natal surrounds South Lake Futululu and is considered an important peat ecoregion within South Africa (Grundling *et al*., 1998). This coastal plain hosts the greatest area of peatland in the country (Grundling et al., 1998). South Lake Futululu is a southward-flowing drainage line that is positioned on the southern margin of the Mfolozi-Msunduze floodplain. This environment presents similar climatic characteristics to that of the Mfolozi coastal plain. According to Scott-Shaw & Escott (2011), the South Lake Futululu vegetation biome is described as Inland Azonal Vegetation and the ecoregion is best described as a Subtropical freshwater wetland. A Subtropical Freshwater Wetland environment generally supports a flat topography with an altitude that ranges between 0-1400 m and is calculated to be 246 ha in extent. Below describes the geology, climate, contemporary vegetation and human history of South Lake Futululu.

4.2.2. Geology- Sedimentology

The nature of the Mfolozi system appears to be highly affected by seasonal variable precipitation this is seen from evidence of clastic sediments that dominate the Mfolozi River floodplain. The upper Msunduze catchment is known to drain Mesozoic basalt as compared to the Mfolozi floodplain which is dominated by alluvium which can account for the ca. 60 cm of silt that was deposited in South Lake Futululu during the Domoina Cyclone in 1984 (Neumann *et al.,* 2010; Scott & Steenkamp, 1996).

The Mfolozi floodplain is underlain by Zululand Group siltstones and sandstones that were deposited between *ca.* 145-65 Ma in the Indian Ocean (Porat & Botha, 2008; Botha, 2021)). After the presence of an erosional hiatus, a second hiatus was observed which allowed a second marine transgression and the formation of the Maputaland Group at around *ca.* 50 Ma (Grenfell *et al*., 2010). The Maputaland regional geology is described to be a broad coastal plain that consists of Cenozoic to recent marine sediments, comprising of Berea and Muzi Formations (Botha, 2015; Watkeys, *et al*., 1993). Within the Maputaland area, a system of dune cordons is traced which mark past sea level stillstands of various ages. The coastal plain is recorded within the Plio-Pleistocene age, which ranges between 3 to 10 million years ago and is covered by sandy deposits forming high dune cordons along the coast. Particularly on the coast, young Quaternary sands which are derived from rocks of Cretaceous and Cenozoic origin occur in the form of sand dune cordons. Along the Zululand coast and within Maputaland these sand dunes are recorded to be high (Botha, 2015).

Where the Mfolozi River enters the coastal plain the floodplain widens, which may be associated to the formation of the alluvial fan at the floodplain head (Garden, 2008). Evidence shows that this alluvial fan building is not due to gradual ongoing channel aggradation but rather a sudden rapid aggradation which is associated with infrequent flooding events (Garden, 2008). The origin of the floodplain occurred from the rise in sea level, from 120 m below present sea level during the Last Glacial Maximum (18000 yr BP) (Ramsay, 1995). The sea level then rose steadily at 8 mm yr^{-1} until around *ca.* 8000 yr BP (Grenfell *et al*., 2009; Neumann *et al*., 2010). The sea level at around *ca.* 8000 yr BP reached its highest of +3.5 m, regressed at around *ca.* 3880 yr BP, and then remained stable for 500 years (Grenfell *et al*., 2009; Neumann *et al*., 2010).

Sediment accumulation along Lake Futululu and South Lake Futululu wetland Basin presented a low clastic sediment supply which allowed for the ideal environment for the formation of peat (Garden, 2008). The geomorphic evolution of South Lake Futululu can be described using Lake Eteza and Lake Futululu and later the results from this study. The geomorphic evolution of the Lake Futululu Valley is described from a phase of LGM incision, followed by deposition of an upwardly fining sand sequence, to peat accumulation 3980 yr BP caused by sediment accumulation along the Mfolozi River (Garden, 2008). Lake Eteza suggested the beginning of sedimentation at ca. 10200 cal yr BP with silty sandy soils and later becoming black clay (Neumann *et al*., 2010).

4.2.3. Climate

South Lake Futululu is situated between latitudes 28°S and 32°S and experiences moist sub-tropical coastal conditions with temperatures that often rise above 30°C in the summer (Delfino, 2002; Bate *et al.*, 2011). South Lake Futululu is classified as a Summer Rainfall Zone (SRZ) which is generated by the moist easterly winds and is associated with the South Indian Anticycone (Zhao *et al*., 2016). Humidity within the area is high as opposed to the moderately dry sub-tropical inland climate (Bate *et al.,* 2011). The relative humidity is recorded to have a daily mean of 70% and annual potential evapotranspiration is recorded to be an average of 1800 mm (Delfino, 2002; Grenfell *et al*., 2010).

An average annual rainfall of 1288 mm is recorded in the town of St Lucia which is located 12 km from Lake Futululu and 23 km from South Lake Futululu(Grenfell *et al*., 2010). The precipitation is abundant in the summer months of December to February however around 80% falls particularly between October to April (Delfino, 2002; Grenfell *et al*., 2010). The area presents an east-west rainfall gradient where an average of 1000 mm yr^{-1} (Patrick and Ellery, 2006). Winters are mild to warm with temperatures that average over 20°C (Delfino, 2002; Patrick and Ellery, 2006). The winter rainfalls are represented by troughs moving northeast along the coast which are less widespread and less intense (Bate *et al.,* 2011). The winter conditions are described to be dry as high pressures loom over the SRZ (Zhao *et al*., 2016).

The precipitation within south Lake Futululu is a result of thunderstorms and mid-latitude cyclonic activity (Bate *et al.,* 2011). The intensity of the thunderstorms leads to rapid overland flow, frequent peaks in stream hydrographs and sediment load capacity (Bate *et al.*, 2011). When these disturbances are blocked because of anticyclonic activity, particularly off the coast of KwaZulu-Natal, the continuous widespread rainfall causes extensive flooding inland (Bate *et al.,* 2011). Cyclone Domoina is one example of cyclonic activity that caused widespread flooding in 1984 (Mucina *et al.,* 2006; Grenfell *et* al., 2009; Cyrus *et al*., 2010).

4.3. Contemporary vegetation

4.3.1. Biomes

South Lake Futululu is surrounded by the Indian Ocean Coastal Belt (IOCB) biome and is located within the Inland Azonal Vegetation Biome (Mucina *et al.,* 2006; Scott-Shaw & Escott 2011). The Mfolozi floodplain is diverse and comprises of various vegetation units which include thickets, grasslands, forests and sensitive wetlands (Neumann *et al.* 2010).

South Lake Futululu is surrounded by the Maputaland Coastal Belt which has an extent of 35 km wide and forms part of the IOCB biome (Scott-Shaw & Escott 2011). The study area is located in the subtropical freshwater wetlands and Subtropical Alluvial vegetation ecoregions and forms part of the Inland Azonal Vegetation Biome (Fig. 2) (Scott-Shaw & Escott 2011). South Lake Futululu also presents vegetation from the Northern Coastal Forest and Swamp Forest ecoregion which forms part of the Afrotemperate, Subtropical and Azonal Forests Biome.

South Lake Futululu is represented by the IOCB biome as primary vegetation and encompasses Subtropical Freshwater wetlands, Afrotemperate, Subtropical and Azonal Forests and Subtropical Alluvial Biomes as secondary vegetation. The primary and secondary vegetation are linked spatially in an azonal manner (Mucina *et al.,* 2006). The ICOB biome portrays a tropical appearance of vegetation which is a result of a mixture of growth forms which include, trees, lianas and epiphytes which dominate the (zonal) forest vegetation of the region while grasses appear less dominant (Mucina *et al.,* 2006). Azonal vegetation is located in habitats that are formed in and around flowing and stagnant freshwater bodies which experience waterlogging and flooding that finally lead to the formation of specialized soils (Mucina *et al.,* 2006).

4.3.1.1. Biome Subtypes

South Lake Futululu is characterised by high-density vegetation cover which occurs in large areas between forested dunes and exotic plantations (Mutanga *et al*., 2012). The vegetation present within this area is dominated with reeds and sedges (Cyperaceae) along with various swamp forest taxa, and grasses to a lesser degree (*et al.,* 2006). The land use described is with the help of the information provided from Grundling and Grobler (2005) of the surrounding Maputaland Coastal Belt. The surrounding study area includes intensive in situ horticulture, water abstraction, agriculture, grazing and afforestation (Grundling and Grobler, 2005).

South Lake Futululu is riddled with vegetation that represents the Maputaland coastal belt which represents the coastal grassland thicket mosaic vegetation classification (Figure 4.2) (Mucina *et al.*, 2006). This vegetation unit comprises thickets, grasslands, timber plantations and cane fields (Mucina *et al.,* 2006). The most prominent types of vegetation are low shrubs, small trees and tall shrubs, woody climbers and herbs (Mucina *et al.,* 2006). The dominating taxa within this subtype is *Syzygium cordatum, Euclea natalensis, Ficus burtt-davyi, Searsianatalensis, Phoenix reclinata, Hyphaene coriacea* and various species of grasses.

Forests are an important vegetation unit for South Lake Futululu with small patches surrounding the wetland. Forests are known to be non-flammable because of their vegetation structure which presents unique physio-chemical properties of fuel that contain high moisture and low-fat content within the leaves (Mucina *et al.,* 2006). This vegetation unit is accompanied by vegetation that displays the northern Coastal Forest that occurs along the seaboards of the Indian Ocean in the KwaZulu-Natal province in Maputaland (Mucina *et al.,* 2006). This vegetation unit is present mostly on the sandy-loamy soils near St Lucia (northeast) and to the east near the Mfolozi swamps and along the coast (Neumann *et al*., 2010). The dominating taxa within this subtype are *Celtis gomphophylla, Coffea racemosa, Brachylaena discolor* and *Acacia kosiensis* (Mucina *et al.,* 2006).

In South Africa, swamp forests are regarded as highly threatened ecosystems. The dominating taxa within this subtype is namely *Barringtonia racemosa, Ficus spp., Macaranga capensis, Syzygium cordatum, Phoenix reclinata, Podocarpus falcatus* and ferns which occur frequently (Mucina *et al.,* 2006; Burger, 2009).

The subtropical freshwater wetland subtype is located on flat topography that houses reed, sedges, rushes and waterlogged meadows which are dominated by grasses This subtype includes small trees, geophytic herbs, succulent herbs and aquatic herbs (Mucina *et al.,* 2006). Dominant taxa within this subtype include *Phoenix reclinata, Hyphaene coriacea,* Cyperaceae (Mucina *et al.,* 2006). This ecoregion also includes various grasses and reeds and sedges which include *Typha capensis, Cyperus papyrus* and *Phragmites australis* (Mucina *et al*., 2006).

Subtropical Alluvial Vegetation is a key vegetation type surrounding South Lake Futululu (Fig. 2) (Mucina *et al.*, 2006). The area houses macrophytic vegetation, marginal reed belts and extensive flooded grasslands, herb-lands and riverine thickets (Mucina and Rutherford, 2006). Key taxa include Cyperaceae and Poaceae (Mucina *et al.,* 2006).

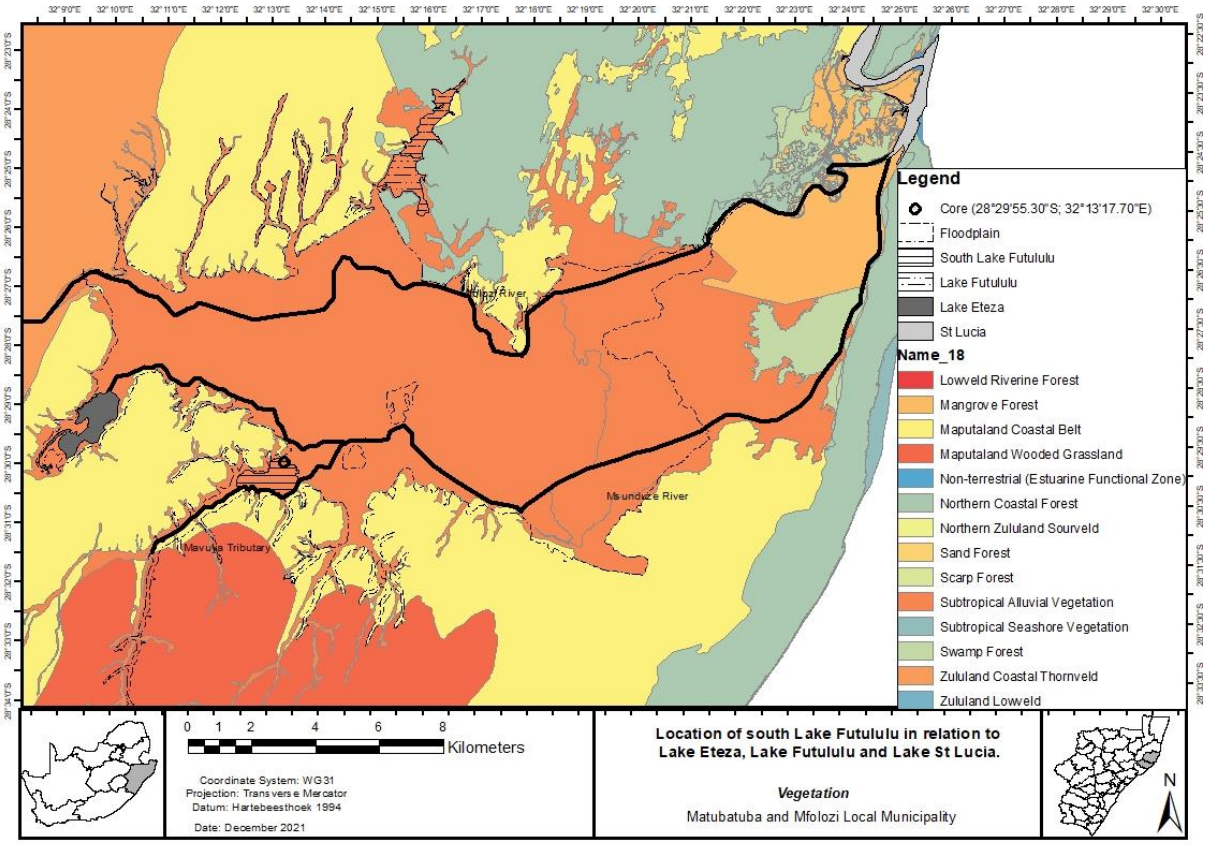

Figure 4.2 Vegetation within south Lake Futululu and the surrounding area (*Source: Mucina et al., 2006; Scott-Shaw and Escott, 2011*)

4.3.1.2. Precolonial Human History

The Mfolozi floodplain and the surrounding area have a history of human occupation. The Bantu farmers and pastoralists were attracted to KwaZulu–Natal because of the humid eastern coast of South Africa (Huffman, 2007). The province of KwaZulu-Natal is known as a prime region for mixed farming because of its permanent rivers, evenly distributed woodlands, grassland, and arable land (Huffman, 2007). Since around *ca.* 1650 cal years, there has been evidence of Early Iron Age pastoralists at Enkwazini which is close to Lake Eteza (Huffman, 2007). The evidence of the Iron Age within southern and eastern Africa is dated to extend over last the *ca.* 2000 years and identified the people as African speaking agriculturalists who used metal, from Later Stone Age Khoisan pastoralists (Huffman, 2007). Early Iron Age farmers practiced cultivation, particularly on the coastal dunes of KwaZulu-Natal *ca.* 950 cal. yr BP and mostly cultivated sorghum and millet (Huffman, 2007). Following the early Iron Age farmers and the secondary communities that followed were more productive in livestock grazing (Hall, 1984). This is supported by the species representation of the modern grassland of the Mfolozi Valley (Hall, 1984). The species representation indicates that the clearance of

fields gave way to the succession of cereal grasses which are most likely to become established in bare fields (Hall, 1984). The succession and presence of grass species were most likely maintained by the selective grazing of their livestock (Hall, 1984).

The discovery of evidence of the use of pottery proved that the Nguni farmers who were known for their herding moved into the coastal region at *ca.* 900 yr BP (Neumann *et al*., 2010; van der Merwe, 2014). The Africans arrived in KwaZulu-Natal during the 15th century, the Late Iron Age (Neumann *et al*., 2010; van der Merwe, 2014). The pre-European settlers may have been part of forest clearing for space, pastures and timber for cooking, house construction, domestic heating, and iron smelting (Neumann *et al*., 2010; van der Merwe, 2014). Human activities influenced coastal plains at both the St Lucia Estuary and the lower Mfolozi River (Bate *et al*., 2011).

4.3.2. Anthropogenic Impacts

In KwaZulu-Natal plantations of exotic trees such as Eucalyptus and Pines and sugar cane took over parts of the coastal forest since 1928 and it is observed that a further expansion took place in the 1940s and 1970s (Neumann, 2010). During the 1930s forest regulations and forced removals ensured that little permanent habituation occurred within the forest until the informal settlements in the 1980s (Nustad *et al*., 2013). Most of the households found along the Mfolozi floodplain were of sugarcane farmers, particularly in the south-eastern section of the Dukuduku forest known as Monzi (Nustad *et al*., 2013). This provided evidence that the transitional areas (forest to swamp) such as the riverbank is an important asset (Nustad *et al*., 2013). Evidence shows that during the invasion in the late 1980s settlers first moved to areas that provided water and good land for cultivation (Nustad *et al*., 2013). In the mid 1960s roads were formalized to the southern area of the Mfolozi (Nustad *et al*., 2013).

Both palaeoriver systems (Mfolozi and Msunduze) occupied a common mouth until human interference in the early 1950s (Bate *et al*., 2011). In 1952, the Mfolozi River was given an artificial mouth with the absence of the Mfolozi River flood and tidal basin scour effect, therefore dredging became a perennial activity (Bates *et al*., 2011). In the late 1970s a canal from the Mfolozi River to the estuary was built to allow excess water into the estuary system (Nustad *et al*., 2013). During the late 1980s, a high influx of people appeared to be present after the two major tropical cyclones. These cyclones shifted the Mfolozi River to its southern course and in 1988 the river moved back to its original channel (Nustad *et al*.,

2013). This opened up new areas for small-scale agricultural farmers in the late 1980s which supported the influx of people into the area (Nustad *et al*., 2013).

4.3.2.1. Recent Landuse Management

The study site presents an ecology much described by the above vegetation units. According to the spatial data majority of the Mfolozi catchment is described as natural vegetation, particularly in areas that fall within the Mfolozi-Hhluhluwe Nature Reserve (Grenfell *et al*., 2009). South Lake forms part of the Eteza Nature Reserve corridor which is classified as natural vegetation however this area is surrounded by plantations and cultivation (Fig. 3) (SANBI & CSIR, 2010). This is made up of exotic vegetation namely, *Eucalyptus* and *Pinus* plantations and sugar cane fields. (Scott and Steenkamp, 1996). The remaining natural vegetation is categorised as 60% grassland, 15% natural forest and woodland and 21% thicket and bush (Grenfell *et al*., 2009). Apart from the natural vegetation less than a quarter of the catchment is categorised as agriculture and the majority is small-scale subsistence and commercial forest classifying this system as not pristine (Grenfell *et al*., 2009). Around 13% of the catchment has been degraded due to over-grazing or excessive use of resources (Grenfell *et al*., 2009). Degraded *Acacia* woodlands are located upstream of the Umfolozi catchment particularly in over-grazed areas (Neumann *et al*., 2010). Less than 1% is categorised as urban including major industrial centers belonging to Mtubatuba and Vryheid in the lower and upper sections of the catchment respectively (Grenfell *et al*., 2009). The ecology includes a surrounding vegetation environment which may be classified as both subsistence and commercial agriculture (Grenfell *et al*., 2009). Crops such as sugarcane, maize, bananas and various vegetables are cultivated within the floodplain (Grenfell *et al*., 2009).

According to a study done by Bate *et al*. (2011), the vegetation distribution within the Mfolozi catchment including Lake Futululu and Eteza was described and identified from aerial photographs. The aerial photography study indicated a pristine environment with large stands of reeds that were present on either side of the Mfolozi and Msunduzi river banks in the earliest imagery taken in 1937 (Bate *et al*., 2011). With time the imagery indicated isolated swamp forests which were observed to be disturbed particularly in 2011 (Bate *et al*., 2011). The flooding of the Msunduzi appeared to alter the distribution and cover of the swamp forest (Bate *et al*., 2011). The swamp forest vegetation appeared to be concentrated around the old Msunduzi River course (Bate *et al*., 2011). With time the swamp forest vegetation migrated southward and developed dense forests (Bate *et al*., 2011). The first

indication of agriculture in the imagery was observed in 1975 which continued to expand with time (Bate *et al*., 2011). With the expansion of agriculture, the swamp forest continued to spread south and encroach into Reeds (Bate *et al*., 2011). Reeds and sedges mosaicked with Cyperaceae and *Phragmites* species made up 34% (1118.3 ha) of the wetland vegetation observed in the imagery of 2006 (Garden, 2008; Bate *et al*., 2011). Imagery in 2006 also indicated that almost 9.1% of the land which was previously wetland vegetation was used for subsistence agriculture (Garden, 2008; Bate *et al*., 2011). On the banks of abandoned and active channel courses *Ficus trichopoda* was found (Bate *et al*., 2011). The grassland vegetation unit experienced a loss in grassland habitat which was observed as time passed throughout the Mfolozi floodplain (Weisser, 1978). It is however noted that presently the catchment is well populated with a great presence of erosion which leads to vast amounts of sediment being dumped into the Umfolozi floodplain. This is mostly due to settlements, overgrazing and poor cultivation practices in both commercial, small subsistence farming and forestry.

4.4. Methodology of the Study Site

Within the Methodology section, the following methods completed by Jamie Wood (Doctor of Philosophy candidate) included: core extraction, stratigraphy, Optical Stimulated Luminescence (OSL) Dating and Loss of Ignition (LOI).

4.4.1. Field Techniques

4.4.1.1. Core Extraction

A 4.78 cm sediment core (South Lake 1B- Section 1 & 2) was extracted from South Lake Futululu (28°29’55.3” S; 32°13’17.7” E) in November 2014 using a 76-mm diameter vibracorer (Figure 4.3). The core was extracted in an area of blocked-valley marsh, near the toe-end of the large alluvial fan deposit that was laid down during the 1984 Domoina floods (Lund, 1984). The core was housed in aluminum tubing and wrapped in cling wrap for transport back to the laboratory. Usually, the colour changes and physical appearances sediment core would be described in the field, however this could not be done because of the risk of light contamination so Optical Stimulated Luminescence (OSL) may be conducted on the core.

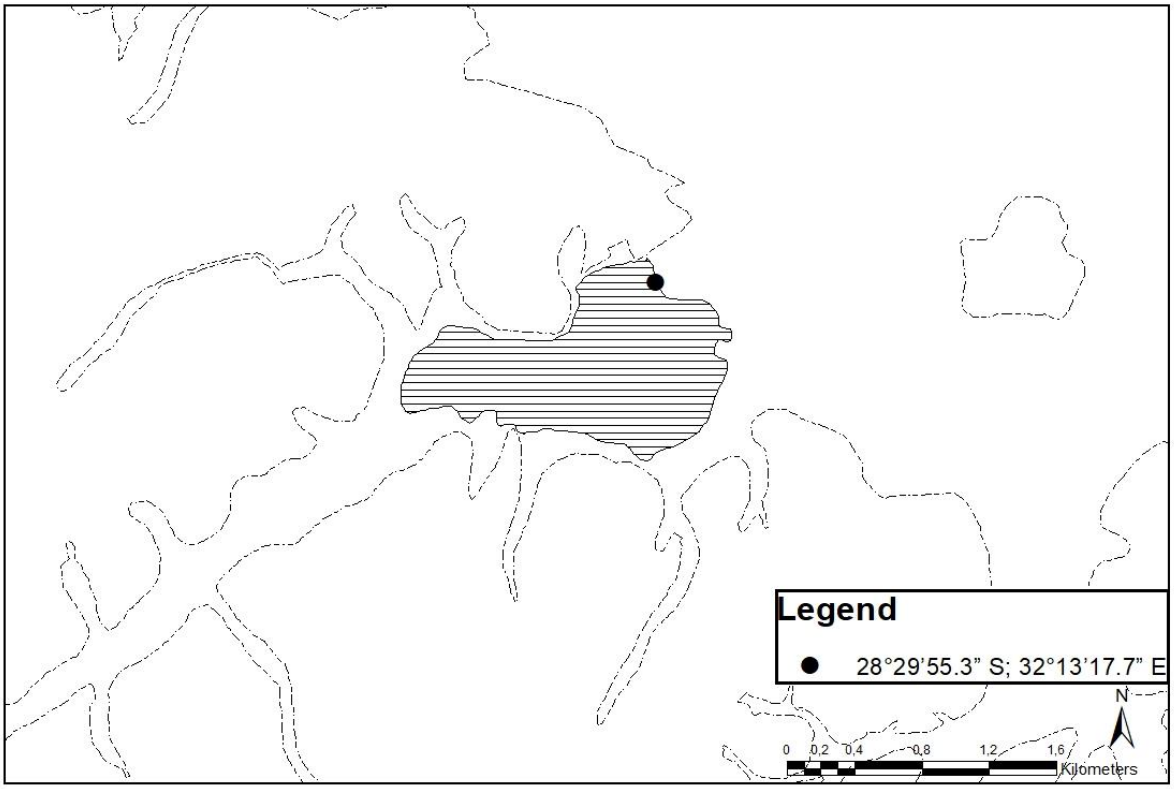

Figure 4.3 Location of the 4.78 cm sediment core extracted from South Lake Futululu

The core barrel was manually extracted from the vibracore (Figure 4.4) in an OSL preparation laboratory to avoid light contamination. The core was cut into 1 m lengths and thereafter cut on opposite sides using a carbide-tipped handheld circular saw which is modified with a cutting guide. Thereafter, the core was cleaned by gently scraping the material off the surface ensuring this was done parallel to the strata to avoid contamination using a scalpel or razor. Once the sediment core was cut open in the OSL laboratory the sediment was examined and described. Subsamples of 1 cm^3 were extracted at 10 cm intervals for pollen and charcoal analysis.

Along the Mfolozi-Msunduze floodplain plant reference material of 13 species was collected. These species were cut using a scalpel from the parent plant and stored in zip lock bags containing silica gel to prevent moisture accumulation within the specimen. These specimens were left unopened till they were processed at the University of KwaZulu-Natal using Appendix C: Procedure for preparing fossil pollen samples.

(a) (b)

Figure 4.4 (a) Using a vibracorer to extract a sediment core (b) from South Lake Futululu (*Source: Jamie Wood*)

4.4.2. Chronology

Five AMS and eighteen OSL subsamples were extracted to determine sedimentation rates. The five AMS samples were obtained from suitable basal and intermediate layers, which is based on the stratigraphy description for radiocarbon dating. Unidentified plant materials and bulk sediments which were in organic rich regions of the core were subsampled for AMS radiocarbon dating. The samples were sent to Beta Analytical Inc. In Miami Florida for analysis. The radiocarbon ages were calibrated using the southern hemisphere calibration model (SHCal20) dataset (Hogg *et al*., 2013).

The eighteen OSL samples were obtained from areas in the core that were described as silt and clays or fine/medium sand particles for OSL dating (Table 5.1 and Appendix Figure 1.1).

A Bayesian age-depth model for the sediment core was produced using Bacon (Blaauw and Christen, 2011). The age model was based on both AMS and OSL age determinations obtained from the core.

4.4.3. Loss of Ignition (LOI)

A total of 478 subsamples were taken at the University of Gloucestershire and further analysed along the length of the core for bulk density, moisture and organic content which is accomplished through loss of ignition (0).

4.4.4. Pollen analysis

A total of 47 samples for pollen were subsampled, labeled, and sealed in centrifuge tubes and transported from the University of Gloucestershire to the University of KwaZulu-Natal (Pietermaritzburg) and then refrigerated. To achieve relative pollen counts, a known quantity of pollen microsphere solution or spike (LacCore- Appendix D) was added to each sample before processing (Carcaillet *et al*., 2001). The spike was placed on a magnetic stirrer for an hour before to evenly distribute the microspheres within the solution. Pollen samples were chemically processed using standard palynological methods of sodium hydroxide (NaOH), hydrochloric acid (HCl), hydrofluoric acid (HF) digestion and acetolysis by means of acetic anhydride and sulphuric acid ($[CH_3CO]_2O$ and H_2SO_4) (Faegri and Iverson, 1989). Samples were rinsed multiple times and were stained using saffranine. The slides were mounted onto a semi-permanent microscope slide using Aquatex solution. Plant reference material of 13 species was collected from the Mfolozi-Msunduze floodplains and was chemically treated using standard HCl and NaOH digestion (Appendix C). Thereafter pollen reference slides were mounted, photographed, and archived. These species include *Grewia flavescens, Imperata cylindricum, Syzygium cordatum, Hibiscus tiliaeceus, Saccharum officinarum, Microsorum scolopendria, Cephalanthus natalensis, Sterculia murex, Passerina corymbosa, Peddiea africana, Crythira coffea, Turraeafloribunda* and *Buddleja racemosa*.

4.4.4.1. Microscopy

Identification and counts of pollen were achieved using regular traverses across the slide using a Leica DM750 light microscope at 400 x and 1000 x magnification. The sample size and the minimum pollen count were determined to allow for an accurate representation of pollen assemblages in all samples. A total of 48 samples were counted, with a minimum of 300 pollen grains counted for each sample. Taxonomic resolution was limited to the family level for most taxa due to the lack of available reference material. Pollen counts excluded indeterminable pollen grains which were broken folded or damaged. Pollen grains that were identified in clumps were counted as a single unit to avoid overrepresentation (Faegri and Iverson, 1989). The identification of pollen was accomplished using the UKZN reference

collection (Appendix B). This was aided using a local pollen reference collection of 13 species from the Mfolozi floodplain.

Palynomorphs were identified and grouped as regional (Coastland grassland thicket mosaic, Swamp forest and Coastal forest), or locally dominant and aquatic (Reed sedge wetland and Ubiquitous) taxa. These ecological groupings were based on nearby pollen records from lakes Eteza and Sibaya (Neumann *et al*., 2008; 2010).

Final pollen counts were entered into Microsoft Excel (2010) before being imported to Psimpoll (Bennett, 2005). This allowed the interpretation of the pollen data and their changes in pollen counts or percentages which were plotted against the interpolated ages from the age model.

The Constrained Incremental Sum of Squares (CONISS) cluster technique was used to define boundaries between the most distinguishable pollen zones. The CONISS algorithm was applied to the regional pollen data to produce a dendrogram (Bennett, 2005). The algorithm divided the pollen diagram into four zones namely: S1 (470-290 cm), S2 (290-120 cm), S3 (120-50 cm) and S4 (50-0 cm). These zones are primarily used for descriptive purposes to identify zones of homogenous pollen content (Grimm, 1987). Pollen samples were divided into zones using CONISS in Psimpoll. This is in the form of a dendrogram that illustrates the hierarchical relationship of clusters defined by the analysis (Fig. 5.3). The CONISS algorithm was applied to regional pollen data (Fig 5.3) to produce a dendrogram. The algorithm divided the pollen diagram into four zones which is based on the hierarchal arrangement of clusters within the dendrogram such that the second order splits were given precedence over the third order splits. The zonation process presents limitations where sections of the profile are not divided uniformly. The zonation profile was based on a combination of CONISS and visual interpretation.

Summary diagrams which include local, regional, charcoal, organic and moisture content were plotted along with their corresponding depths and using Craticula (C2) (Juggins, 2007).

4.4.5. Macroscopic charcoal analysis

All 47 samples were processed using the deflocculation and bleaching method as described by Aleman *et al*. (2013) and Carcaillet *et al*. (2001). This process is achieved by utilizing potassium hydroxide (KOH) for deflocculation and by KOH and sodium chloride (NaCl) for bleaching (Stevenson and Haberle, 2005; Mooney and Tinner, 2011).

A total of 47 samples for macroscopic charcoal were subsampled from the core. The charcoal particles were analysed under a Leica M60 stereomicroscope coupled with a digital camera and image analysis software (WinSeedle 2009). This software provided grouped fragment (Global) and individual fragment (Seedle) data. Seedle data was chosen for analysis and interpretation. This image analysis software provided Area, Volume, Average Straight Length, Width Length Ratio and Charcoal Concentration. Macroscopic charcoal counts were plotted against depth and interpolated ages from the age model.

The variables that were provided by the software that were used to calculate Charcoal Accumulation Rates (CHAR), using the age–depth model by number (CHAR in particles/cm^3/yr^{-1}) and surface area (CHAR in mm^2/cm^2/yr), charcoal area (mm^2); length (μm) and lastly sample average W/L ratio of charcoal particles (ratio). The W/L was analysed such that the fragments were categorised by their W/L calculation. As such grasses produced elongated particles and the W/L was interpreted as <0.5, whereas woody material produced charcoal that was visibly squarer and the W/L would be interpreted as >0.5 (Aleman *et al*., 2013). μm

CHAPTER FIVE: RESULTS

5.1. Stratigraphy

The profile was split into four units for ease of description during the subsampling process. Basal sediments 470-240 cm observed a clastic-rich sequence, which alternates between fine/medium sand and clay rich beds (Figure 5.1). Fine/Medium sand beds occupy the majority of this part of the profile. It is noted that some coarse sands are incorporated within the fine/medium sand beds, but again this represents a small proportion of the matrix. From 250-150 cm a pattern of peat/organic and fine clastic interlamination is observed. Clastic beds within the unit are dominated by silts and clays, some fine/medium sands are incorporated within their matrix. A bed formed solely of fine/medium sands is preserved at 210 cm. Between 140-50 cm the profile is organic rich, containing peat and well-preserved leaf and root litter. The fluctuation in organic content is created by clastic bands (formed by silts and clays) preserved amongst the peat/organic units occurring at 114 cm. A fine/medium sand bed is preserved between 40-50 cm. Between 30-0 cm the core is predominately characterised by silts and clays and remains organic poor throughout. On occasion the matrix supports fine sands, however, at these locations, silts and clays remain the dominant material. The profile stratigraphy indicated that there was less than 30% organic content making this section organic rich soil and not peat.

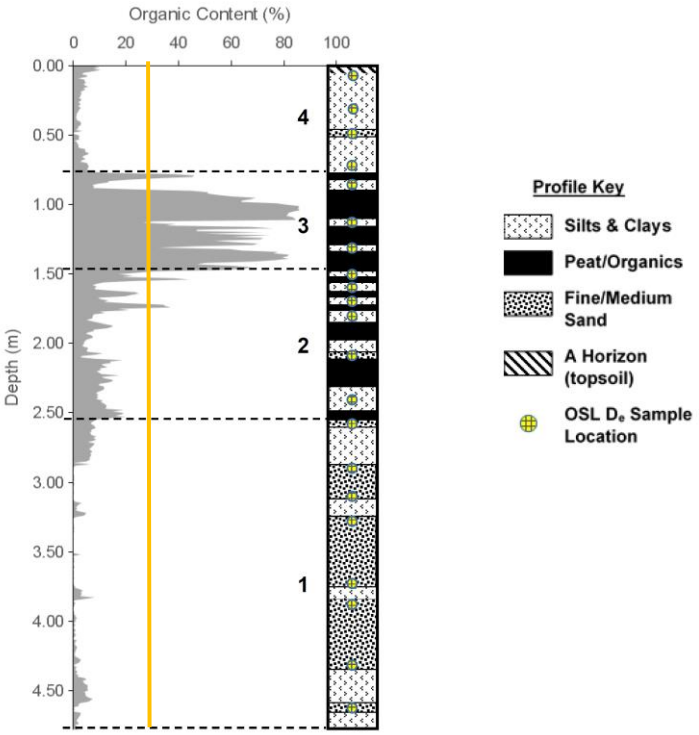

Figure 5.1. Profile stratigraphy description of the South Lake Futululu core *(Source: Jamie Wood)*

5.2. Chronology

The chronology of South Lake Futululu is based on five calibrated accelerator mass spectrometry (AMS) radiocarbon dates taken from unidentified plant material (Appendix 1, Section 1.3; Table 5.1 in addition to 18 Optically Stimulated Luminescence (OSL) age determinations from a previous study (Wood, 2020).

Table 5.1 AMS and OSL results for South Lake Futululu core. AMS results are calibrated using SHCal 20 (Hogg *et al.*, 2013).

Sample ID	Lab code	Method	Core depth (cm)	Grain fraction	^{14}C yr BP	Cal BP range	Material
South Lake AMS_4	Beta-526301	AMS	10		1833	1720±30	Bulk sediment
OSL1	GL15157	OSL	17	180-250		40±10	Quartz particle
OSL2	GL15158	OSL	32	180-250		50±10	Quartz particle

OSL3	GL15015	OSL	48	180-250		270±40	Quartz particle
OSL4	GL16099	OSL	72	5-15		1540±190	Quartz particle
OSL5	GL15016	OSL	85	5-15		2810±360	Quartz particle
South Lake AMS_2	Beta-469558	AMS	90		1470	1350±30	Macrofossil
South Lake AMS_1	Beta-446039	AMS	120		1251	1240±30	Macrofossil
OSL6	GL15020	OSL	158	5-15		3670±470	Quartz particle
OSL7	GL15021	OSL	168	5-15		3470±430	Quartz particle
South Lake AMS_3	Beta-485916	AMS	172		1603	1480±30	Macrofossil
OSL8	GL15022	OSL	181	5-15		1850±230	Quartz particle
OSL9	GL15023	OSL	209	180-250		2650±390	Quartz particle
OSL10	GL15024	OSL	258	180-250		3530±480	Quartz particle
South Lake AMS_5	Beta-526302	AMS	271		3779	4150±30	Bulk sediment
OSL11	GL15025	OSL	288	180-250		5240±730	Quartz particle
OSL12	GL15026	OSL	313	180-250		5820±830	Quartz particle
OSL13	GL15027	OSL	327	180-250		5770±810	Quartz particle
OSL14	GL15028	OSL	374	180-250		5740±810	Quartz particle
OSL15	GL15029	OSL	387	180-250		6390±910	Quartz particle
OSL16	GL15030	OSL	410	125-180		7150±1020	Quartz particle
OSL17	GL15031	OSL	433	125-180		7150±1020	Quartz particle
OSL18	GL15032	OSL	462	125-180		6590±940	Quartz particle

(OSL ages from Wood (2020) have been converted from ka to yr BP for ease of comparison with AMS results)

Basal sediments of the South Lake Futululu core are dated to ca. 7000 yr BP using OSL on quartz. A Bayesian age-depth model was developed based on OSL and AMS ages (Figure 5 1). Between 181 cm and 0 cm, multiple age reversals are present. These age reversals are

observed in fine grained particles from 1850 ± 230 to 1540±190 yr BP(181-72 cm) these layers may also represent past erosional events. The age reversals occur within areas of low organic and moisture content which gradually increased from 180 to 0 cm (Appendix 1; Section 1.2.1). The Bayesian Age model indicated four ages as outliers at depths of 10, 85, 158 and 168 cm.

The age-depth model shows three distinct changes in sedimentation, with an average sediment accumulation rate (SAR) of 0.060 cm/yr recorded between 470 and 259 cm depth (Table 5.2). The average SAR decreased to 0.031 cm/yr from 258 and 173 cm. From 172-86 cm the average SAR was 0.243 cm/yr. From 85 to 0 cm a lower average SAR of 0.083 cm/yr was recorded.

Table 5.2 Average sediment accumulation rates for South Lake Futululu.

Depth range (cm)	Age range (cal yr BP)	Average sediment accumulation rate (SAR) (cm/yr)
0 -85	Present – 1021	0.083
86-172	1047 - 1401	0.243
173-258	1406 - 4148	0.031
259-470	4182 – 7674	0.060

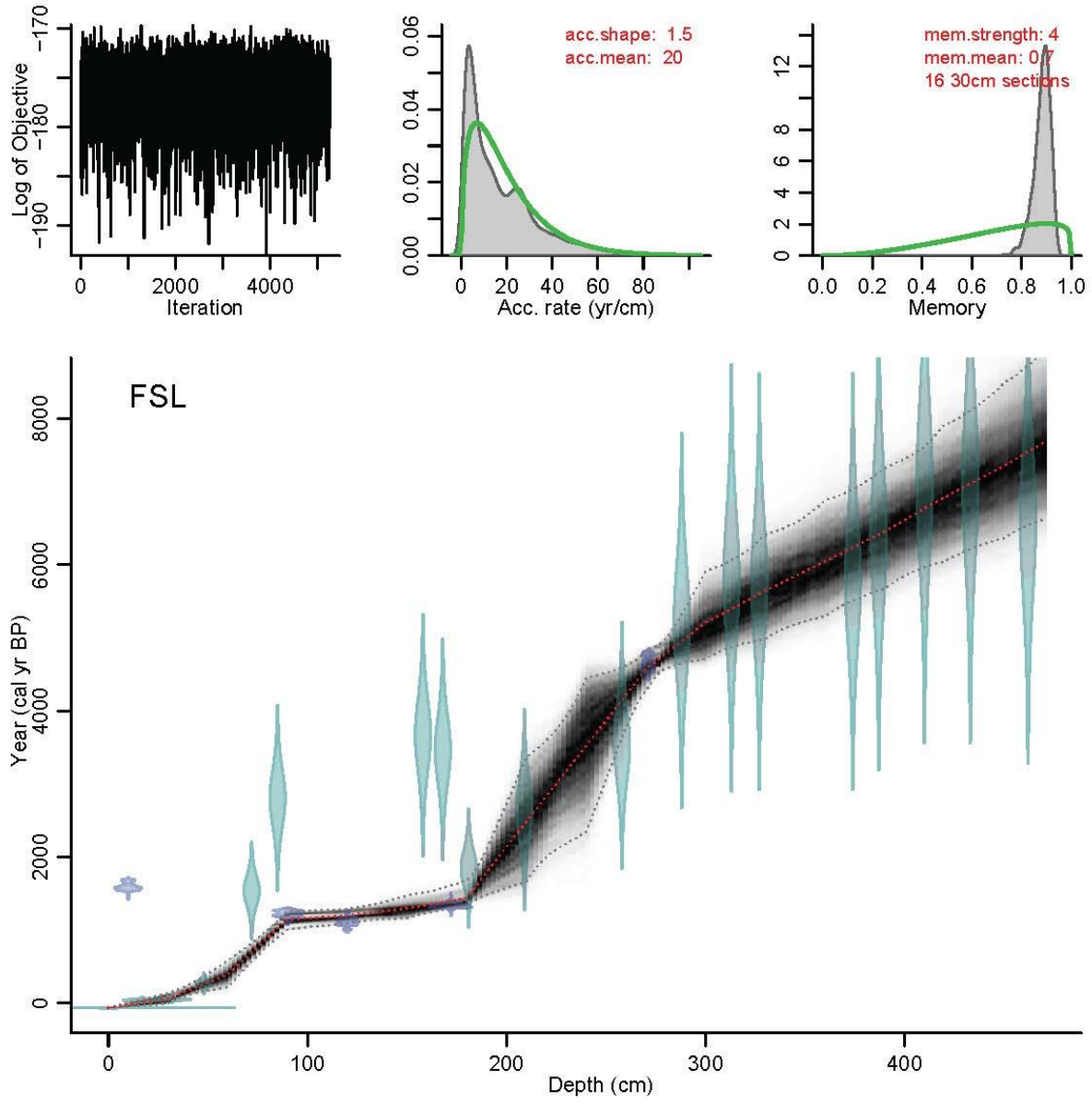

Figure 5.2 Bayesian age-depth model for South Lake Futululu with OSL (green wider error bars) and Radiocarbon dates (blues horter error bars).

5.3. Zonation

Constrained Incremental Sum of Squares (CONISS) was performed on the relative pollen dataset, yielding four stratigraphic zones for descriptive purposes: S1 (470-290 cm), S-2 (290-120 cm), S-3 (120-50 cm), S-4 (50-0 cm). The zones are determined using the agglomerative and hierarchal approach to create the clusters that are indicated on the dendrogram plotted alongside the pollen diagram (Figure 5.3 and Figure 5.4). The dendrogram allows for the appropriate zones to be delineated according to the analysis so that the pollen data may be described in an orderly fashion.

Zone S-1 was identified due to the low to no pollen counts present which displayed their own degrees of relative homogeneity. Within zone S-1 a hiatus was identified and manually inserted between depths 400 and 350 cm due to the low pollen preservation. The pollen zonation was applied to all stratigraphic diagrams.

5.4. Pollen and Charcoal analysis

Of the original 48 pollen samples, 10 were excluded as they did not meet the minimum count threshold of 300 pollen grains. A minimum count of 300 pollen grains was achieved in 16 of the 48 samples where preservation was relatively good, with a total of 53 pollen taxa recorded. However, between 400-350 cm, sediments presented low levels of pollen preservation with many barren samples thus a hiatus in pollen preservation was designated. The pollen taxa in the dataset were divided into four groups including coastal grassland thicket mosaic, swamp forest, coastal forest, and reed sedge wetland (Table 5.3 Figure 5.3 and Figure 5.4**Error! Reference source not found.**). Macrocharcoal data include W/L ratio, length, CHARn and CHARa from which inferences were made (Figure 5.5).

Table 5.3 Classification of pollen taxa according to regional (Coastal Grassland Thicket Mosaic, Coastal Forest, Swamp Forest and Reed Sedge wetlands) (*indicates rare taxa with total counts of <1%, L= Local pollen taxa).

Coastal Grassland Thicket Mosaic	**Swamp Forest**
ACANTHACEAE undiff.	APOCYNACEAE *Rauvolfia*
ASTERACEAE *Ambrosia*	EUPHORBIACEAE *Macaranga*
*ASTERACEAE *Artemisia**	LECYTHIDACEAE *Barringtonia*
*ASTERACEAE *Crassocephalum**	HIBISCUS undiff.
ASTERACEAE *Tubuliflorae*	MORACEAE *Ficus*
ASTERACEAE *Vernonia*	MYRICACEAE *Morella*
CHENO-AM-type undiff.	MYRTACEAE *Syzygium*
COMMELINACEAE undiff.	
ERICACEAE undiff.	
EUPHORBIACEAE undiff.	
GERANIACEAE undiff.*	**Coastal Forest**
NYCTAGINACEAE*	*ANACARDIACEAE *Rhus**
PALMAE *Hyphaene*	AQUIFOLIACEAE *Ilex*
POACEAE undiff.	*CELASTRACEAE *Maytenus**
*THYMELEACEAE *Passerina**	*COMBRETACEAE *Combretum**
THYMELEACEAE undiff.	*EBENACEAE *Euclea**
	EUPHORBIACEAE *Alcornea*
Reed Sedge Wetland	*EUPHORBIACEAE *Bridelia**
POLYGONUM **(L)**	*EUPHORBIACEAE *Cleistanthus**
CYPERACEAE undiff. **(L)**	EUPHORBIACEAE *Sapium*
GUNNERACEAE *Gunnera* **(L)**	FABACEAE undiff.
HALORAGACEAE undiff. **(L)**	MIMOSACEAE *Acacia*
IRIDACEAE undiff. **(L)**	MYRSINACEAE undiff.
LILIACEAE undiff. **(L)**	OLEACEAE *Olea**
NYMPHAEACEAE **(L)**	PODOCARPACEAE *Podocarpus*
TYPHACEAE *Typha* **(L)**	RUBIACEAE undiff.*
*LYCOPODIACEAE *Lycopodium jussiae** **(L)**	*STERCULIACEAE *Dombeya**
Ubiquitous	ULMACEAE *Celtis*
PTERIDOPHYTA Monoletes **(L)**	ULMACEAE *Trema*
PTERIDOPHYTA Triletes **(L)**	

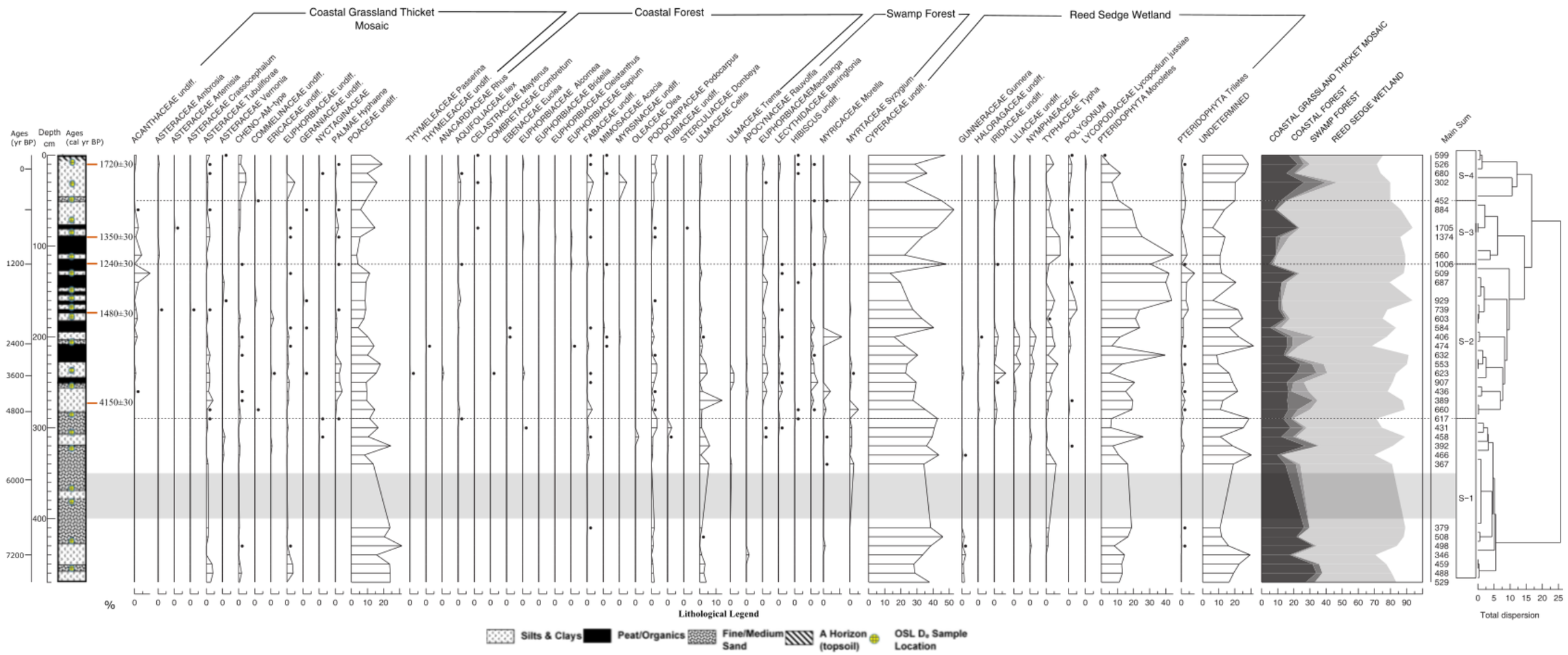

Figure 5.3 Pollen diagram plotted against a dual age-depth axis indicating the main sum and dendrogram with associated Troels Smith lithology. The age axis is based on the age-depth model presented in Fig. 5.1 based on both OSL and AMS ages of which their position are indicated on the diagram. The grey area on the diagram indicates the position of a low pollen preservation hiatus from 400-350 cm.

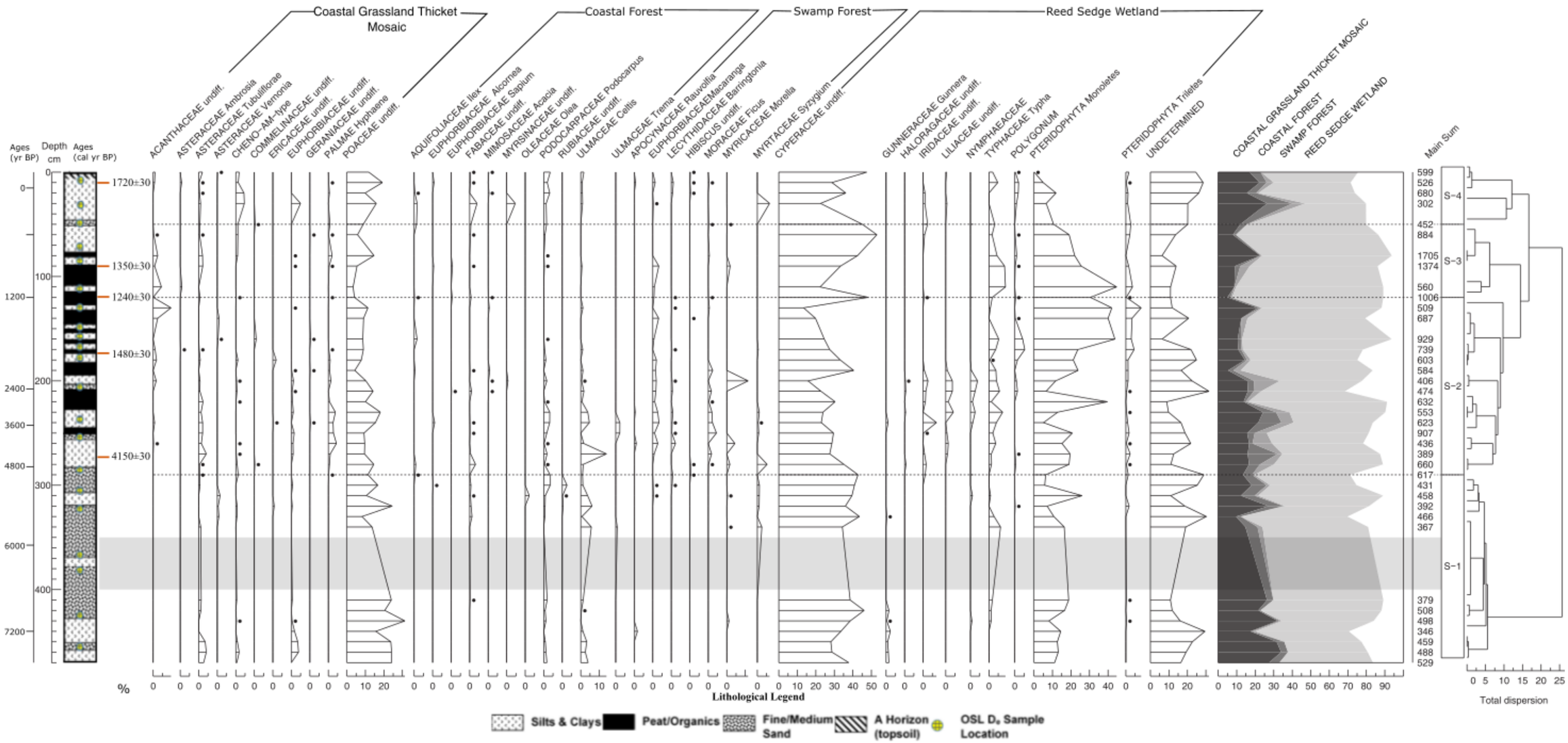

Figure 5.4 Pollen diagram excluding rare taxa (<1%) plotted against a dual age-depth axis indicating the main sum and dendrogram with associated Troels Smith lithology. The age axis is based on the age-depth model presented in Fig. 5.1 based on both OSL and AMS ages of which their position are indicated on the diagram. The grey area on the diagram indicates the position of a low pollen preservation hiatus from 400-350 cm.

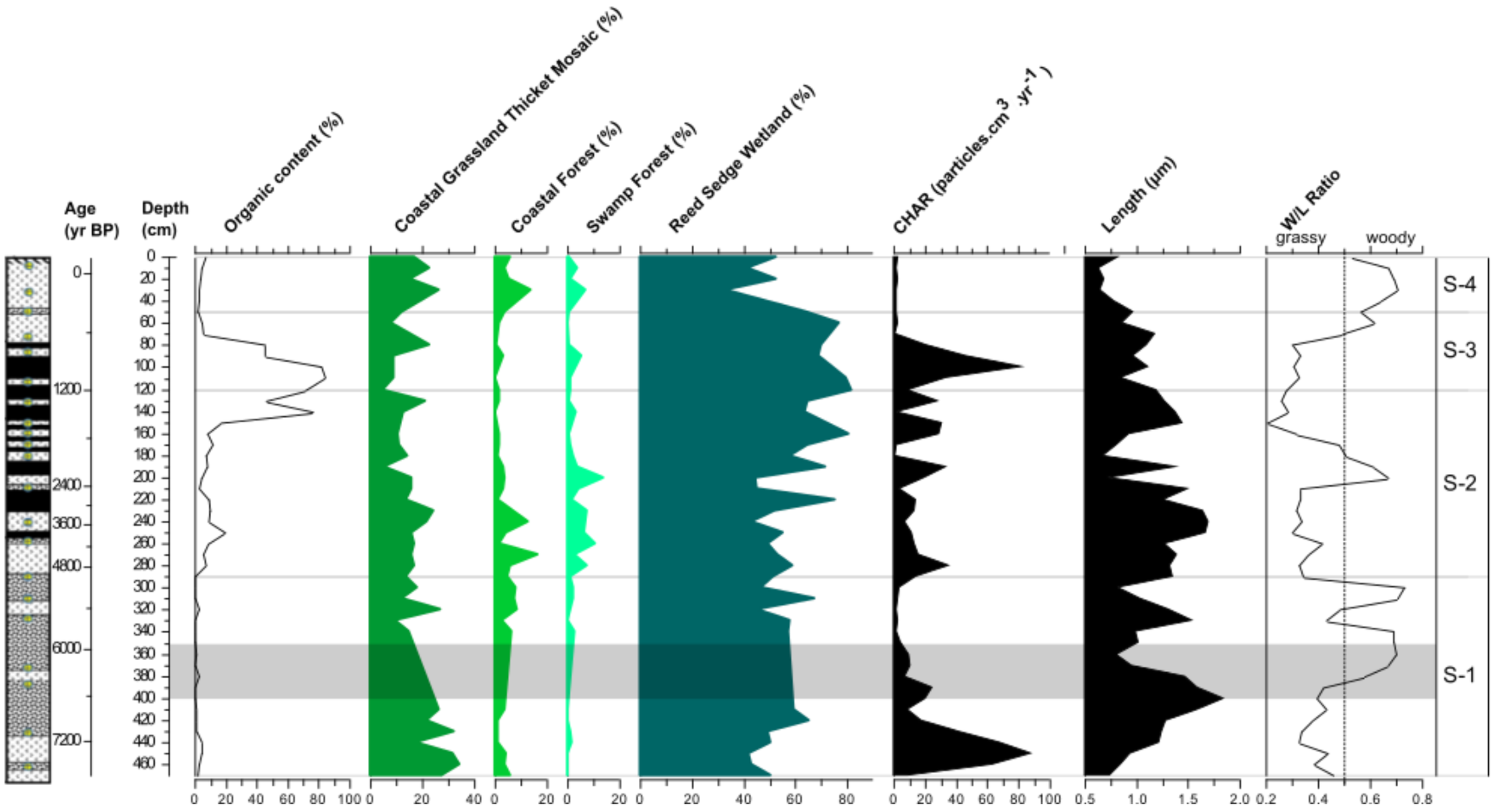

Figure 5.5 Summary diagram of organic content, pollen ecological groupings and macroscopic charcoal which includes $CHAR_n$, length and W/L plotted against a dual age-depth with associated Troels Smith lithology.. The age axis is based on the age-depth model presented in Fig. 5.1 is based on both OSL and AMS ages of which their position are indicated on the diagram. The grey area on the diagram indicates the position of a low pollen preservation hiatus from 400-350 cm. The dashed line represents the W/L cut off between predominantly woody (>0.5) and grassy (<0.5) fuel types.

5.4.1. Zone S-1 (470-290 cm; ca. 7600-4900 yr BP)

Within zone S-1 the record presents a hiatus in pollen preservation between ca. 6600 to 5900 yr BP (400 – 350 depth). As such, the preservation of pollen in this zone was not sufficient to provide a reliable pollen count within this time period, so data for this section of the record is absent.

The pollen signal in zone S-1 was dominated by the reed sedge wetland pollen types from *ca.* 7600-5300 yr BP (Figure 5.2; average 53%), with coastal grassland thicket mosaic subdominant (22%). Coastal forest (4%) and swamp forest (1%) types are poorly represented (Figure 5.3).

Within zone S-1 the general trend indicates an increase in reed sedge wetland abundance and a decrease in coastal grassland thicket mosaic. This is driven by changes in dominant pollen types Cyperaceae and Poaceae, which exhibit a parallel trend. Zone S-1 commences at *ca.* 7600 yr BP with a domination of Cyperaceae (37%) which continues to increase to 46% by *ca.* 7000 yr BP, and remaining high thereafter. The coastal grassland thicket mosaic is dominated by Poaceae (19%, peaking at 31%). Poaceae decreases throughout Zone S-1.

Within the reed sedge wetland grouping, monolete spores were dominant within zone S-1 (13%). Within the coastal forest group, *Podocarpus* appears within the profile *ca.* 7600 yr BP (2%) and proceeded to increase to 4% by *ca.* 5600 yr BP. *Celtis* becomes increasingly dominant towards the zone boundary, reaching 6% by *ca.* 5700 yr BP.

Within the coastal grassland thicket mosaic Tubuliflorae indicated a high of 4% at *ca.* 7600 yr BP and decreased to a low abundance of <1% at *ca.* 5300 yr BP. Euphorbiaceae is present at 4% at *ca.* 7600 yr BP however decreased to 1% at *ca.* 5500 yr BP within S-1. Cheno-AM-type presented an average of 1% within zone S-1 with a high of 2% at *ca.* 7600 yr BP and decreased to 1% at *ca.* 5000 yr BP. Zone S-1 proceeded to indicate an increase in the coastal grassland thicket mosaic ecological group at *ca.* 5900-5300 yr BP which presented the appearance of rare taxa such as *Vernonia*, Ericaceae, Nyctaginaceae *and Hyphaene* which were only indicated at low abundance (<1%).

The reed sedge wetland ecological group recorded the presence of *Gunnera* (average of 1%) evident between *ca.* 7600 and 5900 yr BP. Within zone S-1 the presence of *Typha* increased with time with the highest abundance (6%) recorded *ca.* 5700 yr BP and thereafter decreased in abundance to 1% *ca.* 5300 yr BP. The reed sedge wetland ecological group continued to

indicate the presence of rare occurring taxon such as Nymphaeaceae (>1%) which occurred only twice during zone S-1 only between *ca.* 7000 and 5300 yr BP and Iridaceae (>1%) which appeared only once *ca.* 5000 yr BP.

The presence of the coastal forest ecological group remains constant in zone S-1 however fluctuates between *ca.* 7600-5200 yr BP. The coastal forest ecological group presented an increase in zone S-1 between *ca.* 5600 and 5200 yr BP indicating the appearance of Fabaceae with a high of 1% which proceeded to decrease to <1%. The presence of Rubiaceae was indicated at a low 1% however increased to 3% between *ca.* 5400-5200 yr BP. The presence of *Olea (2%), Ilex, Alcornea* and *Trema* are all rare appearing taxon which presented low abundance (<1%) within zone S-1.

The swamp forest ecological group was the lowest representation within the S-1 zone which only appeared in the profile *ca.* 7200 yr BP. The group commenced with rare occurring taxon such as *Rauvolfia* (1%), *Morella* (1%), *Hibiscus* (<1%), *Macaranga* (<1%) and *Barringtonia* (1%) between *ca.* 7200-5000 yr BP. The presence of *Syzygium* remained constant within zone S-1 averaging 1% from *ca.* 5400 and 5200 yr BP. Within S-1 *Syzygium* (2%) peaked *ca.* 5700 yr BP and appeared to decrease with time in zone 1. Within zone S-1 the presence of *Barringtonia* averaged 1% between *ca.* 5200-5000 yr BP. The presence of *Macaranga* was indicated at a low <1% between *ca.* 5300-5200 yr BP.

The charcoal data within this zone presents the highest average CHAR of 24 particles. cm^2. yr. The highest CHAR was recorded at *ca.* 7300 yr BP (88 particles.cm^{-2}.yr^{-1}) and the lowest 2 particles. cm^3. yr^{-1} at *ca.* 5500 yr BP (Figure 5.4). The average W/L ratio is recorded within this zone (0.5). The highest W/L ratio recorded in zone S-1 was 0.7 at *ca.* 5200 yr BP and the lowest was 0.3 at *ca.* 7200 yr BP (Figure 5.4). This zone presented the highest average W/L ratio (0.7) within the entire core at *ca.* 5200 yr BP. The average particle length presented in this zone was recorded to be 1.1 μm. The longest particle length was recorded to be 1.5 μm *ca.* 6700 yr BP and the shortest 0.7 mm^2 *ca.* 7600 yr BP.

The hiatus within S-1 presented a higher average CHAR of 12 particles.cm^{-2}.yr^{-1}. The CHAR fluctuated slightly where the highest recorded CHAR peak was presented at *ca.* 6400 yr BP (24 particles. cm^3. yr^{-1} and the lowest at *ca.* 5900 yr BP (4 particles. cm^3. yr^{-1}) (Figure 5.4). The highest average W/L ratio of 0.7 recorded within the hiatus occurred at *ca.* 6000 yr BP. The charcoal particle lengths fluctuate drastically within the zone and present the highest average length (1.3 μm). The hiatus presents the longest length at *ca.* 6600 yr BP (1.8 μm)

and the shortest at *ca.* 6000 yr BP (0.8mm^2) (Figure 5.4). The hiatus presented the longest charcoal particle length (1.8 μm) within the entire core (Figure 5.4).

5.4.2. Zone S-2 (290-120 cm; ca. 4900-1200 yr BP)

Zone S-2 commenced with a clear indication of the presence of swamp forest and coastal forest between *ca.* 4700-3100 yr BP. The parallel trend between coastal grassland thicket mosaic and reed sedge wetlands is evident in zone S-2. The reed sedge ecological group dominated zone S-2 of the profile with an average of 60% of the profile this was followed by coastal grassland thicket mosaic (14%), swamp forest (5%) and coastal forest (4%).

Cyperaceae dominated zone S-2 with a high (28%) abundance. Poaceae was recorded to be the second most dominant taxon (10%) within zone S-2. Poaceae and Cyperaceae shared a parallel trend within zone S-2. Between *ca.* 4700-4200 yr BP Poaceae increased whereas Cyperaceae decreased. A similar trend was observed from *ca.* 3800-2800 yr BP where Poaceae was observed to decrease and Cyperaceae increased with time in zone 2. The trend continued from *ca.* 2400-1700 yr BP where Poaceae was observed to decrease while Cyperaceae increased. From *ca.* 1400-1300 yr BP Poaceae decreased whereas Cyperaceae increased. Finally, between *ca.* 1200-1100 yr BP Poaceae decreased and Cyperaceae increased.

The Monoletes within the reed sedge wetland ecological group and appeared to present an expected trend like that of Cyperaceae. The Monoletes dominated the ecological group with an overall average of (23%). The Monoletes presented the lowest (5%) abundance *ca.* 3500 yr BP and the highest (43%) abundance within the profile between 1300-1100 yr BP. Monoletes presented an increase in moving from zone S-1 to S-2 within zone S-2. Triletes were also present in zone S-2 which presented a constant trend between 8 - <1% between *ca.* 4700-1100 yr BP.

Within the swamp forest ecological group, the presence of *Syzygium* (5%), *Morella* (2%), *Ficus* (1%) and the rare occurring *Hibiscus* (<1%) appear. These taxa are present throughout zone S-2 apart from the rare presence of *Hibiscus*. The presence of *Macaranga* was indicated at *ca.* 4500 yr BP which fluctuated between 3%-<1% throughout zone S-2.

Around *ca.* 4700 yr BP the coastal forest ecological group presented a relatively high abundance (14%) of *Celtis,* which continued to fluctuate over time. With this fluctuation the

lowest (<1%) recorded abundance occurred *ca.* 2100 yr BP. *Podocarpus* (<1%), Fabaceae (1%) and *Ilex* (<1%) appeared by *ca.* 4700 yr BP.

From *ca.* 4200-3100 yr BP the coastal forest ecological group increased whereas the swamp forest decreased displaying a parallel trend. The swamp forest group presented the appearance of *Rauvolfia* (1%) and *Barringtonia* (2%) *ca.* 4200 yr BP which both appeared to decrease with time. Within the coastal forest ecological group from *ca.* 4200 yr BP the presence of the rare occurring taxa such as *Trema* (2%), *Alcornea* (1%), *Combretum* (<1%) and *Searsia* (1%) which all appeared for the first time within zone S-2. All the mentioned taxa are present throughout zone S-2 of the profile.

The exception of the parallel trend between the coastal forest and swamp forest occurred from *ca.* 2800-2100 yr BP where both the coastal forest and swamp forest indicated an opposite trend. The change in the parallel trend continued from *ca.* 1700-1400 yr BP where both coastal forest and swamp forest decreased. From *ca.* 2800-1400 yr BP the pollen signal remained constant. The coastal forest ecological group displayed the appearance of *Acacia* (1%), *Sapium* (<1), *Euclea* (<1%) and the rare occurring Myrsinaceae (1%).

From *ca.* 1300-1100 yr BP coastal forest and swamp forest continued a parallel trend. Where coastal forest increased swamp forest decreased and vice versa. From *ca.* 1300-1100 yr BP the highest abundance recorded for *Ilex* (1%) and *Sapium* (<1%) with zone S-2. The general trend from *ca.* 1300-1100 yr BP indicates a decrease in the abundance of swamp forest and coastal forest in zone S-2.

As mentioned above zone S-2 presented a visible increase in coastal forest taxa as compared to the previously mentioned zone S-1.

The coastal grassland thicket mosaic ecological group within zone S-2 indicates the presence of *Hyphaene* particularly *ca.* 4200 yr BP where the highest abundance (4%) occurs. It is evident from Figure 5.3 that *Hyphaene* appears to decrease between 4200-2100 cal yr BP. Within zone S2 Tubuliflorae presented a high abundance from *ca.* 4700-3100 yr BP. This period presented a general increase in coastal grassland thicket mosaic taxa. The presence of Acanthaceae (1%), Cheno-AM-type (1%), Commelinaceae (<1%), Euphorbiaceae (2%) and Geraniaceae (<1%) increased from *ca.* 4700-3100 yr BP and fluctuated with time. Within the reed sedge wetland ecological group, the presence of *Typha* occurred from *ca.* 4700-1100 yr BP where the highest abundance (7%) was recorded at *ca.* 3100 yr BP. The presence of

Holoragaceae (1%), Iridaceae (7%), Liliaceae (4%), Nympheaceae (2%) and *Polygonum* (1%) occurred from *ca.* 4500 yr BP. The rare occurrence of *Gunnera* (1%) was indicated *ca.* 3500 yr BP. From *ca.* 2100-1200 yr BP *Polygonum* indicated a high abundance (5%) and presented a general increase between *ca.* 1400-1100 cal yr BP. *Typha* indicated a decrease between 3100-1200 cal yr BP where the lowest abundance (<1%) was recorded *ca.* 1265-1233 yr BP. *Hyphaene* presented a similar trend where the lowest abundance (<1%) was recorded *ca.* 1100 yr BP

Zone S-2 indicated areas between *ca.* 4700-2400 yr BP where the W/L ratio ranged between 0.3-0.4. Within zone S-2 where the W/L ratio was <0.5, a high particle length and an increase in CHAR were observed. Between *ca.* 2100-1300 yr BP the W/L ratio increased to above 0.5 which also presented a decrease in particle length and CHAR. From *ca.* 1300-1100 yr BP the W/L ratio decreased to below 0.5 as such particle length increased and CHAR continued to increase.

Zone S-2 presented an average W/L ratio of 0.4 and was dominated by particles that fall below 0.5 however between *ca.* 2100-1300 yr BP a small number of fragments fall above the W/L ratio of 0.5 (Figure 5.4). The charcoal particle lengths fluctuate drastically within the zone and present a high average length of 1.3 μm. The longest particle length within Zone S-2 is recorded at *ca.* 3500 yr BP (1.7 μm) and the shortest at *ca.* 1400 yr BP (0.7 μm) (Figure 5.4).

5.4.3. Zone S-3 (120-50 cm; ca. 1100-280 yr BP)

Zone S-3 indicated a dominance in reed sedge wetland taxa with a high overall average (71%) followed by coastal grassland thicket mosaic (12%), coastal forest (2%) and swamp forest (1%). The peak in coastal grassland thicket mosaic and reed sedge wetlands that is seen in Figure 5.3 is attributed to the high abundance of Cyperaceae (53%) *ca.* 390 yr BP and Poaceae (15%) *ca.* 890 yr BP. Both Cyperaceae and Poaceae displayed a trend that increases between 1100-280 cal yr BP.

Within the reeds sedge wetland ecological group, Monoletes occurred within zone S-3 in high abundance (44%) and thereafter decreased from 1100-280 cal r BP. *Typha* was present (8%) from 1100 yr BP and proceeded to decrease thereafter. *Polygonum* (1%) and *Iridacea* (2%) were both present at *ca.* 1100-280 yr BP.

The coastal grassland thicket mosaic indicated the presence of Acanthaceae (4%), *Tubuliflorae* (2%), *Cheno-AM-type* (1%), *Hyphaene* (2%) at their highest abundance between *ca.* 1100-390 yr BP. The taxa such as Geraniaceae (<1%), Commelinaceae (<1%), *Artemisia* (<1%) and *Ambrosia* (1%) are rare and occur within zone S-3.

From 1140-890 yr BP coastal forest and swamp forest indicated an increase in abundance. The coastal forest ecological group indicated the presence of rare occurring taxa such as *Maytenus* (<1%), *Alcornea* (1%), *Cleistanthus* (1%), *Sapium* (1%), Fabaceae (1%), *Dombeya* (<1%) and *Celtis* (1%). The presence of *Podocarpus* increased with time where initially <1% was recorded at *ca.* 1140 yr BP with a relatively high abundance of 2% *ca.* 280 yr BP when compared to other zones. Within zone S-3 the swamp forest *Macaranga* presented a relatively high (3%) abundance *ca.* 1140 yr BP when compared to the rest of the profile. The rare occurring *Ficus* and *Morella* appeared for the first time within zone S-3 *ca.* 1140 yr BP which both decreased with time.

Zone S-3 presented the highest average CHAR (26 particles. cm^3. yr^{-1}). Between *ca.* 1100-900 yr BP W/L ratio remained below 0.5 whereas CHAR presented high values ranging between 20-81 particles. cm^3. yr^{-1} with a relative average length of 1 μm. Between *ca.* 600-200 yr BP the W/L ratio ranged above 0.5 whereas the CHAR decreased to an average of 2 particles. cm^3. yr^{-1} and an average length of 1 μm.

The CHAR fluctuated drastically within this zone where the highest CHAR of 81 particles. cm^3. yr^{-1} and the lowest 1 particles. cm^3. yr^{-1} (Figure 5.4). A low average W/L ratio was recorded in this zone (0.4). The highest W/L ratio within this zone is recorded *ca.* 400 yr BP (0.6) and the lowest *ca.* 900 yr BP (0.3) (Figure 5.4). The greatest length was recorded *ca.* 600 yr BP (1.2 μm) and the shortest length *ca.* 1100 yr BP (0.8 μm) (Figure 5.4).

5.4.4. Zone S-4 (50-0 cm; ca. 60 yr BP - present)

From *ca.* 170-0 yr BP reed sedge wetlands indicate the highest abundance (44%) coastal grassland thicket mosaic (24%) coastal forest (13%) and swamp forest (7%). Zone S-4 presented a parallel trend between Cyperaceae and Poaceae. From *ca.* 60 yr BP to present, Cyperaceae increased in abundance (22-36%) with a decrease in depth. Poaceae decreased in abundance with a decrease in depth (15-9%).

The coastal grassland thicket mosaic indicated an increase in Tubuliflorae (2%) which increased with the decrease in depth. Cheno-AM-type indicated a decrease with the decrease

in depth where a high abundance (5%) was recorded at the earlier section of the zone and proceeded to decrease to 1% toward the surface of the core. The presence of *Hyphaene* indicated a decrease with the decrease in depth. Taxa such as *Ambrosia* (1%), Euphorbiaceae (5%) and Nyctaginaceae (<1%) are rare occurring taxa within zone S-4. Except for Tubuliflorae, the general trend in the coastal grassland thicket mosaic ecological group presented a similar trend to that of Poaceae.

The reed sedge wetland ecological group presented a high abundance of Monoletes (7%) which decreased with time. Triletes were indicated within the zone which fluctuated between (1%-<1%). The presence of *Typha* presented a high 5% however decreased from 5700 cal yr BP. *Polygonum* was present throughout zone S-4 however fluctuated between a high abundance of 2% and a low of <1%. Taxa such as Iridaceae (1%), Liliaceae (1%) and *Lycopodium* (1%) are rare occurring taxa within zone S-4.

Zone S-4 indicates a significant peak in coastal and swamp forests like the increase in zone S-2. Within the coastal forest ecological group, Fabaceae indicated a high abundance (4%) dominating the ecological group which decreased from 60 cal yr BP (<1%). *Podocarpus* was present at low abundance (1%) earlier in the zone and increased from 280 cal yr BP (to 3%). *Celtis* presented a low abundance (1%) within zone S-4 which increased from 60 cal yr BP. Taxa such as *Combretum* (1%), *Alchornea* (1%), Myrsinaceae (4%) are all rare occurring taxa within zone S-4. The swamp forest ecological group indicated an increase in *Barringtonia* (1%) and *Macaranga* (1%) which increased from 170 cal yr BP. Taxa such as *Syzygium* (6%), *Ficus* (<1%) and *Rauvolfia* (1%) are all rare occurring taxa with zone S-4. The presence of *Hibiscus* was indicated at a low abundance (<1%) throughout the zone.

Zone S-4 indicated the lowest average CHAR (2 particles. cm^3. yr^{-1}) and particle length (0.7 μm). The highest CHAR (3 particles. cm^3. yr^{-1}) was indicated at present and the lowest (2 particles. cm^3. yr^{-1}) *ca.* 60 yr BP. An average particle length of 0.7 μm. The W/L ratio within this zone remained above 0.5. The W/L average within S-4 was recorded as 0.6. The highest W/L ratio (0.7) was indicated *ca.* 60 yr BP and the lowest (0.5) at present.

5.5. Summary

The pollen record which was divided into 4 zones included a hiatus. Zone S-1 presented low organic content. The pollen signal was dominated by the reed sedge wetland ecological group. Zone S-1 recorded a high Cyperaceae abundance as compared to the other taxa within the profile. The charcoal dataset indicated a low W/L ratio and an increase in CHAR,

however, particle length fluctuated for the remainder of the zone without a clear trend. Zone S-1 also included a hiatus which provided poor preservation of pollen and could not provide reliable pollen counts within the hiatus time period (Figure 5.4).

Zone S-2 commenced with a low organic content but increased over time. The pollen signal within this zone indicated a dominance in reed sedge wetlands however presented the introduction of coastal and swamp forest taxa. The spike in coastal and forest taxa fitted well with the charcoal W/L ratio. The W/L ratio of the charcoal fragments varied between 0.2 and >0.7. Where W/L ratios were <0.5 CHAR particles increased and where the W/L ratios were >0.5 CHAR particles decreased.

Zone S-3 indicated a similar high organic content and a strong presence of coastal and swamp forest taxa and reed sedge wetland ecological groups that dominated this zone. The charcoal presented areas where the W/L ratio <0.5 the CHAR values increased and where the W/L ratios were >0.5 the CHAR values decreased.

Zone S-4 indicated a dominance in reed sedge wetland pollen taxa. However, a strong presence of coastal and swamp forests was evident. The charcoal W/L ratio presented fragments only >0.5 within this zone.

CHAPTER SIX: DISCUSSION

Fossil pollen and macroscopic charcoal data will be used to produce a Holocene palaeoenvironmental reconstruction for the Mfolozi Floodplain, drawing on morphological, ecological and distributional information for key pollen taxa. This will be compared with previous palaeoenvironmental work conducted on the eastern coastline, and more broadly from the summer rainfall zone of southern Africa. In this chapter, the pollen data and charcoal data will be discussed and interpreted collectively.

6.1. Holocene palaeoenvironmental reconstruction for the Mfolozi Floodplain

6.1.1. Early reed sedge wetland phase (470-390 cm; ca. 7600 – 6600 yr BP)

The record commences at *ca.* 7600 yr BP during the early Holocene period at 470 cm in depth. It should be noted that the age model shows fairly good agreement between OSL and AMS dates between 7150±1020 to 4150±30 yr BP (433-271 cm). The pollen assemblage for this phase has a low diversity dominated by a few types which include Cyperaceae, Poaceae, Monolete ferns spores and Cheno/AM (in decreasing order of importance). The local signal inferred during this phase is reed-sedge wetland vegetation, which is dominated by Cyperaceae, Poaceae and Monolete ferns. Poaceae pollen in this assemblage may originate from surrounding grasslands or from the wetland environment, which often includes a mix of grasses. Regionally the pollen signal indicated the presence of *Celtis* and the low abundance of *Podocarpus.* The South Lake record inferred relatively dry conditions in the early parts of the record with the presence of Cheno/AM (**Table 6.1**) (Scott, 1999). This inference is supported by the low arboreal pollen signal. During the initial dry Early Holocene phase South Lake Futululu describes a wetland environment that favors the presence of wetland taxa and grassland taxa.

Several regional records show evidence of dry conditions during this period and the prevalence of open grassland vegetation. Between *ca.* 8000 and 7000 yr BP, relatively dry grassy ecosystems are inferred from the Lake Eteza record (IOCB Biome) located only 20 km south west of Lake Futululu (Neumann *et al.,* 2010). The Mfabeni record (IOCB Biome) located 88 km northwest of South Lake Futululu, also indicates the presence of grassy conditions during this time period (Finch and Hill, 2008). Baker *et al*. (2014) contradicted the trend observed in the South Lake Futululu record by describing the $\delta^{13}C$ signal of the

Mfabeni record as negative suggesting the return to swamp forest environments that favour humid and warm climatic conditions *ca.* 7000 yr BP. In the Mahwaqa record, 240 km south west of South Lake Futululu, Neumann et al. (2014) interpret Poaceae pollen as an indicator of warming of the atmosphere. Mahwaqa showed an increase in non-arboreal pollen taxa including Poaceae and Asteraceae between *ca.* 8500 and 4600 yr BP similar to that of South Lake Futululu between *ca.* 7600-6600 yr BP (Neumann *et al*., 2014). From *ca.* 7500 - 2500 yr BP, Norström et al. (2010) inferred drier conditions from the Braamhoek record (Grassland Biome) in the Eastern Free State. The Clarens record located 605 km west of South Lake Futululu, inferred relatively warm and dry conditions during the early Holocene with the presence of grasslands, similar to South Lake Futululu (Scott, 1989). This is also supported by the Makapansgat record located 650 km northwest of the South Lake Futululu record, which suggests drier regional conditions are inferred from increased grassy environments after *ca.* 8500 yr BP (Holmgren *et al.* 2003). The increased arid and temperature conditions are similarly displayed in the Tswaing Crater 530 km North in the province of Mpumalanga (Finch and Hill, 2008; Scott, 1990; Scott et al., 2003). The Rietvlei (Grassland Biome wetland in the Western Free State) record supported the South Lake Futululu record between 7600-6600 yr BP which indicated a decrease in moisture between *ca.* 8500 and 680 yr BP indicating a drier environment (Neumann *et al*., 2014).

The increase of temperature as seen in Rietvlei and Braamhoek may be linked to the global Holocene Thermal Maximum which is known to be associated with the orbitally forced summer insolation maximum (Neumann et al., 2014). Further evidence of dry conditions was documented at Mutale pollen record between *ca.* 10 000-6700 yr BP (Scott, 1987). The contradiction of the Mafadi record (high in altitude) in Lesotho inferred cold wet conditions during *ca.* 8140 and 7580 yr BP (Fitchett et al., 2016b). Later, the Mafadi record inferred similar conditions to South Lake Futululu with evidence of drier conditions between *ca.* 7520 and 6680 yr BP (Fitchett et al., 2016b). Chevalier and Chase (2015) supported the South Lake Futululu record between *ca.*, 7600-6600 yr BP indicating a dry event between *ca.* 7000 – 5000 yr BP from the central and eastern sites namely the Blydefontein, Equus Cave and Florisbad records. The northern sites which include the Tswaing Crater and Rietvlei Dam records indicate an increase in moisture during *ca.* 7600-6600 yr BP contradicting the South Lake Futululu Record (Chevalier and Chase, 2015). The Tate Vondo record inferred warm conditions at around *ca.* 7400 yr BP and later contradicted the South Lake Futululu record

(between 7600-6600 yr BP) indicating wet conditions after *ca.* 7400 to 2000 yr BP (Scott, 1987).

The low W/L values between *ca.* 7600 – 6600 yr BP suggest a predominantly grassy fuel type in South Lake Futululu. It is most likely that the majority of macroscopic charcoal particles (<1 μm) originated from local fires but we cannot exclude the possibility of long-distance transport, particularly in the smaller size classes (Ali et al., 2009). The values of CHAR between *ca.* 7600-7000 yr BP were higher than those in any of the following zones, mostly because around South Lake Futululu the grass cover is highly productive with respect to biomass which would result in greater amounts of charcoal particles present due to a greater fire frequency. Pollen preservation hiatus (400-350 cm; ca. 6600-5900 yr BP)

A pollen preservation hiatus was observed in the South Lake Futululu record between 6600-5900 yr BP. No pollen was located in this section of the profile due to poor preservation. The profile stratigraphy indicated that there was less than 30% organic content making this section organic rich soil and not peat. This is likely due to the medium fine sand sediments with very low organics in this section being non-conducive to pollen preservation. The lack of organics may reflect the dynamic nature of the wetland system being subject to fluvial activity and flooding events. This section of the record could not be utilised to infer vegetation history, thus we are reliant on other published records. Between *ca.* 6000 – 5000 yr BP, Lake Eteza recorded swamp forest conditions which were interpreted to be cool and moist (Neumann *et al*. 2010). The Lake Sibaya pollen record, located 130 km northeast of South Lake Futululu, indicated a shift from freshwater to swamp conditions during *ca.* 5500 yr BP (Neumann *et al.*, 2008). The Matitimani peat forming macrofossil record, located 180 km north east of South Lake Futululu, indicated a rise in sea level and humid conditions at *ca.* 6000 yr BP (Gabriel *et al*., 2017). A similar trend is supported by the Mfabeni pollen record which inferred warmer wetter conditions at 6000 yr BP indicating a forest expansion with the increase in arboreal pollen after *ca.* 6300 yr BP (Finch and Hill, 2008). The Mfabeni $\delta^{13}C$ record supported the establishment of swamp forests after *ca.* 5400 yr BP, suggesting humid and warm climatic conditions (Baker et al., 2014). Between *ca.* 6200-6000 yr BP a high occurrence of Rosaceae and *Podocarpus* pollen types was present within the Cathedral Peak record, located in Drakensberg 500 km south west of South Lake Futululu, which favoured moist conditions (Lodder, 2010). The Lake Eteza record indicated an increase in arboreal pollen taxa at *ca.* 6500 yr BP inferring moist subtropical conditions with high

precipitation (Neumann *et al*., 2010). The pollen preservation period infers a shift from dry to an increase in precipitation.

6.1.2. Mid Holocene Transition phase (380-290cm; ca. 5900-4900 yr BP)

This section of the profile presents an initial continuation of trends recorded in the early reed sedge wetland phase. The key difference within this phase is the appearance of coastal forest pollen (*Celtis*, Rubiaceae, *Podocarpus, Syzygium* and *Olea*) and swamp forest pollen (*Rauvolfia*, *Morella* and *Syzygium*) from *ca*. 5500 yr BP onwards. Between *ca.* 5200–4600 yr BP the South Lake Futululu indicated the presence of coastal forest type pollen taxa such as *Celtis*, Rubiaceae, *Podocarpus* and *Olea*, a decrease in Poaceae and a gradual increase in Cyperaceae which continues into the Mid to Late Holocene phase. These changes suggest a transition towards more moist conditions at South Lake Futululu, an inference supported by a decrease in Cheno/AM pollen. The shift during the latter part of the Early Holocene is portrayed during the Mid Holocene which transitions South Lake Futululu to a wetter type of wetland with a climate that favours reed sedge taxa moving away from the drier grassland taxa.

The Mfabeni, Lake Eteza and Lake Sibaya records indicated a high abundance of forest pollen taxa and low Poaceae abundance during the Mid Holocene. These records infer cooler, moist conditions with the presence of *Podocarpus* forest (Finch and Hill, 2008; Neumann *et al*., 2008; Neumann *et al*. 2010). However, the Matitimani, Braamhoek and Rietvlei records inferred drier conditions at around ca. 6000 – 4000 yr BP contradicting the South Lake Futululu record (Gabriel et al., 2017; Norström et al., 2008).

During *ca.* 6000 - 4300 yr BP the South Lake Futululu charcoal record indicates a predominantly woody fuel type (W/L ratio greater than 0.5) which may be due to the higher representation of woody vegetation in the surrounding landscape as indicated in the pollen recordThe CHAR within this period indicated a decrease in burned biomass which could be linked to wetter conditions. However inferring climatic changes from charcoal frequencies remains difficult as fire frequencies may not always be associated with drier conditions (Breman *et al*., 2011). The Matitimani record indicated low fire frequencies in vegetation that is dominated by peat swamp forest (Gabriel *et al*., 2007). This is supported in the South Lake Futululu record which indicates low CHAR values *ca.* 5000 yr BP

6.1.3. Mid to Late Holocene (280-120 cm; 4900-1200 yr BP)

At *ca.* 4900 yr BP South Lake Futululu record shows the appearance of a high diversity of regional taxa from coastal grassland thicket, coastal forest and swamp forest taxa entering the pollen assemblage, suggesting the onset of regionally wet climatic conditions. Locally, the record provides evidence of the establishment of swamp forests including *Rauvolfia, Macaranga, Barringtonia, Hibiscus, Ficus, Morella* and *Syzygium*. The coastal forest and swamp forest ecological groups within zone S-2 displayed a similar trend to that of the coastal grassland thicket mosaic and the reed sedge wetlands. The coastal forest and swamp forest share a parallel trend. Between ca. 4700-4500 yr BP the coastal forest ecological group fluctuated where an increase was observed whereas the swamp forest presented a decrease in abundance. This is later followed by the appearance of a greater diversity of reed sedge wetland taxa indicating a peak in local wetness from *ca.* 4200 to 1700 yr BP. The wet conditions displayed in the South Lake Futululu record and the possibility of a lacustrine environment may be evident with evidence of a few taxa observed during this period that favour open water.

The possibility of open water is supported by the presence of *Typha* within the South Lake Futululu record which represents the presence of fresh water and the presence of Nymphaeaceae which may have grown along freshwater pools or streams (Neumann, 2008). Following the peak in reed sedge wetland, swamp forest continues however with lower abundance than recorded earlier in this period. During the mid Holocene (from *ca.* 6500-3600 yr BP), Neumann *et al*. (2010) inferred high precipitation, high SST and a higher sea level from the Lake Eteza record. This implies that the general spread of moisture from north to south and the simultaneous development of the warmer Agulhas current may have together played a part in the increase in moisture at the coast in South Lake Futululu just like it may have in the Lake Eteza record (Partridge, 1997; Scott *et al*., 2012). A neoglacial event was reported between *ca.* 3200 – 2500 yr BP which resulted in a lowering sea level indicating cooler and drier conditions within this region (Grenfell *et al*., 2010).

Regionally, a diverse representation of coastal forest types is present in the South Lake Futululu record from *ca.* 4900-1400 yr BP. The key coastal forest taxa present in the record include Fabaceae, *Acacia*, Myrsinaceae, *Podocarpus*, *Celtis* and *Trema*. Both *Podocarpus* and *Celtis* record their highest abundances of the profile during this period. Similarly, the coastal grassland thicket mosaic is diversely represented. Notably, the pollen of *Hyphaene* is relatively abundant, probably associated with the lala palm *Hyphaene coriacea*, a

characteristic species from the coastal grassland thicket mosaic observed in parts of Maputaland today.

The expansion of coastal and swamp forest stands at South Lake Futululu is supported by the Lake Eteza pollen record which indicated similar trends between *ca.* 6500-3600 yr BP (Neumann *et al*., 2010). In the Lake Muzi record, both geochemical variations and the diversity of diatoms also inferred a wet environment between *ca.* 5000 and 4600 yr BP supporting the inference made in the South Lake Futululu record (Humphries *et al*., 2019). The Mfabeni pollen record indicated an increase in arboreal pollen at around *ca.* 4500 yr BP (Finch and Hill, 2008) supporting the inference of the South Lake Futululu record. The Umzimvubu, Muzi- Oos and Tswaing Crater records all inferred drier conditions between *ca.* 5500 – 3100 yr BP (Hahn *et al*., 2021; Grundling et al., 1998; Scott et al., 2003 and Scott 1990) contradicting the trend indicated at South Lake Futululu. The Clarens record indicated an expansion of grassland and inferred sub humid conditions with summer rains similar to the South Lake Futululu record (Scott, 1989). The Lake Eteza record indicated a strong presence of swamp, riverine and mangrove forest elements during *ca.* 1700-1500 yr BP similar to South Lake Futululu (Neumann et al., 2010). The Umzimvubu record reflected a similar trend to the South Lake Futululu record which indicated an increase in arboreal taxa such as *Podocarpus*, *Macaranga* and *Olea* during *ca.* 1500 yr BP (Hahn *et al*., 2021). The trend observed at Umzimvubu reflected sufficient rainfall which supports forests similar to that of Lake Futululu (Hahn *et al*., 2021). The Mfabeni record however contradicted the South Lake Futululu record suggesting dry conditions after *ca.* 2000 yr BP (Finch and Hill, 2008). The Transvaal records (, Moreletta Stream and Rietvlei) contradicting South Lake Futululu suggested dry conditions present during this period (Scott and Vogel, 1978; Finch and Hill, 2008).

Between *ca.* 4500 - 2000 yr BP the charcoal W/L ratio remained below 0.5 indicating grassy type vegetation. During this period, the low CHAR value suggests an increase in biomass burned within the area. The forest vegetation established within this period may have acted as a physical filter for wind transportation of charcoal affecting the charcoal record during this period (Aleman et al, 2013). Clark (1988) provided evidence that convection during fires causes turbulence which suspends particles within the combustion zone causing thermal buoyancy which provides the energy that is needed to lift particles above the canopy. Based on this evidence, we may assume that only small sized particles would be transported above

the forests and further deposited into the lake or rather deposited directly by runoff (Whitlock and Larsen 2001, Carcaillet et al., 2007).

The W/L ratio indicated woody type vegetation supporting the pollen record between *ca.* 2600 and 2000 yr BP. The CHAR value remained low indicating low burned biomass. The South Lake Futululu record indicated a slight elevation in the CHAR value between *ca.* 3200 and 2000 yr BP. Davies *et al* . (2022) explained that at around *ca.* 2000 yr BP in southern Africa the increased regional fire activity coincides with archaeological changes, particularly within the intensification of food production across the region which may have contributed to the woody type vegetation represented in the South Lake Futululu record. Olayoyan *et al*. (2022) indicated evidence of anthropogenic impacts in the form of pastoralism and farming from *ca.* 1900 to 1600 yr BP within the Savanna, Grassland, Fynbos and IOCB Biomes, and ~1450–1300 BP in the Nama-Karoo and Desert. Evidence of the low CHAR values may be indicative of low biomass burned due to the low available biomass as a result of anthropogenic activities.

From 1400 yr BP onwards the South Lake Futululu record presents the beginning of a retreat in coastal forest which continues into the next phase. Arboreal pollen taxa such as *Ilex*, Fabaceae, *Podocarpus*, *Celtis*, *Macaranga*, *Barringtonia*, *Hibiscus* and *Ficus* decrease during this period indicating forest retreat. The coastal forest taxa become less diverse and taxa such as *Ficus, Morella* and Liliaceae gradually disappear entirely from the record indicating a forest retreat and a decline in *Podocarpus,* which may be better dispersed than other arboreal pollen types (Coetzee, 1967; Hamilton, 1972; Scott et al., 1992). This period presents high percentages of Poaceae and Asteraceae along with the presence of Cheno-AM-type, *Typha,* and *Polygonum*. The South Lake Futululu record indicated less Asteraceae pollen and a higher abundance of Poaceae pollen in relation to Asteraceae which signifies a shift to more open dry vegetation. The occurrence of dry conditions after 1400 yr BP infers a return to cyclical climate conditions and provides clear evidence of the various climate fluctuations which is a well-known characteristic of the Holocene period (Baker *et al*., 2014).

The Lake Eteza record displayed a similar trend to that of South Lake Futululu indicating a high Poaceae and Asteraceae presence between 2500-1400 yr BP (Neumann *et al*., 2010). Grundling *et al*. (1998) supported the South Lake Futululu trend by describing the decrease in forest and dryland herbs from *ca.* 2450 yr BP. This trend may be due to climatic stress which may be attributed to drier conditions. which suggests the onset of warmer temperatures and

sub-humid conditions (Table 6.1). The Mdlanzi Swamp indicated a similar trend with high grasses and Monolete spores suggesting sandy wet depressions (Turner and Plater, 2004). The Matitimani record however contradicted the trends displayed in the South Lake Futululu record which indicated the emergence of swamp forest after *ca.* 1200 yr BP (Gabriel *et al*., 2017).

Between *ca.* 2000 - 1700 yr BP where the W/L ratio increased to greater than 0.5 (woody) and between *ca.* 1500 - 1200 yr BP the charcoal data indicated W/L ratios that ranged below 0.5 (grassy) where the Mid to Late Holocene phase indicated both grassy and woody type environments. The CHAR values during this period fluctuated indicating increased fire frequencies and intensities during this time. A similar trend is observed in the Umzimvubu record which indicated a dominance of smaller charred particles during *ca.* 1500 yr BP suggesting the reduction of burned biomass due to high fuel moisture (Hahn et al., 2021).

6.1.4. Coastal Forest retreat phase (110-50 cm; 1200-300 yr BP)

This phase demonstrates a continuation of a coastal forest retreat recorded in the previous period. Coastal forest taxa are present (*Dombeya, Acacia* and *Ilex*), however, their diversity and abundance were very low as compared with the Mid Holocene. Swamp forest taxa (*Barringtonia, Morella* and *Macaranga*) presented a similar trend indicating evidence of a retreat. During this coastal retreat phase, the area favours a shift to a wetland environment with the presence of wetland taxa similar to what is seen currently in certain parts of the area.

The charcoal data links well with the pollen in this phase. Between *ca.* 1100 and 600 yr BP the charcoal W/L ratios described a grassy environment (less than 0.5). The CHAR values at around *ca.* 1100 yr BP were the highest within the South Lake Futululu record. The high CHAR values correspond to the increase of charcoal flux which is linked to the type of biomass that was burned indicating a high burned biomass. This drastic increase may be attributed to the number of fire occurrences which is dependent on the availability of rainfall (Bond, 1997). High CHAR values combined with the W/L ratio of less than 0.5 provide evidence for the understanding of structural changes in forest disturbances and if CHAR was associated with land use changes (Aleman *et al*., 2013).

The Lake Sibaya charcoal record supported the high CHAR value within this period indicating evidence of high fuel type taxa like grassy vegetation rather than forest taxa which have a high leaf moisture content (Neumann *et al*., 2008). The Drakensberg record indicated around *ca.* 550 yr BP evidence of changes in fire regimes was evident which may be

associated with the arrival of early agro pastoralists (Finch *et al*., 2021). Both the Drakensberg and South Lake Futululu records indicate grass as the dominant fuel load during this time which provides evidence of a seasonal shift from high intensity late season lightning fires to low intensity early season anthropogenic fires (Finch *et al*., 2021). The record also describes low intensity fires as fires that are less damaging to woody vegetation hence making grass the dominant fuel load. Fire occurrence may be a major factor in charcoal accumulation as forests retreat and the environment shifts to grassland thicket. After *ca.* 600 yr BP the charcoal record indicated low CHAR values resulting in lower burned biomass. The W/L provides evidence of a shift to that of a woody environment after *ca.* 600 yr BP giving evidence to possible forest clearance. Neumann *et al.*(2008) suggested evidence of the Late Iron Age settlers during *ca.*850-350 yr BP, these W/L ratio changes coincide with the timing of the arrival of the settlers and provide the possibility that these changes could have been linked to human activity. In the Umzimvubu record evidence of erosion rates may provide evidence of the presence of increased anthropogenic impacts (Hahn *et al*., 2021).

The Umzimvubu record however indicated signs of human impacts after *ca.* 1500 yr BP with the presence of Asteraceae and the presence of Acanthaceae (Hahn *et al*., 2021). The Umzimvubu record indicated the presence of Poaceae pollen (>40 µm) at around *ca.* 1400 yr BP with the arrival of the Early Iron Age farmers in Mpondoland (Hahn *et al*., 2021). Neumann *et al*. (2010) interpreted the low arboreal taxa present after *ca.* 800 yr BP with the arrival of the Iron Age Settlers. Neumann *et al*. (2010) also indicated a decline in *Podocarpus* forest paving the way for the Iron Age cultivation and herding in open landscapes (Neumann et al., 2010). The low tree taxa and the spread of grass taxa are attributed to the combination of unfavorable climatic conditions and human pressure (Neumann et al., 2010). The Umzimvubu record indicated humid conditions between *ca.* 900 to 300 yr BP (Hahn *et al*., 2021). similar to the trend reflected at South Lake Futululu.

After *ca.* 600 yr BP the Umzimvubu record indicated the expansion of floodplains and swamps during a humid climate (Hahn et al., 2021). The Lake Eteza record however supported this trend indicating a decrease in arboreal and shrub taxa with an increase in Poaceae inferring a shift to drier conditions and a retreat of forest taxa (Neumann *et al*., 2008). The Mfabeni and Muzi-Oos record supported this trend suggesting the establishment of swamp forest vegetation after *ca.* 600 yr BP (Grundling *et al.* 1998). The Braamhoek and Tswaing records support the South Lake Futululu record by describing a similar environment which may be characterised as wetter conditions and a wetland type area (Norström *et al*.,

2008). Lake Muzi indicated wetter conditions during this period (Humphries *et al*., 2019). The Ladybird high altitude record (located west of South Lake Futululu) in Lesotho, inferred an increase in aridity between *ca.* 1200 to 900 yr BP supporting the trend observed in the South Lake Futululu record. (Norström *et al*., 2018). The Ladybird record later indicated an anomalous phase at around *ca.* 1100 yr BP when monsoon activities and SSTs declined to result in a shift to drier conditions which supported the South Lake Futululu record (Norström *et al*., 2018).

After *ca.* 600 yr BP, south Lake Futululu indicated a shift to a grassland type environment which is maintained in the Late Holocene phase.

6.1.5. Late Holocene Phase (40-0 cm; 300 yr BP -present)

The retreat of the forest continues within this phase indicating a very low abundance of arboreal pollen taxa. The coastal grassland thicket indicated a prominent Cheno/AM taxa. The coastal forest, swamp forest and reed sedge wetland taxa are not well represented within this phase with all contributing to the inferred dry conditions during this phase. The Late Holocene includes colonial activities described in Turner and Plater (2004) such as water management schemes, the excavation of canals and clearance of various riparian forest areas, commercial forestry (*Pinus*, *Casuarina* and *Eucalyptus*) and changes in the nature and extent of agriculture. The Late Holocene phase portrays an environment that is surrounded by plantations and cultivated land which is a result of human activities.

The presence of a grassland type environment between *ca.* 200 - 60 yr BP may be attributed to human control of grazing intensity. A high proportion of Cheno-AM-type, Asteraceae and Poaceae were present during *ca.* 40 yr BP section. From *ca.* 100 to the present day, arboreal taxa particularly pioneer taxa such as *Macaranga* and *Celtis* (Taylor and Marchant, 1994; Jolly et al., 1997; Hamilton, 1982; Friis, 1992; Beentje, 1994 and Finch *et al*., 2017), suggest characteristics of secondary regenerating forests, particularly in the recent portion of the record. These taxa may also be interpreted as disturbance indicators much like the trends observed in the Umzimvubu record *ca.* 800 yr BP (Hahn *et al*., 2021). The South Lake Futululu pollen record indicated recent landscape transformation which was observed on site and described in Grenfell *et al*. (2009). The upper parts of the catchment have been transformed to cultivate sugar cane and may contribute to the high presence of Poaceae within the recent portion of the South Lake Futululu record. A full understanding of human activity within the South Lake Futululu record may be lost due to the absence of present-day

sediments due to erosion that may have occurred during flooding events. There are many records of flooding in the area. One was described during 1918 resulting in the destruction of farms, another in 1925 and 1984 where the Domoina Cyclone caused widespread flooding in 1984 and resulted in the lower Mfolozi being established (Neumann *et al.,* 2010; Scott & Steenkamp, 1996) and later resulted in the channelization of the river.

The charcoal record between *ca.* 300 yr BP - present day indicated the W/L ratio of a woody nature (greater than 0.5). This supported the low presence of diverse arboreal taxa within this period. The CHAR value within this period remains low and indicates low fire frequencies. The shift to grasslands infers a drier climate during this period (**Table 6.1**). Nustad *et al*. (2013) indicated that large parts of the Dukuduku forest which borders Lake Futululu had been cleared by colonial invaders who have since taken over the area by a process described as an invasion from the 1880s. History describes that Zululand was open to settlers following the work of the Zululand Delimitation Commission between 1902 and 1904 (Nustad *et* al., 2013). The first known settlers arrived around 1911 after the Mfolozi flats were surveyed and allotted (Nustad *et al*., 2013). In 1916 a sugar mill was formalized which drove the expansion of the cultivation of sugarcane in the area (Nustad *et al*., 2013).

Between ca. 1000 yr BP and present the sediment accumulation was the highest of all the zones which may be attributed to a large sediment deposition due to the flooding events within the more recent period of the record (Grenfell et al., 2010). Low CHAR values were observed within the South Lake Futululu record within this period. This period indicated a W/L ratio of greater than 0.5 indicating woody vegetation (Plate 6.1).

Table 6.1 Summary of vegetation history and inferred palaeoenvironmental changes at south Lake Futululu.

Time Period (yr BP)	**Vegetation History**	**Inferred environmental conditions**
7600-6600	Locally, reed sedge wetland vegetation is inferred, dominated by Cyperaceae. Wetland may also have included prominent grasses, given the poor representation of other coastal	Dry conditions

	grassland/thicket taxa. Regional pollen signal is represented by *Celtis* and a low abundance of *Podocarpus*. Cheno/Am is prominent in the early part of this phase.	
6600-5900	Pollen preservation hiatus	The lack of preservation of pollen during this period inhibited the inference
5900-4900	Continuation of trends recorded in the early reed sedge wetland phase. But the key difference in the later part – from 5500 yr BP onwards we see the appearance of coastal forest (*Celtis*, Rubiaceae, *Podocarpus, Syzygium* and *Olea*) and swamp forest (*Rauvolfia, Morella* and *Syzygium*). Lower abundance of Cheno-Am.	Wetter conditions
4900-1200	High diversity of coastal grassland thicket taxa, coastal forest taxa, and swamp forest taxa entering the pollen assemblage, suggesting the onset of wet climatic conditions. Locally we see the establishment of swamp forests *Rauvolfia, Macaranga, Barringtonia, Hibiscus, Ficus, Morella* and *Syzygium.* Followed later by a greater diversity of reed/sedge wetland taxa like *Typha* and *Nymphaea.* Regionally a diverse representation of coastal	Peak in local wetness

	forest types is present. Key coastal forest taxa present in the record include Fabaceae, *Acacia,* Myrsinaceae, *Podocarpus*, *Celtis* and *Trema*. Both *Podocarpus* and *Celtis* record their highest abundances. From 1400 yr BP onwards the South Lake Futululu record presents the beginning of a retreat in coastal forest which continues into the next phase.	
1200-300	The coastal forest retreat provided the presence of coastal forest taxa (*Dombeya*, *Acacia* and *Ilex*) however their diversity and abundance were very low indicating the retreat. Charcoal data links well with the pollen data in this phase indicating the shift to a woody environment after *ca.* 600 yr BP giving evidence to possible forest clearance.	There are few to no signals to make a climate inference.
300-present	Forest retreat continued. Coastal grassland indicated a prominent high proportion of Cheno-AM-type, Asteraceae and Poaceae taxa. Both coastal forest, swamp forest and reed sedge wetland taxa are not well represented within this phase.	Dry conditions

  Early reed sedge wetland phase (470-390 cm; ca. 7600 – 6600 yr BP)	  Mid Holocene Transition phase (380-290cm; ca. 5900-4900 yr BP)	  Mid to Late Holocene (280-120 cm; 4900-1200 yr BP)	   Late Holocene Phase (110-0 cm; 1200 yr BP-present)

Plate 6.1 Descriptive images of the four phases within the South Futululu Record.

6.2. Limitations

Taphonomic studies of pollen preservation have been proven to serve as a useful tool in pollen studies. These help with interpreting a wider pollen analytical dataset despite the sites displaying characteristics suitable for palynological analysis (Tweddle and Edwards, 2010).

For the majority of the South, Lake Futululu record, pollen preservation was classified with good preservation, however, between *ca.* 7300 – 5000 yr BP was characterised with low organic content and resulted in poor preservation. For this reason, pollen data were obtained primarily in the upper part of the core and from the very bottom of the core where the organic content was higher. The areas with low preservation were either classified as the hiatus or indicated few pollen numbers which did not meet the minimum number of grains per sample.

Lower pollen preservation can be attributed to the lowering of the blocked valley lake water table, weathering, increased run-off, or a disturbance event that causes sediment mixing and results in the removal of organic pollen containing material. Low pollen preservation can be explained by the variation in the hydrology so that sediment may have become dry (Kirleis *et al*., 2011). In most cases, it is almost impossible to find the root cause of low pollen preservation but the evidence in this scenario is a result of a combination of factors. The low percentage of moisture and organic content could be explained by an increased run-off which possibly caused the mixing of sediment. This mixing would result in two problems which indicate that the section of the core is unreliable and that it presents low preservation quality within this section.

Pollen preservation combined with LOI data and the frequency of pteridophyte spores makes it possible to assess the reliability of the conventional pollen record although it is not possible to pinpoint the main cause of any changes in preservation. It is suggested by Tweddle and Edwards (2010) that the presence of Pteridophyta (Monoletes) spores is accompanied by areas that display significant levels of corrosion. This could be because Monolete spores are resistant to corrosion in the form of chemical oxidation, repeated wet and dry cycles and various other actions that entail bacteria and fungi (Tweddle and Edwards, 2010). In the area between *ca.* 6900 to 5600 yr BP, it is evident that there is a peak in Monolete spores and other pollen absent indicating the area of a hiatus. The South Lake Futululu record indicated low palynomorph diversity in some parts of the record (400-350 cm; *ca.* 6600-5900 yr BP) which may also be linked to preservation. Different pollen grains are preserved differently some are robust and some are delicate and easily destroyed. Triletes are often well

represented within the profile when compared to other palynomorphs, particularly in samples where the total sum of pollen grains is low indicating that these grains may have been destroyed.

The South Lake Futululu core represented a good variation of climatic changes and vegetation changes between 7500 and to present day. This sediment core indicated past flooding events and the indication of human inferences. It is important to understand that this study has contributed to the existing bodies of information and provides insight into the poorly studied Msunduze Floodplain. The South Lake Futululu record also experiences the possible loss of the uppermost sediments to recent flooding events. Since the record indicated a lack of exotic neophytes associated with human activity the support of flooding events may be a strong possibility.

The profile indicated a limited taxonomic resolution of pollen identification particularly for groups like Poaceae where a good taxonomic resolution would be useful to understand grassland dynamics. Progress in the identification of common pollen types such as Cyperaceae and Poaceae is slow and limits the identification of wetland and grassland dynamics. This would be useful to help with the separation of sugarcane from the record. The South Lake Futululu record presented a lack of unequivocal pollen markers for human activity such as *Zea Mays* and also more recent markers such as exotic neophytes (Pinus, Eucalyptus, Casuarina). At times the general lack of available markers is linked to taxonomic resolution as in the case of Poaceae and sugarcane.

The South Lake Futululu record acknowledges the differences in production and dispersal characteristics of pollen types for example Podocarpus and Poaceae which are wind pollinated and likely over represent the assemblage (Coetzee 1967; Hamilton 1972; Scott *et al.* 1992). It must be noted that in the South Lake Futululu record taxa such as grasses, sedges, and pteridophyte spores tend to be overrepresented, muting the regional pollen signal.

Conclusion

7.1. Key Findings

South Lake Futululu inferred dry conditions which shifted to wetter conditions during the early Holocene (*ca.* 7600 – 6600 yr BP). The Early Holocene indicated a high presence of reed sedge wetland with a presence of coastal grassland thicket locally and coastal forest regionally. The early Holocene (*ca.* 6600-5900 yr BP) also presented a section of the profile that can be described as a pollen preservation hiatus due to the lowest moisture and organics of the entire profile. The South Lake Futululu pollen record indicates vast fluctuations in the pollen assemblage observed within the core, reflecting a complex range of drivers of change including regional changes in climate and local changes in hydrology, fire or disturbance, and human activity.

The mid Holocene indicated some interesting highlights. These include a transition phase, during which coastal and swamp forest taxa appeared, indicating a shift to wetter conditions. Within this phase, coastal grasslands indicated lower Cheno/AM abundance supporting the shift to moist conditions. Thereafter, a high diversity of coastal grassland thickets, coastal forests and swamp forests enter the pollen assemblage. These suggest the onset of wet climatic conditions, an inference supported by several regional palaeoclimate records. Locally the establishment of swamp forest taxa is observed and later a greater diversity of reed sedge wetland taxa. This inferred a peak in local wetness between *ca.* 4200 to 1700 yr BP. Once this peak in local wetland taxa declines the appearance of swamp forests is evident however the abundance is not as high as in the earlier part of this phase. Regionally a diverse representation of coastal forest taxa is evident with key taxa such as *Podocarpus* and *Celtis* which recorded their highest abundance in the profile. Similarly, coastal grassland thicket mosaic is diversely represented with the characteristic genus *Hyphaene* which is relatively abundant. Later in this phase, another important highlight is observed of a coastal forest retreat which continues into the Late Holocene.

The Late Holocene presents the coastal forest retreat after *ca.* 1200 yr BP. This phase indicated the presence of coastal forest taxa however their diversity and abundance were very low. What is most interesting in this phase is that the charcoal data supports the pollen profile. The high CHAR values combined with the W/L ratio of less than 0.5 provide

evidence for the understanding of structural changes in forest disturbances which may be associated with land use changes. Neumann (2008) described the arrival of the Iron herders from central Africa to the eastern coasts of South Africa *ca*. 2000 yr BP who were likely to influence the change in landscape. Following the forest retreat to the present day, the record suggests dry conditions. This final phase continued with coastal forest retreat indicating very low abundance. The coastal grassland thicket indicated a prominent high abundance in Cheno/AM, suggesting dry conditions. Coastal forest, swamp forest and reed sedge wetland taxa were poorly represented within this phase. A full understanding of human activity within the South Lake Futululu record may be lost due to the absence of present-day sediments due to erosion during flooding events of 1918, 1925 and 1984. The highest sediment accumulation was observed during this phase which may be attributed to a large sediment deposition due to the flooding events within the more recent period of the record. The charcoal record of the South Lake Futululu record provided insight into past fire regimes and fuel types, reflecting the interplay between changes in available fuel within the landscape, and shifts between natural fires and anthropogenic burning. The combined record provides insights into the dynamic nature of this wetland ecosystem and surrounding landscape through time, which can be used to conserve and manage these ecosystems going forward.

7.1.1. Aims and Objectives Review

This research aimed to investigate the Holocene palaeoenvironmental change in the Mfolozi-Msunduze catchment through fossil pollen and charcoal analysis of a sediment core from South Lake Futululu. This was achieved through the completion of several specific objectives of which are described below:

i. **To produce an age-depth model for the sedimentary sequence based on a combination of accelerator mass spectrometry (AMS) radiocarbon and optically stimulated luminescence (OSL) ages.**

A total of eighteen OSL and 5 AMS radiocarbon ages were used to obtain the age-depth model. These ages were calibrated in Bacon software (Blaauw and Christen, 2011) together with the SHCal 20 (Hogg *et al*., 2013) dataset. A Bayesian age-depth model for the sediment core was produced using Bacon. The age model displayed multiple age reversals between 1700 yr BP and present these layers may also represent past erosional events.

ii. **To conduct relative fossil pollen counts along the length of the core with the aim of reconstructing the Holocene vegetation history for the area;**

Relative pollen counts were conducted at 10 cm resolution along the South Lake Futululu profile with a minimum count of 300 pollen grains.

Final pollen counts were entered into Microsoft Excel (2010) before being imported to Psimpoll (Bennett, 2005). This allowed the interpretation of the pollen data and their changes in pollen counts or percentages which were plotted against the interpolated ages from the age model. The Constrained Incremental Sum of Squares (CONISS) cluster technique was used to define boundaries between the most distinguishable pollen zones. The CONISS algorithm was applied to regional pollen data to produce the dendrogram. The pollen diagrams included a main sum pollen diagram of all taxa; and a pollen diagram excluding rare taxa (<1%). The pollen main sum was adjusted to produce a summary pollen diagram to aid interpretation. The pollen record was described according to the pollen assemblages indicated in each pollen zone.

iii. To conduct macroscopic charcoal counts along the length of the core, such that fire history may be reconstructed for the area; and

This was achieved by the use of the Leica M60 steromicroscope coupled with a digital camera and image analysis software (WinSeedle 2009) for ease of counting. The image analysis provided multiple datasets which were analysed to produce three macrocharcoal main indicators. These indicators include CHAR, W/L ratio and Length which were all plotted along with the summary pollen diagrams for ease of analysis and comparison.

iv. To infer past environmental conditions in the Mfolozi-Msunduze catchment during the Holocene period.

Pollen data was analysed using the indicator species approach. This approach uses the presence or absence of indicator taxa to draw conclusive statements which help infer past environmental conditions. The modern ecological tolerances of these indicator species are well understood and may be used as a basis for reconstructing palaeoenvironments. The environmental inferences derived from the pollen record were integrated with the inferences from the charcoal record for a better understanding of the palaeoreconstruction. Hence a detailed palaeoreconstruction of the South Lake Futululu record during the Holocene was provided.

7.1.2. Future research directions

Blocked valley lakes are poorly researched, and dynamic and require multiproxy palaeoenvironmental research to fully understand the past climatic changes in the subregion by taking advantage of the organic rich peat deposits of the Maputaland Coastal Plain. This research has provided a greater understanding of the South Lake Futululu wetland area and surrounding landscape, however, a closer grid of sites should be studied to help understand regional patterns of past climate. The pollen and charcoal data worked together to help the inferences particularly where the pollen was muted charcoal aided inferences. This research provided a Holocene record covering the past *ca.* 7600 years from the South Lake Futululu blocked valley lake furthering the palaeoenvironmental research into the Mfolozi-Msunduze catchment, and contributing to our understanding of Holocene palaeoenvironments in the Maputaland region of southern Africa.

References

Aaby, B., and & Berglund, B. E. (1986). *Characterization of peat and lake deposits*. In: Berglund BE (ed) Handbook of Holocene palaeoecology and palaeohydrology. Wiley, Chichester, pp 231–246

Adeeyo, A. O., Ndlovu, S. S., Ngwagwe, L. M., Mudau, M., Alabi, M. A., and & Edokpayi, J. N., 2022. Wetland Resources in South Africa: Threats and Metadata Study. *Resources*, 11(6), 54.

Aleman, J.C. et al., 2013. Tracking land-cover changes with sedimentary charcoal in the Afrotropics. The Holocene, 23(12), 1853 –1862.

Aleman, J.C., Blarquez, O., Bentaleb, I., Bonté, P., Brossier, B., Carcaillet, C., Gond, V., Gourlet-Fleury, S., Kpolita, A., Lefèvre, I. & Oslisly, R. (2013). Tracking land-cover changes with sedimentary charcoal in the Afrotropics. *The Holocene*, *23*(12), 1853-1862.

Al-Ghussain, L. (2019). Global warming: Review on driving forces and mitigation. *Environmental Progress and Sustainable Energy*, 38(1), 13-21.

Ali, A., Higuera, P.E., Bergeron, Y. and & Carcaillet, C., (2009). Comparing fire-history interpretations based on area, number and estimated volume of macroscopic charcoal in lake sediments. *Quaternary Research*, 72, 462-468.

Anderson, D. E., Goudie, A. S. and & Parker, A. G. (2007): Global environments through the Quaternary. Exploring environmental change. *Oxford University Press*.

Baker, A. (2016b). Bulk geochemical, biomarker and leaf wax isotope records of Mfabeni peatland, KwaZulu Natal, South Africa since the late Pleistocene (*Doctoral dissertation, Stellenbosch: Stellenbosch University*).

Baker, A., Pedentchouk, N., Routh, J., and & Roychoudhury, A. N. (2017). Climatic variability in Mfabeni peatlands (South Africa) since the late Pleistocene. *Quaternary Science Reviews*, 160, 57-66.

Baker, A., Routh, J., and & Roychoudhury, A. N. (2016a). Biomarker records of palaeoenvironmental variations in subtropical Southern Africa since the late Pleistocene:

Evidences from a coastal peatland. *Palaeogeography, Palaeoclimatology, Palaeoecology*, 451, 1-12.

Baker, A., Routh, J., and & Roychoudhury, A. N. (2018). n-Alkan-2-one biomarkers as a proxy for palaeoclimate reconstruction in the Mfabeni fen, South Africa. *Organic Geochemistry*, 120, 75-85.

Baker, A., Routh, J., Blaauw, M., and & Roychoudhury, A. N. (2014). Geochemical records of palaeoenvironmental controls on peat forming processes in the Mfabeni peatland, Kwazulu Natal, South Africa since the Late Pleistocene. *Palaeogeography, Palaeoclimatology, Palaeoecology*, 395, 95-106.

Bamford, M.K., (2021). Pollen, charcoal and phytolith records from the Late Quaternary of southern Africa: vegetation and climate interpretations. *South African Journal of Geology*, 124(4), 1047-1054. or future reconnection of the river to the St Lucia system, Water Research Commission.

Bate, G.C., Whitfield, A.K. and & Forbes, A.T., (2011). A review of studies on the Mfolozi Estuary and associated flood plain, with emphasis on information required by management for future reconnection of the river to the St Lucia system, *Water Research Commission*.

Bennett, K.D., (2005). Psimpoll. Uppsala Universitet, Villavgen.

Bennett, W. L. (1990_. Toward a theory of press-state. *Journal of communication*, 40(2), 103-127.

Berger, A. and & Yin, Q. (2011). Chapter 13: Astronomical theory and orbital forcing. In: *The SAGE Handbook of Environmental Change Volume 1*, Mathhews, J. A., Bartlein, P. J., Briffa, K. R., Dawson, A. G., De Vernal, A., Denham, T., Fritz, S. C. and Oldfield, F. (eds). SAGE Publications Ltd, London, pp. 254-283.

Berger, A. L. (1978). Longterm variations of daily insolation and Quaternary climatic changes. *Journal of Atmospheric Science*, 35, 2362-2367.

Berger, A., and & Loutre, M. F. (2004). Astronomical theory of climate change. In *Journal de Physique IV (Proceedings)*. *EDP sciences*, 121, 1-35.

Berger, A., Guiot, J., Kukla, G., and & Pestiaux, P. (1981). Long-term variations of monthly insolation as related to climatic changes. *Geologische Rundschau*, 70(2), 748-758.

Birks H. J. B. and & Birks H. H. (1980).:*Quaternary paleoecology*, Edward Arnold, London

Birks, H. H. 1980. Paleolimnological applications. *Encyclopedia of Quaternary Science*, 2337-2356.

Birks, H. H. and & Birks, H. J. B. (2000). Future uses of pollen analysis must include plant macrofossils. *Journal of Biogeography*. 27: 31-35.

Birks, H. H. and & Birks, H. J. B. (2000). Future uses of pollen analysis must include plant macrofossils. *Journal of Biogeography*. 27: 31-35.

Birks, H. H., and & Birks, H. J. B. (2006). Multi-proxy studies in palaeolimnology. Vegetation history and Archaeobotany, 15(4), 235-251.

Birks, H. J. B., and & Berglund, B. E. . (2017). One hundred years of Quaternary pollen analysis 1916–2016. *Vegetation History and Archaeobotany*, 2(27), 271-309. doi:10.1007/s00334-017-0630-2

Birks, H. J. B., Heiri, O., Seppä, H. &, and Bjune, A. E. (2010). Strengths and weaknesses of quantitative climate reconstructions based on Late-Quaternary. *The Open Ecology Journal*, 3(1).

Blaauw, M. &, and Christen, J. A. (2011). Flexible paleoclimate age-depth models using an autoregressive gamma process. *Bayesian analysis*, 6(3), 457-474.

Blaauw, M., (2010). Methods and code for 'classical'age-modelling of radiocarbon sequences. *Quaternary geochronology*, 5(5), 512-518.Blaauw, M. 2010. Methods and code for 'classical'age-modelling of radiocarbon sequences. quaternary geochronology, 5(5), 512-518.

Blaauw, M., Christen, J. A., Mauquoy, D., van der Plicht, J., and & Bennett, K. D. (2007). Testing the timing of radiocarbon-dated events between proxy archives. *The Holocene*, 17(2), 283-288.

Boelter, D. H. (1968). Important physical properties of peat materials. In In: Proceedings, third international lpeat congress; 1968 August 18-23; Quebec, Canada.[Place of publication unknown]: *Department of Energy, Minds and Resources and National Research Council of Canada,*: 150-154..

Boreux, J. J., Pesti, G., Duckstein, L., and & Nicolas, J. (1997). Age model estimation in paleoclimatic research: fuzzy regression and radiocarbon uncertainties. *Palaeogeography, Palaeoclimatology, Palaeoecology*, 128(1-4), 29-37.

Breman, E., Gillson, L. and & Willis, K., (2011). How fire and climate shaped grass dominated vegetation and forest mosaics in the northern South Africa during the past millennia. *The Holocene*, 1, 1-13.

Broecker, W. S., and & Stocker, T. F. (2006). The Holocene CO2 rise: anthropogenic or natural?. Eos, *Transactions American Geophysical Union*, 87(3), 27-27.

Brook, G.A., Scott, L., Railsback, L.B. and & Goddard, E.A., (2010). A 35 ka pollen and isotope record of environmental change along the southern margin of the Kalahari from a stalagmite and animal dung deposits in Wonderwerk Cave, South Africa. *Journal of Arid Environments*, 74, 870-884.

Brossier, B., Oris, F., Finsinger, W., Asselin, H., Bergeron, Y. &, and Ali, A. A. (2014). Using tree-ring records to calibrate peak detection in fire reconstructions based on sedimentary charcoal records. *The Holocene*, 24(6), 635-645.

Brown, T. A., Farwell, G. W., Grootes, P. M. and & Schmidt. (1992). Radiocarbon AMS dating of pollen extracted from peat samples. *Radiocarbon*. 34(3):55-556.

Brown, T. A., Nelson, D. E., Mathewes, R. W., Vogel, J. S. and & Southon, J. R. (1989). Radiocarbon dating of pollen by accelerator mass spectrometry. *Quarternary Research*. 32: 205- 212.

Burger, J., (2008). Vegetation of Richards Bay municipal area, KwaZulu-Natal, South Africa, with specific reference to wetlands, *University of Pretoria, Pretoria*.

Calov, R., Ganopolski, A., Claussen, M., Petoukhov, V. &, and Greve, R. (2005). Transient simulation of the last glacial inception. Part I: glacial inception as a bifurcation in the climate system. *Climate Dynamics*, 24(6), 545-561.

Cao, Y., Zhao, Y., Wen, L., Li, Y., Wang, S., Liu, Y., Shi, Q. and & Weng, J. (2019). System dynamics simulation for CO2 emission mitigation in green electric-coal supply chain. *Journal of Cleaner Production*, 232, 759-773.

Carcaillet, C., Bergeron, Y., Richard, P.J., Fréchette, B., Gauthier, S. & Prairie, Y.T. (2001a). Change of fire frequency in the eastern Canadian boreal forests during the Holocene: does vegetation composition or climate trigger the fire regime?. *Journal of Ecology*, 89(6), 930-946.Carcaillet, C. et al., 2001. Change of fire frequency in the eastern Canadian boreal forests during the Holocene: does vegetation composition or climate trigger the fire regime? Journal of Ecology, 89: 930-945.

Carcaillet, C., Bouvier, M., Frechette, B., Larouche, A. C. and & Richard, P. J. H. (2001b). Comparison of pollen-slide and sieving methods in lacustrine charcoal analysis or local and regional fire history. *The Holocene*. 11(4): 467-476.

Carcaillet, C., Perroux, A.-S., Genries, A. and & Perrette, Y., (2007). Sedimentary charcoal pattern in a karstic underground lake, Vercors massif, French Alps, implications for palaeo-fire history. *The Holocene,* 17(6), 845–850.

Chappell, J. (1973). Astronomical theory of climatic change: Status and problem. *Quaternary Research*, 3(2), 221-236.

Chappellaz, J. A., Fung, I. Y., and & Thompson, A. M. (1993). The atmospheric CH4 increase since the Last Glacial Maximum. Tellus B: *Chemical and Physical Meteorology*, 45(3), 228-241.

Chase, B.M. a Norström nd & Meadows, M.E., (2007). Late Quaternary dynamics of southern Africa's winter rainfall zone. *Earth-Science Reviews*, 84(3-4), 103-138.

Chevalier, M. &, and Chase, B. M. (2015). Southeast African records reveal a coherent shift from high-to low-latitude forcing mechanisms along the east African margin across last glacial–interglacial transition. *Quaternary Science Reviews*, 125, 117-130.

Chevalier, M., Davis, B. A., Heiri, O., Seppä, H., Chase, B. M., Gajewski, K., Lacourse, T., Telford, R. J., Finsinger, W., Guiot, J. and & Kupriyanov, D. (2020). Pollen-based climate reconstruction techniques for late Quaternary studies. *Earth-Science Reviews*, 210, 103384.

Chmura, G.L., Anisfeld, S.C., Cahoon, D.R. and & Lynch, J.C., (2003). Global carbon sequestration in tidal, saline wetland soils. *Global biogeochemical cycles*, 17(4).

Clark, J.S., 1988. Particle motion and the theory of charcoal analysis, source area, transport, deposition, and sampling. *Quaternary Research*, 30, 67-80.

Cole-Dai, J. (2010). Volcanoes and climate. *Wiley Interdisciplinary Reviews: Climate Change*, 1(6), 824-839.

Conedera, M., Tinner, W., Neff, C., Meurer, M., Dickens, A. F., and& Krebs, P. (2009). Reconstructing past fire regimes: methods, applications, and relevance to fire management and conservation. *Quaternary Science Reviews*, 28(5-6), 555-576.

Cyrus, D. P., Vivier, L., Owen, R. K. &, and Jerling, H. L. (2010). Ecological status and role of the Mfolozi–Msunduzi estuarine system within the iSimangaliso Wetland Park, a World Heritage Site on the south-east coast of South Africa. African *Journal of Aquatic Science*, 35(2), 109-116.

Davies, A. and & Bunting, J. M., (2010). Applications of Palaeoecology in Conservation. *The Open Ecology Journal*. 3, 54-67.

Davis, M. B., (1963): The theory of pollen analysis. *American Journal of Science*. 261: 897-912.

Delfino, A.J.A., (2002). Control of invasive Chromoleana odorata (L.) R.M. King and & H. Robinson, an evaluation of its efficacy in Futululu State Forest, *South Africa International Institute for Geo-Information Science and Earth observation*.

Dreibrodt, S., Hofmann, R., Sipos, G., Schwark, L., Videiko, M., Shatilo, L., Martini, S., Saggau, P., Duttmann, R. and & Bork, H.R., (2019). Dreibrodt et al.-Holocene erosion history in central Ukraine.

Duffin, K.I., (2008): The representation of rainfall and fire intensity in fossil pollen and charcoal records from a South African savanna. *Review of Palaeobotany and Palynology*. 151: 59-71.

Dunker, S., Motivans, E., Rakosy, D., Boho, D., Maeder, P., Hornick, T., and& Knight, T. M. (2021). Pollen analysis using multispectral imaging flow cytometry and deep learning. N*ew Phytologist*, 229(1), 593-606.

Ekblom, A., and& Gillson, L. (2010). Dung fungi as indicators of past herbivore abundance, Kruger and Limpopo National Park. *Palaeogeography, Palaeoclimatology, Palaeoecology*, 296(1-2), 14-27.

Ellery, W.N., Grenfell, S. E., Grenfell, M. C., Humphries, M. S., Barnes, K., Dahlberg, A. and & Kindness, A., (2012). Peat formation in the context of the development of the Mkuze floodplain on the coastal plain of Maputaland, South Africa. *Geomorphology*, 141-142, 11-20.

Ellison, J. C. (2008). Long-term retrospection on mangrove development using sediment cores and pollen analysis. *Aquatic Botany*, 89, 93-104.

Fadnavis, S., Müller, R., Chakraborty, T., Sabin, T. P., Laakso, A., Rap, A., Griessbach, S., Vernier, J. P. &, Tilmes, S. (2021). The role of tropical volcanic eruptions in exacerbating Indian droughts. *Scientific Reports*, 11(1):2714

Faegri, K. and & Iverson, J., (1989): Textbook of pollen analysis. Chichester. John Wiley and Sons.

Feely, J. M., and & Bell-Cross, S. M. (2011). The distribution of early iron age settlement in the Eastern Cape: some historical and ecological implications. *The South African Archaeol Logical Bulletin*, 105-112.

Feurdean, A., Spessa, A., Magyari, E.K., Willis, K.J., Veres, D. and Hickler, T. (2012). Trends in biomass burning in the Carpathian region over the last 15,000 years. *Quaternary Science Reviews*, 45, 111-125.

Figueiral, I. and & Mosbrugger, V. (2000): Areview of charcoal analysis as a tool for assessing Quarternary and Tertiary environments: achievements and limits. *Paleogeography, Paleoclimatology, Paleoecology*. 164: 397-407.

Finch, J. M., and & Hill, T. R. (2008). A late Quaternary pollen sequence from Mfabeni Peatland, South Africa: Reconstructing forest history in Maputaland. *Quaternary Research*, 70(3), 442-450.

Finch, J. M., Hill, T. R., Meadows, M. E., Lodder, J., and & Bodmann, L. (2022). Fire and montane vegetation dynamics through successive phases of human occupation in the northern Drakensberg, South Africa. *Quaternary International*, 611, 70-80.

Finch, J.M. and & Hill, T. R., (2008). A late Quaternary pollen sequence from Mfabeni Peatland, South Africa, Reconstructing forest history in Maputaland. *Quaternary Research*, 70, 442–450.

Finsinger, W. and & Tinner, W. (2005): Minimum count sums for charcoal-concentration estimates in pollen slide accuracy and potential errors. *The Holocene*: 15(2): 293-297.

Fisher, T. G., (2004): Vibracoring from lake ice with a lightweight monopod and piston coring apparatus. *Journal of Paleolimnology*. 31: 377-382.

Fitchett, J. M. &, and Bamford, M. K. (2017). The validity of the Asteraceae: Poaceae fossil pollen ratio in discrimination of the southern African summer-and winter-rainfall zones. *Quaternary Science Reviews*, 160, 85-95.

Fitchett, J. M., Grab, S. W., Bamford, M. K., and& Mackay, A. W. (2016a). A multi-proxy analysis of late Quaternary palaeoenvironments, Sekhokong Range, eastern Lesotho. *Journal of Quaternary Science*, 31(7), 788-798.

Fitchett, J. M., Mackay, A. W., Grab, S. W., and& Bamford, M. K. 2016b. Holocene climatic variability indicated by a multi-proxy record from southern Africa's highest wetland. *The Holocene*, 27(5), 638-650.

Garden, S., (2008). Wetland geomorphology and floodplain dynamics on the hydrologically variable Mfolozi River, KwaZulu-Natal, South Africa, *University of KwaZulu-Natal, Durban*, 243 pp.

Gardner, R. C., Barchiesi, S., Beltrame, C., Finlayson, C., Galewski, T., Harrison, I., Paganini, M., Perennou, C., Pritchard, D., Rosenqvist, A., Walpole, M. and & Walpole, M., (2015). State of the World's Wetlands and Their Services to People: A Compilation of Recent Analyses. 12th Meeting of the Conference of the Parties to the Convention on Wetlands, *Ramsar COP12 DOC.23*.

Gerstell, M. F., Crisp, J. &, and Crisp, D. (1995). Radiative forcing of the stratosphere by SO 2 gas, silicate ash, and H 2 SO 4 aerosols shortly after the 1982 eruptions of El Chichón. *Journal of climate*, 8(5), 1060-1070.

Gillespie, R., Magee, J.W., Luly, J.G., Dlugokencky, E., Sparks, R.J. & Wallace, G. (1991). *Palaeogeography, Paleoclimatology, Palaeoecology*.Gillespie, R., Magee, J. W., Luly, J. G., Dlugokencky, E., Sparks, R. J. and Wallace, G. 1991. 84: 333-338.

Gillson, L., Ekblom, A., Willis, K. and & Froyd, C. A., (2008). Holocene palaeo-invasions: The link between pattern, process and scale in invasion ecology? *Landscape Ecology*, 23, 757-769.

Glew, J. R., Smol, J. P., and& Last, W. M. (2002). Sediment core collection and extrusion. In Tracking environmental change using lake sediments (pp. 73-105). *Springer, Dordrecht*.

Gordon, A.D. &, Birks, H.J.B., (1972). Numerical methods in quaternary palaecology. I. Zonation of pollen diagrams. *New Phytologist*, 71: 961-979.

Gosling, W. D., Mayle, F. E., Killeen, T. J., Siles, M., Sanchez, L., and& Boreham, S. (2003). A simple and effective methodology for sampling modern pollen rain in tropical environments. *The Holocene*, 13(4), 613-618.

Goudie, A. S. (2018). Human impact on the natural environment. John Wiley and Sons.

Green, A. N., Humphries, M. S., Cooper, J. A. G., Strachan, K. L., Gomes, M., and& Dladla, N. N. (2022). The Holocene evolution of Lake St Lucia, Africa's largest estuary: Geological implications for contemporary management. *Estuarine, Coastal and Shelf Science*, 266, 107745.

Green, D. G.&, and Dolman, G. S. (1988). Fine resolution pollen analysis. *Journal of Biogeography*, 685-701.

Grenfell, S., Ellery, W.N., Grenfell, M.C., Ramsay, L.F. and & Flugel, T.J., (2010). Sedimentary facies and geomorphic evolution of a blocked-valley lake, Lake Futululu, northern Kwazulu-Natal, South Africa. *Sedimentology*, 57, 1159-1174.

Grenfell, S.E. and & Ellery, W.N., (2009). Hydrology, sediment transport dynamics and geomorphology of a variable flow river, The Mfolozi River, South Africa. *Water South Africa*, 35(3), 271-282.

Grenfell, S.E., Ellery, W.N. and& Grenfell, M.C.,(2009). Geomorphology and dynamics of the Mfolozi River floodplain, KwaZulu-Natal, South Africa. *Geomorphology*, 107, 226-240.

Grimm, E. C. (1987). CONISS: a FORTRAN 77 program for stratigraphically constrained cluster analysis by the method of incremental sum of squares. *Computers and geosciences*, 13(1), 13-35.

Grundling, P. L., and &Grobler, R. E. T. I. E. F. (2005). Peatlands and mires of South Africa. *Stapfia*, 85, 379-396.

Grundling, P.-L., Mazus, H., and& Baartman, L. (1998). Peat resources in northern KwaZulu-Natal wetlands: Maputaland. Pretoria.

Hahn, A., Neumann, F. H., Miller, C., Finch, J., Frankland, T., Cawthra, H. C., Schefuß, E. and & Zabel M. 2021. Mid-to Late Holocene climatic and anthropogenic influences in Mpondoland, South Africa. *Quaternary Science Reviews*, 261, 106938.

Hall, M., (1984). Prehistoric farming in the mfolozi and hluhluwe valleys of Southeast Africa, an archaeo-botanical survey. *Journal of Archaeological Science*, 11(3), 223–235.

Harder, S. L., Shindell, D. T., Schmidt, G. A.&, and Brook, E. J. (2007). A global climate model study of CH4 emissions during the Holocene and glacial-interglacial transitions constrained by ice core data. *Global Biogeochemical Cycles*, 21(1).

Herzschuh, U., Tarasov, P., Wünnemann, B., and& Hartmann, K. (2004). Holocene vegetation and climate of the Alashan Plateau, NW China, reconstructed from pollen data. *Palaeogeography, Palaeoclimatology*, Palaeoecology, 211(1-2), 1-17.

Higuera, P. E., Brubaker, L. B., Anderson, P. M., Hu, F. S., and& Brown, T. A. (2009). Vegetation mediated the impacts of postglacial climate change on fire regimes in the south-central Brooks Range,. *Alaska. Ecological Monographs*, 79(2), 201-219.

Higuera, P. E., Peters, M. E., Brubaker, L. B., and& Gavin, D. G. (2007). Understanding the origin and analysis of sediment-charcoal records with a simulation model. *Quaternary Science Reviews*, 26(13-14), 1790-1809.

Hill, T. R., Duthie, T. J., and &Bunting, J. (2021). Pollen productivity estimates from KwaZulu-Natal Drakensberg, South Africa. In Quaternary Vegetation Dynamics–The African Pollen Database (pp. 259-274). CRC Press.

Hogg, A. G., Hua, Q., Blackwell, P. G., Niu, M., Buck, C. E., Guilderson, T. P., Heaton, T. J., Palmer, J. G., Reimer, P. J., Riemer, R. W., Turney, C. S. &, Zimmerman, S. R. H., (2013): SHCal13 Southern hemisphere calibration, 0-50000 years Cal BP. *Radiocarbon*. 55(2): 1-15.

Holmgren, K., Karlén, W., Lauritzen, S. E., Lee-Thorp, J. A., Partridge, T. C., Piketh, S., Repinski, P., Stevenson, C., Svanered, O. & Tyson, P. D. (1999). A 3000-year high-resolution stalagmitebased record of palaeoclimate for northeastern South Africa. *The Holocene*, 9(3), 295-309.

Holmgren, K., Lee-Thorp, J. A., Cooper, G. R., Lundblad, K., Partridge, T. C., Scott, L., Sithaldeen R, Talma AS. &, Tyson PD. (2003). Persistent millennial-scale climatic variability over the past 25,000 years in Southern Africa. *Quaternary Science Reviews*, 22(21-22), 2311-2326.

Holmgren, K., Tyson, P. D., Moberg, A.&, and Svanered, O. (2001). A preliminary 3000-year regional temperature reconstruction for South Africa. *South African Journal of Science*, 97(1), 49-51.

Huffman, T.N., (2007). Handbook of the Iron Age: The Archaeology of Pre-Colonial Farming Societies in Southern Africa. *University of KwaZulu-Natal Press, Pietermaritzburg*.

Humphries, M. S., Kirsten, K. L.&, and McCarthy, T. S. (2019). Rapid changes in the hydroclimate of southeast Africa during the mid-to late-Holocene. *Quaternary Science Reviews*, 212, 178-186.

Humphries, M., Green, A., Benallack, K., Finch, J., de Lecea, A., Gomes, M., Strachan, K. and & Kirsten K. (2015). A multi-proxy investigation into past and present environmental change at Lake St Lucia. *Water Research Commission Report*.

Huntley, B., Banard, P., Altwegg, R., Chambers, L., Coetzee, W. T., Gibson, L., Hockey, P. A. R., Hole, D. G., Midgley, G. F., Underhill, L. G. and & Willis, S. G., (2010): Beyond bioclimatic envelopes: dynamic species range anf abundance modelling in the context of climatic change. *Ecography*. 33: 621-626.

IPCC 2022, Climate Change (2022): Impacts, Adaptation and Vulnerability, the Working Group II contribution to the Sixth Assessment Report, Cambridge University Press, Cambridge, UK.

Iversen, J. (1941). Land occupation in Denmark's stone age. Danmarks Geologiske Undersøgelse II. række, 66, 1-68.

Juggins, S., (2007). C2 vrsionversion 1.5 user guide. Software for Ecological and Paleoecological Data Analysisand Visualisation., Department of Geography, New Castle upon Tyne.

Kayranli, B., Scholz, M., Mustafa, A. and & Hedmark, A.,(2010). Carbon storage and fluxes within freshwater wetlands: A critical review. *Wetlands*, 30, 111-124.

Kim, J. H., Schneider, R. R., Mulitza, S., and& Müller, P. J. (2003). Reconstruction of SE trade-wind intensity based on sea-surface temperature gradients in the Southeast Atlantic over the last 25 kyr. *Geophysical Research Letters*, 30(22).

Kirleis, W., Pillar, V.D. and & Behling, H., (2011). Human-environmental interactions in mountain rain forests, archaeobotanical evidence from central Sulawesi, Indonesia. *Vegetation History and Archaebotany*, 20(3), 165-179.

Kristen, I., Fuhrmann, A., Thorpe, J., Rohl, U., Wilkes, H., and& Oberhansli, H. (2007). Hydrological changes in southern Africa over the last 200 Ka as recorded in lake sediments from the Tswaing impact crater. *South African Journal of Geology*, 110(2-3), 311-326.

Lian, O. B. and & Roberts, R. G., (2006): Dating the Quaternary: progress in luminescence dating of sediments. *Quaternary Science Review*. 25: 2449-2468.

Loader, N. J., and& Hemming, D. L. (2004). The stable isotope analysis of pollen as an indicator of terrestrial palaeoenvironmental change: a review of progress and recent developments. *Quaternary Science Reviews*, 23(7-8), 893-900.

Lodder, J. (2011). The Late Quaternary palaeoenvironments of a subalpine wetland in Cathedreal Peak, KwaZulu-Natal Drakensberg. Doctoral Dissertation, *University of KwaZulu-Natal*.

Long, A., Davis, O. K. and de Lanois, J. (1992): Seperation and ^{14}C 14C dating of pure pollen from lake sediments: nanofossil AMS dating. *Radiocarbon*. 34(3): 557-560.

Madsen, A. T. and & Murray, A. S. (2009). Optically stimulated luminescence dating of young sediments: A review. *Geomorphology*. 109: 3-16.

Mazus, H. (1996). Pollen records from Nhlangu Peatland on the Zululand coastal plain, *Council for Geoscience Internal Report no*. 1996-0234, Pretoria.

Mazus, H., (2000). Clues on the history of Podocarpus forest in Maputaland, South Africa, during the Quaternary, based on pollen analysis. *Africa Geoscience Review*, 7, 75–82.

Mbatha, P. (2022). Unravelling the perpetuated marginalization of customary livelihoods on the coast by plural and multi-level conservation governance systems. *Marine Policy*, 143, 105143.

McCormac, F. G., Hogg, A. G., Blackwell, P. G., Higham, T. F. G. and & Reimer, P. J., (2004). SHCAL04 southern Hemisphere Calibration, 0–11.0 CAL KYR BP. *Radiocarbon*, 46 (3), 1087-1092.

Meadows, M. E., Baxter, A. J. and & Parkington, J., (1996): Late Holocene environmnets at Verlorenvlei, Western Cape province, South Africa. *Quaternary International*. 33: 81-95.

Metwally, A.A., Scott, L., Neumann, F.H., Bamford, M.K. & Oberhänsli, H. (2014). Holocene palynology and palaeoenvironments in the Savanna Biome at Tswaing Crater, central South Africa. *Palaeogeography, Palaeoclimatology, Palaeoecology*, 402, pp.125-135.

Miller, C., Finch, J., Hill, T., Peterse, F., Humphries, M., Zabel, M.&, and Schefuß, E. (2019). Late Quaternary climate variability at Mfabeni peatland, eastern South Africa. *Climate of the Past*, 15(3), 1153-1170.

Mitsch, W., Bernal, B.&, and Hernandez, M. E., (2015). Ecosystem services of wetlands. International *Journal of Biodiversity Science, Ecosystem Services and Management*, 11(1), 1-4.

Mooney, S. D. and & Tinner, W., (2010): The analysis of charcoal in peat and organic sediments. *Mines and Peat*. 7(9): 1-18.

Mooney, S. D. and & Tinner, W., (2011): The analysis of charcoal in peat and organic sediments. *Mines and Peat*. 7(9): 1-18.

Moore, P. D. and & Webb, T. I. (1978). An illustrated guide to pollen analysis, Hodder and Stoughton, London

Moore, P. D., Webb, T. I. and& Collinson, M. E. (1991): Pollen Analysis, Hodder and Stoughton, London.

Mucina, L. and& Rutherford, M.C., (2006). The vegetation of South Africa, Lesothoand Swaziland. *South African National Biodiversity Institute Pretoria*.

Mutanga, O., Adam, E. and& Cho, M.A., (2012). High density biomass estimation for wetland vegetation using WorldView-2 imagery and random forest regression algorithm. International *Journal of Applied Earth Observation and Geoinformation*, 18, 399-406.

Nash, D. J. and& Meadows, M. E., (2012). Africa In: Quaternary environmental change in the tropics, Metcalfe S. E. and Nash, D. J. (eds), Wiley-Blackwell, Oxford, UK, pp. 79-150.

Neal, M.J., (2001). The vegetation ecology of the lower Mkuze River floodplain, northern KwaZulu-Natal, A landscape ecology perspective., *University of Natal-Durban, Durban*, 155 pp.

Neumann, F. H., Scott, L., and& Bamford, M. K. (2011). Climate change and human disturbance of fynbos vegetation during the late Holocene at Princess Vlei, Western Cape, South Africa. *The Holocene*, 21(7), 1137-1149.

Neumann, F. H., Stager, J. C., Scott, L., Venter, H. J. T. &, Weyhenmeyer, C., (2008): Holocene vegetation and climate records from Lake Sibiya, KwaZulu-Natal (South Africa). *Review of Paleobotany and Palynology*. 152: 113-128.

Neumann, F.H., Botha, G.A., & Scott, L., (2014). 18,000 years of grassland evolution in the summer rainfall region of South Africa: evidence from Mahwaqa Mountain, KwaZulu-Natal. Vegetation. History. *Archaeobotany* 23 (6), 665-681.

Neumann, F.H., Scott, L. and& Bousman, C.B., (2010). A Holocene sequence of vegetation change at Lake Eteza, coastal KwaZulu-Natal, South Africa. *Review of Palaeobotany and Palynology*, 162, 39-53.

Ngqulana, S. G. (2012). Spatial and temporal distribution of the benthos in the Mfolozi-Msunduzi Estuary, *KwaZulu–Natal (Doctoral dissertation).*

Norström, E., Bringensparr, C., Fitchett, J. M., Grab, S. W., Rydberg, J., and& Kylander, M. (2018). Late-Holocene climate and vegetation dynamics in eastern Lesotho highlands. *The Holocene*, 28(9), 1483-1494.

Norström, E., Kylander, M. E., Sitoe, S. R. and& Finch, J. M. (2022). Chronostratigraphic palaeo-climate phasing based on southern African wetlands: From the escarpment to the eastern seaboard. *South African Journal of Geology*, 124(4), 977-994.

Norström, E., Neumann, F. H., Scott, L., Smittenberg, R. H., Holmstrand, H., Lundqvist, S., Snowball, I., Sundqvist, H. S., Risberg, J., and& Bamford, M. (2014). Late Quaternary vegetation dynamics and hydro-climate in the Drakensberg, South Africa. *Quaternary Science Reviews*, 105, 48-65.

Norström, E., Scott, L., Patridge, T.C., Risberg, J. and& Holmgren, K.,(2010). Reconstruction of environmental and climate changes at Braamhoek wetland, eastern escarpment South Africa, during the last 16,000 years with emphasis on the Pleistocene–Holocene transition. *Palaeogeography, Palaeoclimatology, Palaeoecology*, 271, 240–258.

Nustad, K. G., and& Sundnes, F. (2013). The nature of the land: the Dukuduku forest and the Mfolozi flats, KwaZulu-Natal. The Journal of Modern African Studies, 51(3), 487-506.

Oris, F., Ali, A. A., Asselin, H., Paradis, L., Bergeron, Y., and& Finsinger, W. (2014). Charcoal dispersion and deposition in boreal lakes from 3 years of monitoring: Differences between local and regional fires. *Geophysical Research Letters*, 41(19), 6743-6752.

Owens, K. A.,(2004). Global issues - National Politics: Comparing wetland protection policies and perceptions in the Netherlands and the United States (CSTM Studies en Rapporten; No. 211). *Center for Clean Technology and Environmental Policy*. 211, 22

Owens, P.N. (2020). Soil erosion and sediment dynamics in the Anthropocene: a review of human impacts during a period of rapid global environmental change. *Journal of Soils and Sediments*, 20, 4115-4143.

Paeth, H., and& Pollinger, F. (2020). Revisiting the spatiotemporal characteristics of past and future global warming. *Erdkunde*, 4, 225-248.

Patrick, M. J., and Ellery, W. N. 2007. Plant community and landscape patterns of a floodplain wetland in Maputaland, Northern KwaZulu-Natal, South Africa. African Journal of Ecology, 45(2), 175-183.

Patrick, M. J., and& Ellery, W. N. (2007). Plant community and landscape patterns of a floodplain wetland in Maputaland, Northern KwaZulu-Natal, South Africa. *African Journal of Ecology*, 45(2), 175-183.

Pessendra, L. C. R., Gouveia, S. E. M. and& Aravena, R., (2001):. Radiocarbon dating of total soil organic matter and humin fraction and its comparison with ^{14}C 14C ages of fossil charcoal. *Radiocarbon*. 43(2b): 595-601.

Peters, M. E., and & Higuera, P. E. (2007). Quantifying the source area of macroscopic charcoal with a particle dispersal model. *Quaternary Research*, 67(2), 304-310.

Peters, M. E., and Higuera, P. E. 2007. Quantifying the source area of macroscopic charcoal with a particle dispersal model. Quaternary Research, 67(2), 304-310.

Reddad, H., Etabaai, I., Rhoujjati, A., Taieb, M., Thevenon, F., and& Damnati, B. (2013). Fire activity in North West Africa during the last 30,000 cal years BP inferred from a charcoal record from Lake Ifrah (Middle atlas–Morocco): Climatic implications. *Journal of African Earth Sciences*, 84, 47-53.

Repinski, P., Holmgren, K., Lauritzen, S. E., and& Lee-Thorp, J. A. (1999). A late Holocene climate record from a stalagmite, cold air cave, Northern Province, South Africa. *Palaeogeography, Palaeoclimatology, Palaeoecology*, 150(3-4), 269-277.

Rojas-Downing, M. M., Nejadhashemi, A. P., Harrigan, T., and& Woznicki, S. A. (2017). Climate change and livestock: Impacts, adaptation, and mitigation. *Climate Risk Management*, 16, 145-163.

Rose, N. L., Turner, S. D., Unger, L. E., and& Curtis, C. J. (2021). The chronostratigraphy of the Anthropocene in southern Africa: Current status and potential. *South African Journal of Geology* 2021, 124(4), 1093-1106.

Sarmaja-Korjonen, K. 1991: Comparison of two methods of counting microscopic charcoal particles in peat. *Bulletin of the Geology Society of Finland*. 63(1):41-48.

Scott, A. C. (2010): Charcoal recognition, taphonomy and uses in paleoenvironmental analysis. *Paleogeography, Paleoclimatology, Paleoecology*. 291: 11-39.

Scott, L. (1982a). Late Quaternary fossil pollen grains from the Transvaal, South Africa. *Review of Palaeobotany and Palynology*, 36(3-4), 241-278.

Scott, L. (1987). Late Quaternary forest history in Venda, Southern Africa. *Review of Palaeobotany and Palynology*, 53, 1-10.

Scott, L. (1989a). Late Quaternary vegetation history and climatic change in the eastern Orange Free State, South Africa. *South African Journal of Botany*, 55(1), 107-116.

Scott, L. (1989b). Climatic conditions in southern Africa since the last glacial maximum, inferred from pollen analysis. *Palaeogeography, Palaeoclimatology, Palaeoecology*, 70(4), 345-353.

Scott, L. (1993). Palynological evidence for late Quaternary warming episodes in Southern Africa. *Palaeogeography, Palaeoclimatology, Palaeoecology*, 101(3-4), 229-235.

Scott, L. (1999). Vegetation history and climate in the Savanna biome South Africa since 190,000 ka: a comparison of pollen data from the Tswaing Crater (the Pretoria Saltpan) and Wonderkrater. *Quaternary International*, 57, 215-223.

Scott, L. (2002).: Microscopic charcoal in sediments: Quarternary fire history of the grassland and savanna regions in South Africa. *Journal of Quaternary Science*: 17(1): 77-86.

Scott, L. (2016). Fluctuations of vegetation and climate over the last 75 000 years in the Savanna Biome, South Africa: Tswaing Crater and Wonderkrater pollen sequences reviewed. *Quaternary Science Reviews*, 145, 117-133.

Scott, L. and& Vogel, J.C., (1978). Pollen analysis of the thermal spring deposit at Wonderkrater (Transvaal, South Africa). *Palaeoecology of Africa*, 10, 155-162.

Scott, L. and& Vogel, J.C., (1983). Late Quaternary pollen profile from the Transvaal highveld, South Africa. *South African Journal of Science*, 79, 266-272.

Scott, L., (1990). Environmental changes reflected by pollen in some Holocene sediments from Transvaal, South Africa and Marion Island, southern Ocean. *South African Journal of Science*, 86, 464-466.

Scott, L., Holmgren, K., Talma, A.S., Woodborne, S. and& Vogel, J.C., (2003). Age Interpretation of the WonderKrater spring sediments and vegetation change in the Savanna Biome, Limpopo province, South Africa. *South African Journal of Science*, 99, 484-488.

Scott, L., Neumann, F. H., Brook, G. A., Bousman, C. B., Norström, E. and& Metwally, A. A., (2012). Terrestrial fossil-pollen evidence of climate change during the last 26 thousand years in Southern Africa. *Quaternary Science Reviews*, 32, 100-118.

Scott, L., Steenkamp, M., (1996). Environmental history and recent human disturbance at coastal Lake Teza, Kwazulu-Natal. *South African Journal of Science* 92, 348–350.

Scott-Shaw, C.R. and& Escott, B.J. (eds). (2011) KwaZulu-Natal Provincial Pre-Transformation Vegetation Type Map – 2011. Unpublished GIS Coverage [kznveg05v2_011_wll.zip], Biodiversity Conservation Planning Division, Ezemvelo KZN Wildlife, Pietermartizburg, South Africa.

Seppä, H. and& Bennett, K. D., (2003).: Quarternary pollen analysis: recent progress in palaeoeceology and paleoclimate. *Progress in Physical Geography*. 27(4): 548-579.

Sherwood, S. C., Dixit, V., and& Salomez, C. (2018). The global warming potential of near-surface emitted water vapour. *Environmental Research Letters*, 13(10), 104006.

Shotyk, W., and& Noernberg, T. (2020). Sampling, handling, and preparation of peat cores from bogs: review of recent progress and perspectives for trace element research. Canadian *Journal of Soil Science*, 100(4), 363-380.

Slagter, B., Tsendbazar, N., Vollrath, A., and& Reichea, J., (2020). Mapping wetland characteristics using temporally dense Sentinel-1 and Sentinel-2 data: A case study in the St. Lucia wetlands, South Africa. International *Journal of Applied Earth Observation and Geoinformation*, 86, 1-11.

Slayton, I. A. (2010). A vegetation history from Emerald Pond, Great Abaco Island, the Bahamas, based on pollen analysis.

South African National Biodiversity Institute (2006- 2018). The Vegetation Map of South Africa, Lesotho and Swaziland, Mucina, L., Rutherford, M.C. and Powrie, L.W. (Editors), Online, http://bgis.sanbi.org/SpatialDataset/Detail/18, Version 2018

South African National Biodiversity Institute (2006- 2018). The Vegetation Map of South Africa, Lesotho and Swaziland, Mucina, L., Rutherford, M.C. and Powrie, L.W. (Editors), Online, http://bgis.sanbi.org/SpatialDataset/Detail/18, Version 2018

Stager, J. C., Ryves, D. B., King, C., Madson, J., Hazzard, M., Neumann, F. H., and& Maud, R. (2013). Late Holocene precipitation variability in the summer rainfall region of South Africa. *Quaternary science reviews*, 67, 105-120.

Swain, A. M. (1973). A History of Fire and Vegetation in Northeastern Minnesota as Recorded in Lake Sediments1. *Quaternary research*, 3(3), 383-396.

Tabares, X., Zimmermann, H., Dietze, E., Ratzmann, G., Belz, L., Vieth-Hillebrand, A., Dupont, L., Wilkes, H., Mapani, B. and& Herzschuh, U., (2020). Vegetation state changes in the course of shrub encroachment in an African savanna since about 1850 CE and their potential drivers. *Ecology and Evolution*, 10, 962-979.

Thackeray, J. F., Scott, L., and& Pieterse, P. (2019). The Younger Dryas interval at Wonderkrater (South Africa) in the context of a platinum anomaly. *Palaeontol Afr*, 54, 30-35.

Thamm, A. G., Grundling, P., and& Mazus, H. (1996). Holocene and recent peat growth rates on the Zululand coastal plain. *Journal of African Earth Sciences*, 23(1), 119-124.

Thomas, K. W. 1964. A new design for a peat sampler. *New Phytologist*, 63(3)

Tinner, W., Hu, F. S., Beer R., Kaltenrieder, P., Scheurer, B. and& Krähenbühl, U. (2005): Postglacial vegetation and fire history: pollen, plant material and charcoal records from two Alaskan lakes. Vegetation History *Archaeobotany*. 15: 279-293.

Troels-Smith, J. (1955). Characterisation of unconsolidated sediments. *Danmarks Geologiske Undersogelse*, 3, 1-73

Truc, L., Chevalier, M., Favier, C., Cheddadi, R., Meadows, M. E., Scott, L., Carr, A.S., Smith, G.F. and& Chase, B. M. (2013). Quantification of climate change for the last 20,000 years from Wonderkrater, South Africa: Implications for the long-term dynamics of the Intertropical Convergence Zone. *Palaeogeography, Palaeoclimatology, Palaeoecology*, 386, 575-587.

Turner, S.,& Plater, A., (2004). Palynological evidence for the origin and development of late Holocene wetland sediments: Mdlanzi Swamp, KwaZulu-Natal, South Africa. *South African Journal of Science* 100, 220–229.

Tusenius, M. L. (1989). Charcoal analytical studies in the north-eastern Cape,. *South Africa. Goodwin Series*, 77-83.

Tweddle, J.C. and& Edwards, K.J., (2010). Pollen preservation zones as an interpretative tool in Holocene palynology. *Review of Paleobotany and Palynology*, 161, 59-76.

Tyson, P. D. (2000). Late-Quaternary and Holocene palaeoclimates of southern Africa: a synthesis. *South African Journal of Geology*, 102(4), 335-349.

Umbanhowar Jr, C. E., and& Mcgrath, M. J. (1998). Experimental production and analysis of microscopic charcoal from wood, leaves and grasses. *The Holocene*, 8(3), 341-346.

van der Merwe, R.H., (2014). Ikhanda, an ethno-historical archaeological investigation of Nguni military homesteads between the Mfolozi and Tugela Rivers, Kwa-Zulu Natal, South Africa, *University of Pretoria, Pretoria*, 177 pp.

Van Deventer, H., Smith-Adao, L., Mbona, N., Petersen, C., Skowno, A., Collins, N.B., Grenfell, M., Job, N., Lötter, M., Ollis, D., Scherman, P., Sieben, E. and& Snaddon, K. (2018). South African National Biodiversity Assessment 2018: Technical Report. Volume 2a: South African Inventory of Inland Aquatic Ecosystems (SAIIAE). Version 3, final released on 3 October 2019. Council for Scientific and Industrial Research (CSIR) and South African National Biodiversity Institute (SANBI): Pretoria, South Africa. Report Number: CSIR report number CSIR/NRE/ECOS/IR/2018/0001/A; SANBI report number http://hdl.handle.net/20.500.12143/5847.

Van Deventer, H., Smith-Adao, L., Mbona, N., Petersen, C., Skowno, A., Collins, N.B., Grenfell, M., Job, N., Lötter, M., Ollis, D., Scherman, P., Sieben, E. and Snaddon, K. 2018. South African National Biodiversity Assessment 2018: Technical Report. Volume 2a: South African Inventory of Inland Aquatic Ecosystems (SAIIAE). Version 3, final released on 3 October 2019. Council for Scientific and Industrial Research (CSIR) and South African National Biodiversity Institute (SANBI): Pretoria, South Africa. Report Number: CSIR report number CSIR/NRE/ECOS/IR/2018/0001/A; SANBI report number http://hdl.handle.net/20.500.12143/5847.

Vellend, M., Brown, C. D., Kharouba, H. M., McCune, J. L., and& Myers-Smith, I. H. (2013). Historical ecology: using unconventional data sources to test for effects of global environmental change. *American Journal of Botany*, 100(7), 1294-1305.

Waddington, J. C. (1969). A Stratigraphic Record of the Pollen Influx to a Lake in the Big Woods of Minnesota. In United States Contributions to Quaternary Research: Papers

Presented on the Occasion of the VIII Congress of the International Association for Quaternary Research, Paris, France, 1969 (Vol. 123, p. 263). *Geological Society of America*.

Walker, M., (2005): Quaternary dating methods. John Wiley and Sons Ltd. Chichester.

Watkeys, M.K., Mason, T.R.,& Goodman, P.S., (1993). The role of geology in the development of Maputaland, *South Africa. Journal of African Earth Sciences (and the Middle East)*, 16(1-2), 205-221.

Weisser, P.J., (1978). Changes in area of grasslands on the dunes between richards bay and the mfolozi river, 1937 to 1974. Proceedings of the Annual Congresses of the Grassland Society of Southern Africa, 13(1), 95–97.

Whitlock, C. and Larsen, C., 2001. Charcoal as a fire proxy. Tracking Environmental Change Using Lake Sediments. Kluwer Academic Publisher, Dordrecht.

Whitlock, C. and& Larson, C., (2001):Charcoal as a fire proxy. In: Tracking environmental change using lake sediments terrestrial, algal and siliceous indicators, Smol J. P., Birks H. J. B. and Last W. M. (eds), Kluwer Academic Publishers, Dordrecht, pp. 75-97.

Willis, K. J., Bailey, R. M., Bhagwat, S. A. & Birks, H. J. B. (2010). Biodiversity baselines, thresholds and resilience: testing predictions and assumptions using palaeoecological data. *Trends in ecology & evolution*, 25(10), 583-591.

Wood, R., (2015). From revolution to convention: the past, present and future of radiocarbon dating. *Journal of Archaeological Science* 56, 61-72.

Wright, H. E. (1991). Coring tips. Journal of Paleolimnology, 6(1), 37-49.

Xu, C., McDowell, N. G., Fisher, R. A., Wei, L., Sevanto, S., Christoffersen, B. O., Weng, E. and & Middleton, R. S., (2019). Increasing impacts of extreme droughts on vegetation productivity under climate change. *Nature Climate Change*, 9(12), 948-953.

Yi-Lun, H. U., Guo-Xu, J. I., Ji-Hong, L. I., Ganjurjav, H. A. S. B. A. G. A. N., Guo-Zheng, H. U.&, and Qing-Zhu, G. A. O. (2022). Interpretation of IPCC AR6: terrestrial and freshwater ecosystems and their services. *Advances in Climate Change Research*, 0.

Zhao, X., Dupont, L., Schefuß, E., Meadows, M. E., Hahn, A. and & Wefer, G., (2016). Holocene vegetation and climate variability in the winter and summer rainfall zones of South Africa. *The Holocene*, 26(6): 843-857.

Appendix A: Chronologies

OSL dating

To understand geomorphological processes and historical sediment transport it is important to acquire accurate and precise technical chronology more so when existing historical records are sparse. There is vast knowledge that can be extracted from sedimentary archives of the changes that occurred in past environmental conditions but interpretation is based on a confident chronology (Madsen and Murray, 2009). Radiocarbon dating has its limitations where it requires an adequate amount of organic material originating from that area present in the sediment. In samples that are younger than 450years and older than 50years present itself with inaccuracies because of the fluctuations of the C_{14} productions in the atmosphere (Madsen and Murray, 2009). The fluctuations have been thought to cause uncertain calibrations because the C_{14} that was absorbed could have occurred many periods in the past which may results in calibration uncertainties essentially when C_{14} years are converted into calendar years (Madsen and Murray, 2009).

The idea that visible light could be used to stimulate electrons and this idea could establish a date of deposition of sediment was first introduced in a seminal paper by Huntley et al. (1985). Luminescence dating is based on the principal that materials which contain radioactive isotopes or materials which lie close to these isotopes are subject to low levels of radiation (Walker, 2005). Optically stimulated luminescence is a method where the electrons are released from the structural defects by shinning a beam of light onto the sample and the luminescence signal is a reflection of the number of electrons that are trapped in the crystal lattice (Walker, 2005).

To arrive at an estimated age by using TL or OSL there are certain parameters that need to be calculated first the DE known as the equivalent dose that measures the radiation required to generate a TL signal. This signal is equivalent to a recent event of exposure to sunlight (Madsen and Murray, 2009). The second parameter is the environmental dose rate which in essence is the dose of radiation (per unit of time) which is absorbed by the mineral since the zeroing of the luminescence clock was initiated by either the firing or exposure to sunlight. Once these parameters are determined then the TL/OSL age can be calculated from the following equation following equation

$$TL/OSL\ age = \frac{equivatent\ dose}{\text{dose rate}}$$

For many years OSL was not considered as an alternative approach to C_{14} dating. This is mostly due to the possibility of inadequate light exposure to final sedimentation which means that the young ages could potentially be overestimated (Madsen and Murray, 2009). Low sensitivity is expected to prevent the measurement of luminescence particularly in young material which through research has been proven to not be the case (Madsen and Murray, 2009).

OSL is a technique that uses the trapped charge that is stored over long periods of time in natural crystalline materials (Madsen and Murray, 2009). The release of the trapped charge occurs when the material is exposed to heat or light. The trapped charge then recombines and is released by means of heat (Madsen and Murray, 2009). Emission of light where the stimulating mechanism can be in the form of heat is called thermoluminescence where the emission of light where the stimulating mechanism is light is called optically stimulated luminescence (Madsen and Murray, 2009). Calibration of luminescence signal in terms of dose is important to ensure an accurate measure (Madsen and Murray, 2009). This is accomplished by measuring the signal that results from the exposure of naturally occurring radiation. Whereas an OSL signal is then regenerated by the exposure of an artificial dose of radiation stimulated from the laboratory (Madsen and Murray, 2009)

Thermoluminescence is used for dating sediments in recent decades it employs quartz grains and is based on the principal that if a sample has been irradiated and subsequently heated then light is emitted as a function of temperature (Lian and Roberts, 2006). This is known as a ‘glow curve’ which depends on the age of the sample. OSL is closely related to TL this method works well for sediment that is of wind-borne and water-borne origin (Lian and Roberts, 2006).

Limitations of OSL

The depositional environment especially samples that are taken from water-lain deposits where there could be great grain to grain variability where bleaching is considered (Madsen and Murray, 2009). The possible reworking of sediment and the intermittent exposure to sunlight are sources of error in luminescence dating of sediment (Madsen and Murray, 2009). There could be variations in luminescence signals in various grains for example feldspar samples bleaching is less rapid than in quartz (Madsen and Murray, 2009). Some samples may have residual OSL and even with a few minutes of exposure to bright sunlight may be able to reduce this to an acceptable lower level under lower light intensities like cloudy

conditions the zeroing process may be less effective (Madsen and Murray, 2009). Problems may arise from the leakage of electrons from thermally stable traps which is a problem that affects both OSL and TL of feldspar and is referred to as anomalous fading (Madsen and Murray, 2009). With the variations in past water content sediment it gives rise to other sources of error which include systematic errors which occur in the calibration of the laboratory radiation sources, light contamination(Madsen and Murray, 2009)

Appendix B: Grain and Particle size description

The stratigraphy of the core was described using the Malvern method for grain and particle size analysis. The Malvern presented a dominant medium silt percentage which was present between 76- 51 cm of the core (**Figure 8.1**). Upon a visual inspection the core presented a distinct visual increase in sand content between 45-50 cm in depth, however further investigation with the use of the Malvern, the core presented an increase in sand content which extended between 50-0 cm (**Figure 8.1**).

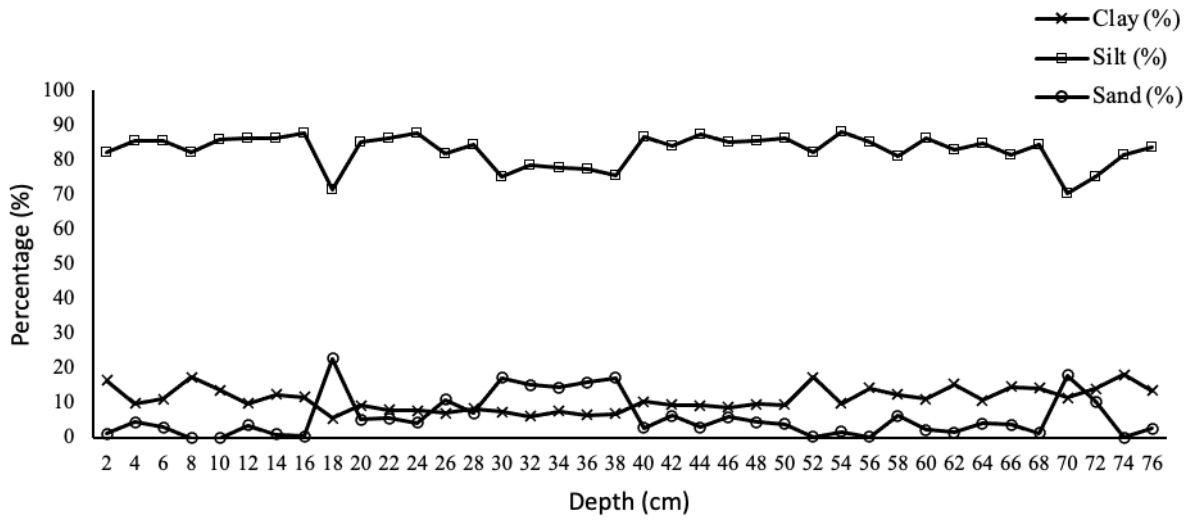

Figure 8.1. Grain particle size along the South Lake profile plotted against depth (Source: Jamie Wood)

Loss of Ignition (LOI)

The samples were initially oven dried at 105°C and weighed prior to the ignition process in the furnace. The samples are weighed after the ignition process and finally the LOI percentage is calculated by determining the weight loss of each sample.

Loss of Ignition description

The record commences with the lowest overall organic (1%) and moisture (22%) content as presented by the loss of ignition (LOI) data within the core (**Figure 8.2**). Within S-1 the

organic percentage was recorded low (1%) and later gradually increased to 4%. The moisture percentage initially recorded at a low 33% within this zone increased to 40% with an increase in depth (**Figure 8.2**). Within the hiatus zone the core presented low average organic and moisture contents (1% and 23%) respectively (**Figure 8.2**).

Zone S-2 presented an overall low organic (19%) and moisture (52%) content within S-2 (**Figure 8.2**). The zone commenced with a low organic (7%) and moisture (44%) content. The organic (72%) and moisture (89%) content gradually increased with depth (**Figure 8.2**).

The organic (38%). and moisture (53%) content were both the highest overall within S-3. The highest organic percentage recorded was 84% which fluctuated between 2% and 84% (**Figure 8.2**). The highest moisture content recorded was 82% and the lowest was 18% within this zone. With the increase in depth zone S-3 presented a decrease in organic (2%) and moisture (21%) content. The organic unit between *ca.* 1300-640 yr BP (70-160 cm) may be a result of two scenarios; either a large/series of depositional events or a short-term change in water table/environment.

Zone S-4 presented low organic and moisture contents. The highest organic content recorded in S-4 was 3% and the highest moisture content recorded was 24%. Zone S-4 indicated a low organic (4%) and the moisture content (30%) content.

Overall, section S-1 had the lowest overall organic (19%) and moisture (52%) content within the core. Zone S-2 and S-3 presented the highest organic (38%) and moisture (53%) contents in the core. Zones S-4 presented low organic (2%) and moisture (21%) contents however zone S-4 did not record LOI results as low as S-1 (**Figure 8.2**).

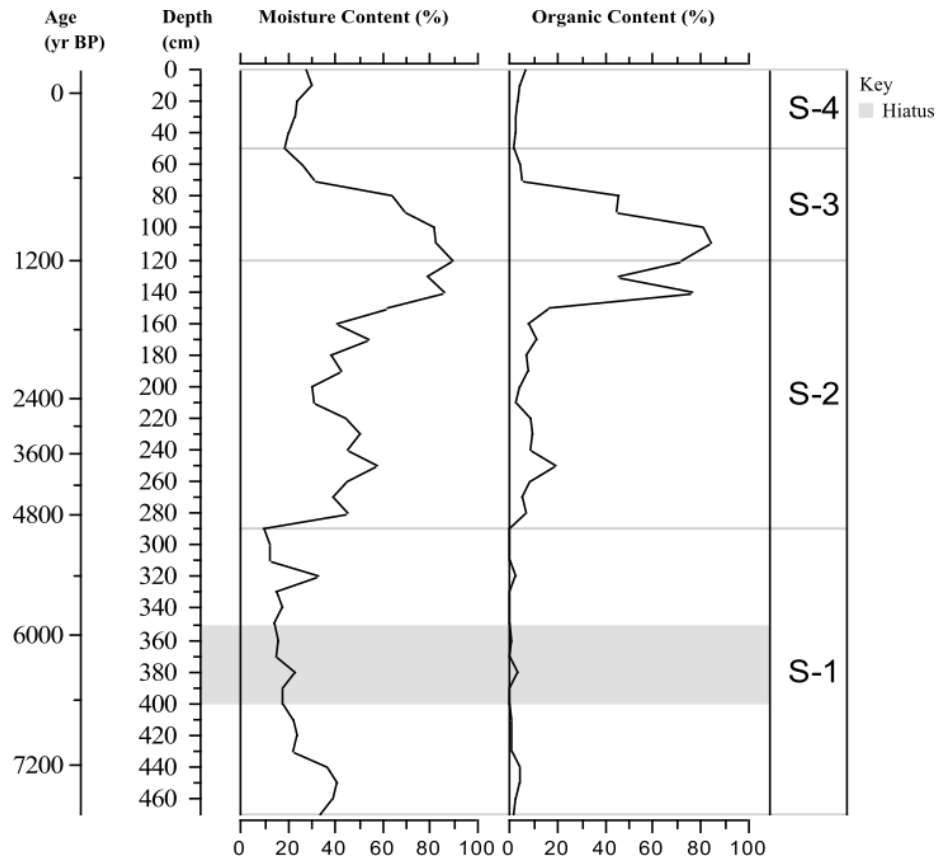

Figure 8.2. Moisture and organic content profiles of core south Lake Futululu plotted against their depth scales along zonations based on pollen data (Source: Jamie Wood)

Chronology

The samples were processed at the University of Gloucestershire in England. The samples were wet sieved and treated with HCl and H_2O_2 to remove organic materials and carbonates. The samples were density separated using heavy liquid techniques. Samples were further refined in HF and was monitored by an IR stimulator. Any further contaminated fluorides were dissolved using HCL and finally rinsed and dried. The particles were then exposed to an intense light source to achieve optical stimulation.

The OSL chronology of core included the findings of sediment particles which were classified into 3 categories: coarse (180-250 µm), medium coarse (125-180 µm) and fine (5-15 µm) grained Quartz particles. The core commenced with particles which ranged from medium course (462-410 cm), course (387-209 cm), fine (181-72 cm) and finally returning to medium course (48-17 cm) Quartz particles (**Table 1.1**).

Table 1.1 GL15015 Single-Grain OSL age summary

Grains (n=)	Zero-dose (%)	CAM Age (ka)	MAM Age (ka)	FMM_{min} Age (ka)	FMM_{max} Age (ka)	FMM_{maj} Age (ka)
115	6	0.19±0.03	0.06±0.01	0.04±0.01	0.27±0.04	0.27±0.04

(Source: Jamie Wood)

Appendix C: Procedure for sub sampling

Source: adapted from Faegri and Iverson (1989) and Finch (2005)

1. With a clean and new scalpel or razor blade, clean the surface of the core by gently scraping material off the surface, parallel to the strata to avoid contamination.

2. Determine a suitable sampling interval by taking into account the estimated age of basal sediments, the total length of the core and the stratigraphy such that samples are taken on either side of distinct chronological or stratigraphic boundaries. Initially a wide sampling interval of 10cm was chosen for pollen and microscopic charcoal analysis of the South Lake core.

3. Each sample contained exactly $1cm^3$ of sediment.

4. Transfer each sample into an airtight plastic storage vial.

5. It is necessary for samples to represent the shortest possible period therefore consisting of thin slices across the entire core. Peat samples of approximately 50g should be stored in polythene bags and refrigerated.

Appendix D: Procedure for preparing fossil pollen samples

Source: adapted from Faegri and Iverson (1989), Moore *et al*. (1991), Baxter (1996) and Finch (2005)

Note:

- Samples will be centrifuged at 4000 rpm for 3 minutes, unless otherwise specified.
- Use 100ml profiled, sealable polypropylene tubes in a swing out centrifuge.
- The temperature of the water bath should be maintained between 50-60°C unless otherwise stated.
- Label all samples clearly.

A. Measurement of sediment

Each sample should contain 1cm^3 of wet sediment. To achieve 1cm^3 of sample the volumetric displacement should be used. This is done by measuring out 9cm^3 of distilled water into a measuring cylinder and adding sediment until the total volume in the measuring cylinder reached 10cm^3.

B. Addition of pollen spike

1. Place pollen spike solution on a magnetic stirrer plate for 1 hour prior to use.
2. Add 1 ml of spike to each peat sample using a graduated plastic syringe.

C. Removal of humic acids and clay materials (sodium hydroxide digestion)

1. To each sample, add 20ml 15% sodium hydroxide (NaOH) and stir.
2. Place samples in a heated water bath for 10 minutes and stir.
3. Wash and stain through a 180µm sieve using distilled water.
4. Centrifuge and decant.

5. Repeat step 3 untill the supernant becomes clear,

D. Removal of clastic material (hydrofluoric acid digestion

1. To each sample, add 20ml of 10% hydrochloric acid (HCl), stir, centrifuge and decant.
2. In a fumehood add 20ml concentrated 40% hydrofluoric acid (HF).
3. Place the polypropylene tubes in a heated water bath for 3 hours, stirring regularly.
4. Seal the centrifuge tubes and centrifuge for 5 minutes and decant.
5. To each sample add 20ml of 10% HCl.
6. Place the samples in a heated water bath for 20 minutes and stir regularly.
7. Remove from the water bath.
8. Stir, centrifuge and decant

E. Acetolysis digestion of extraneous organic detritus

1. Add 20ml glacial acetic acid. Stir, centrifuge and decant making sure to discard as much as the supernatant as possible to avoid remaining acetic acid from reacting with the acetolysis mixture.
2. To each sample add 20ml acetolysis mixture (9 parts acetic anhydride ($[CH_3CO]_2O$) : 1 part concentrated sulphuric acid [H_2SO_4]).
3. Place in a heated water bath for 10-15 minutes, stir regularly.
4. To stop the reaction remove the samples from the water bath and place in cold water for a few seconds. Stir, centrifuge and decant.
5. Add 20ml glacial acetic acid. Stir, centrifuge and decant.
6. Add 9ml distilled water and 1ml NaOH to neutralize samples
7. Rinse samples 3 times with distilled water and add 2 drops of safranine stain to the last rinse.

8. Add 5 ml tertiary butyl (TBA), stir centrifuge and decant.

9. Add 5 ml TBA, transfer the sample from the polypropylene tube into a labelled 30ml storage vial.

F. Mounting

1. Allow the processed solution to settle overnight in a refrigerator. Using a glass pipette remove the clear liquid so as to concentrate the pollen and charcoal.

2. Place a single drop of Aquatex mounting solution on a sterile glass microscope slide.

3. Use a micropipette or a blunt toothpick to extract approximately 3 drops of the pollen solution. Add to the Aquatex, using a toothpick to mix the pollen suspension evenly within the Aquatex.

4. Place a coverslip over the Aquatex suspension and let the mixture spread to all edges. This may be aided by applying light pressure with a dissecting needle.

5. The slide should be allowed to stand for 4 hours prior to counting, to allow the pollen to disperse evenly across the slide.

Appendix E: Preparation procedure for reference collection pollen

Source: adapted from Baxter (1996) and Finch (2004)

Note:

- Centrifuge at 4000 rpm for 3 minutes, unless otherwise stipulated.
- Use 100ml profiled, sealable polypropylene tubes in a swing-out centrifuge
- The temperature of the water bath should be maintained between 50-60°C unless otherwise stipulated.
- Label all samples clearly.

A. Chemical preprocessing

1. Place the specimen in a polypropylene tube
2. Add 20ml of 10% NaOH to the specimen and stir.
3. Place the tube in a heated water bath for 5 minutes and stir regularly.
4. Strain and rinse through 300µm mesh sieve. Gently crush the material on the screen and rise with distilled water.
5. Centrifuge and decant
6. Using glacial acetic acid, transfer the contents into a 10ml centrifuge tube. Stir, centrifuge and decant.
7. To each sample add 20ml acetolysis mixture (9 parts acetic anhydride ($[CH_3CO]_2O$) : 1 part concentrated sulphuric acid [H_2SO_4]).
8. Place in a heated water bath for 5 minutes, stir regularly.
9. To stop the reaction remove the samples from the water bath and place in cold water for a few seconds. Stir, centrifuge and decant.
10. Rinse samples 3 times with distilled water and add 2 drops of safranine stain to the last rinse.

11. To prevent bacteriological and fungal spoilage, rinse in a mild phenol solution.

12. Invert the tubes onto blotting paper and allow to drain.

B. Mounting

1. Clean and label the microscope slides preferably 3 microscope slides per specimen.

2. Cut small cubes of glycerine jelly (ideally phenol impregnated brand), and with a small dissecting needle, collect pollen grains/ spores from the blotting paper. Wipe the glycerine jelly around the inside of the tube to pick up the pollen residue.

3. Place the glycerine jelly in the middle of the microscope slide and heat the slide over a heating plate to melt the jelly, being careful not to allow the jelly to boil as this will cause the texture of the jelly and the structure of the pollen to be damaged.

4. Using a dissecting needle, lower the coverslip over the jelly. While the jelly is allowed to cool and set, invert the slide to allow for the grains to allow for the grains to settle on the inside of the coverslip, to ensure that the pollen grains settle in the same focal plane.

5. After the jelly has set, scrape off the excess that may have been forced out from the coverslip.

6. Clear nail varnish should be used be painted around the edge of the coverslip to act as a sealant.

Appendix F: LacCore Microsphere Pollen Spike

The suspension contains ~16 µm diameter polystyrene microspheres (p= 1.3 g/cm^3), Milli-Q high-purity deionized water, potassium chloride to increase density (25% KCl solution) and <0.1% tween 80 (a surfactant).

The suspension was calibrated by automated Bio-Rad TC10 cell counter at the University of Minnesota Department of Pharmacology. Batch 5 ststistics are as follows: Concentration: 5.0x10^4 spheres/mL ±8% (stdev)

The spike suspension is supplied in individual 250 mL capped Erienmeyer flasks with stir-bars. These flasks are stored dark at room temperature until time of purchase or use. Each flask contains a minimum of 200 mL of usable spike suspension.

Microspheres have a density and chemical resistance similar to that of fossil pollen, and can thus be added to the sample at the beginning of preparation. Spheres are easily recognisable as slightly translucent black-brown balls in the pollen slide.

Spike solution should be kept tightly capped when not in use. Solubility of KCl at 4 deg C is about 280 g/L, so refrigeration should not cause KCl to come out of solution, however, the high salinity of the solution should preclude microbal growth, making refrigeration unnecessary. Place on a magnetic stir plate at room temperature for at least one hour before use. If not consumed within 18 months from time of first opening, solution should be recalibrated using a hemo-cytometer or particle counter. Appearance of KCl precipitate is also an indicator that evaporation has occurred abs suspension concentration should be checked.

Appendix G: Macrocharcoal extraction (Stevenson and Haberle, 2005)

1. Measure out 1 cm^3 wet sediment into a sample vial.
2. Disperse 5-10 ml Potassium Hydroxide (KOH) or Sodium Pyrophosphate ($Na_4P_2O_7$) solution.
3. Add wet sediment to KOH or $Na_4P_2O_7$. Heat sample if rapid dispersal is required or leave overnight.
4. To achieve good separation of clumped sediment use a mechanical mixer or a very gentle stirring action with a stirring rod.
5. Pour off and discard supernatant after sediment settles.
6. Re-suspend in very dilute Hydrogen Peroxide (H_2O_2) (4-6% only), or alternatively Sodium Hypochlorite (ClO^-) (4-6%), leaving it overnight. This will be enough to bleach the organics excluding the charcoal.
7. Mix well and wet sieve this through a 125 µm sieve (150/210/250 µm or a combination of these, and then put the course fractions back into a test tube in water. This can be stored until counting is done.
8. Pour the solution into a petri dish with graph paper underneath and place under a binocular microscope (approximately x10-15 magnification). Count the angular black (opaque) particles.
9. Alternative to Step 8. Pour the solution into a petri dish with graph paper underneath and place underneath and place under a Leica M60 steromicroscope coupled with a digital camera and image analysis software (WinSeedle 2009).

Appendix H: Bayesian Model Calibrated Ages

depth	min	max	median	wmean
0	-66.9	-60.8	-63.9	-63.8
1	-63.6	-55.6	-59.7	-59.6
2	-61	-49.5	-55.7	-55.3
3	-58.8	-43	-51.8	-51.1
4	-56.6	-36.5	-47.9	-46.8
5	-54.5	-29.9	-43.9	-42.6
6	-52.5	-23.3	-40	-38.4
7	-50.4	-16.7	-36	-34.1
8	-48.4	-10.1	-32.1	-29.9
9	-46.6	-3.4	-28.1	-25.7
10	-44.6	3.2	-24.2	-21.4
11	-42.7	10	-20.3	-17.2
12	-40.8	16.6	-16.3	-12.9
13	-38.8	23.3	-12.4	-8.7
14	-36.8	30.2	-8.4	-4.5
15	-34.9	36.7	-4.5	-0.2
16	-32.9	43.4	-0.5	4
17	-31	50	3.4	8.3
18	-29	56.7	7.4	12.5
19	-27	63.4	11.4	16.8
20	-25.3	70.2	15.3	21
21	-23.3	76.9	19.2	25.2
22	-21.3	83.5	23.2	29.5
23	-19.3	90.3	27.2	33.7
24	-17.3	97.1	31.2	38
25	-15.5	103.7	35.2	42.2
26	-13.5	110.4	39.2	46.4

27	-11.5	117.1	43.1	50.7
28	-9.6	123.9	47	54.9
29	-7.7	130.5	51.1	59.2
30	-5.8	137.3	55.1	63.4
31	11.5	145.6	65.5	74.4
32	27.7	154.7	76.2	85.5
33	42.1	165.1	86.8	96.3
34	54.8	175.7	97.7	107.2
35	66.4	185.7	109.4	118.1
36	77	197.5	121.3	129
37	86	208.6	133.4	140
38	94.6	220.9	145.5	150.9
39	102.5	233.6	157.3	161.8
40	110.2	246.7	169.1	172.8
41	117.7	260.1	180.7	183.7
42	124.6	274.4	191.8	194.7
43	130.8	289.8	202.8	205.6
44	137	305.4	213.8	216.6
45	142.4	320.8	224.7	227.4
46	148.5	336.5	235.5	238.4
47	153.4	352.5	246	249.3
48	159.4	368.9	256.9	260.2
49	164.3	385.2	267.4	271.1
50	169.8	401.4	278.2	282.1
51	174	419.4	289.2	293.1
52	178.2	436.7	299.7	304
53	183.1	455.1	310.3	315
54	188.7	472	321.2	325.9
55	192.8	490	331.8	337
56	196.5	507.9	342.7	347.8
57	201	527	353.5	358.8
58	205.4	546.3	364.2	369.7
59	209.3	565.2	374.8	380.8

60	213.8	582.1	385.7	391.7
61	244.4	601.9	411.1	416.8
62	276.6	620.4	436.4	442
63	306.5	640.1	461.6	467.1
64	337.2	659	487.2	492.2
65	367	678.5	512.4	517.3
66	397.5	698.3	537.7	542.5
67	427.1	718.5	563.1	567.7
68	455.5	738.1	588.8	592.8
69	485.4	758.3	614	617.9
70	514.5	778.5	639.7	643.1
71	543.1	799.1	665.2	668.3
72	571	820.7	690.4	693.4
73	598.7	841.7	716.2	718.6
74	626.6	863.7	741.5	743.7
75	653.4	884.9	767	768.8
76	680.2	908.3	792.3	794
77	707.2	930.9	817.4	819.2
78	733.3	954.9	842.4	844.6
79	758.5	978	867.2	869.8
80	783.2	1001	892.2	895.1
81	806	1024.5	916.9	920.3
82	828.5	1048.5	941.3	945.6
83	851.2	1073.6	965.6	970.9
84	873.4	1098	990.4	996.2
85	896.9	1123.3	1014.9	1021.4
86	919.8	1149.3	1039.8	1046.7
87	942.1	1175.1	1064.5	1071.8
88	963.4	1202	1089.5	1096.9
89	985.1	1229	1114.3	1121.9
90	1006.3	1257.2	1139.2	1146.9
91	1009.7	1258.3	1140.7	1148.7
92	1013.5	1259.3	1142.3	1150.4

93	1017.1	1259.5	1143.5	1152.1
94	1020.7	1260.2	1145.1	1153.8
95	1024.6	1261.3	1146.5	1155.5
96	1027.9	1261.8	1147.9	1157.2
97	1031	1262.6	1149.4	1158.9
98	1033.6	1263.2	1150.8	1160.6
99	1037.7	1263.9	1152.1	1162.3
100	1040.1	1265	1153.9	1164
101	1042.8	1265.3	1155.3	1165.7
102	1045.7	1266.3	1157	1167.4
103	1048.7	1267.4	1158.3	1169
104	1051	1268.1	1159.9	1170.7
105	1053.3	1269	1161.3	1172.5
106	1055.6	1270.2	1162.9	1174.3
107	1058.5	1271.2	1164.4	1176
108	1060.6	1272.2	1166.2	1177.8
109	1063.9	1273.7	1167.6	1179.5
110	1066.1	1274.6	1169.3	1181.2
111	1067.7	1276.2	1170.7	1183
112	1070.4	1277.3	1172.2	1184.7
113	1073.1	1278.9	1174.3	1186.6
114	1075.2	1280.1	1175.7	1188.2
115	1078.8	1281.7	1177.6	1190
116	1080.9	1283.5	1179.3	1191.8
117	1082.6	1284.9	1180.9	1193.5
118	1086.3	1286.7	1182.7	1195.3
119	1089.2	1288.8	1184.7	1197.1
120	1090.6	1291.4	1186.7	1198.9
121	1095.2	1293.3	1190.1	1202.4
122	1100	1295.3	1193.6	1205.8
123	1104.6	1298.2	1197	1209.1
124	1108.9	1302.3	1200.5	1212.6
125	1113.3	1306.6	1204.2	1216.1

126	1117.8	1311.3	1207.8	1219.5
127	1121.8	1316.1	1211.4	1222.9
128	1125.2	1321.5	1215.4	1226.5
129	1128.7	1327	1219.1	1229.8
130	1131.4	1333	1223.1	1233.2
131	1134.3	1339.1	1226.7	1236.3
132	1137.6	1344.9	1230.9	1239.6
133	1139.6	1350.3	1234.7	1242.8
134	1142.2	1357.2	1238.7	1246
135	1144.5	1363.3	1242.6	1249.3
136	1146.2	1369.6	1246.6	1252.5
137	1148.3	1375.8	1250.3	1255.8
138	1150.6	1383.4	1253.7	1258.9
139	1151.8	1389.5	1257.1	1262.2
140	1152.8	1396.6	1260.4	1265.4
141	1155.1	1403.1	1263.6	1268.6
142	1156.2	1411.9	1266.6	1271.8
143	1157.6	1419.2	1269.5	1275
144	1158.9	1427.7	1272.9	1278.4
145	1160.3	1433.9	1275.6	1281.6
146	1161.5	1441.9	1278.2	1284.8
147	1163	1451	1281.1	1288
148	1164	1458.4	1283.9	1291.2
149	1165.1	1465.4	1286.7	1294.5
150	1166.7	1473.5	1289	1297.6
151	1173.9	1479.9	1293.2	1302.4
152	1181.6	1483.1	1297.3	1307.1
153	1189.4	1485.4	1301.1	1311.7
154	1196.1	1492.4	1305.1	1316.6
155	1202.9	1497	1308.7	1320.9
156	1210.5	1500.3	1312.7	1325.9
157	1217.4	1506.4	1316.4	1330.5
158	1222.8	1510.5	1320.2	1335.2

159	1229.6	1515.7	1323.8	1339.8
160	1236.4	1521.9	1327.6	1344.5
161	1242	1525	1331.6	1349.3
162	1247.9	1530.6	1335.3	1353.8
163	1254.1	1537.5	1338.9	1358.6
164	1259	1546.4	1342.6	1363.4
165	1264.9	1553.7	1346.3	1368.2
166	1270	1562.5	1350	1372.8
167	1275	1571.5	1353.7	1377.5
168	1280.1	1579	1357.4	1382.2
169	1285	1588.7	1361.4	1387.1
170	1289.5	1592.6	1365.6	1391.9
171	1293.6	1601.7	1369.8	1396.7
172	1297.4	1607.8	1373.9	1401.4
173	1300.5	1617.1	1378.4	1406.3
174	1304	1625.8	1382.5	1411.1
175	1307.5	1633.5	1386.5	1415.7
176	1310.4	1642.6	1390.8	1420.5
177	1313.4	1651.8	1394.4	1425.2
178	1316.6	1662.4	1398.1	1429.9
179	1319.4	1672.5	1402.5	1434.6
180	1322	1680.4	1407.2	1439.3
181	1353.9	1704.6	1444.8	1474.3
182	1376.9	1730.8	1484.6	1509.4
183	1394	1763.9	1525.3	1544.6
184	1408.8	1804	1565.2	1580
185	1422.7	1846.5	1604.3	1615.4
186	1435.5	1893	1641.7	1650.5
187	1449.3	1941.6	1678.7	1685.8
188	1460.1	1996.6	1714.5	1721.1
189	1471.3	2052.2	1749.6	1756.3
190	1484	2111.9	1785.9	1791.9
191	1493.4	2169.7	1820.6	1826.7

192	1504.2	2227.9	1856.2	1862.1
193	1515.4	2290.7	1891.3	1897.4
194	1524.8	2354.3	1926.7	1932.5
195	1533.1	2417.7	1960.1	1967.2
196	1543.4	2480.1	1994.7	2002
197	1553.2	2541.3	2028.3	2036.4
198	1561.9	2603.2	2062	2070.9
199	1571.1	2665	2096.5	2105.6
200	1579.3	2728.3	2130.2	2140.3
201	1589	2790.4	2163.8	2174.8
202	1596.6	2853.1	2197.2	2209.5
203	1604.9	2918.1	2229.4	2243.7
204	1614.3	2982.4	2262.6	2278.1
205	1622.6	3047.7	2297	2312.6
206	1628.8	3110.3	2330.8	2346.8
207	1637.9	3173.7	2365.4	2381.4
208	1645.8	3238.5	2398.4	2415.8
209	1654.9	3302.6	2432.4	2450.2
210	1663.9	3367.3	2466.4	2484.7
211	1710	3389.8	2501	2519.4
212	1747.1	3410.7	2535.6	2553.5
213	1785	3432.2	2571.5	2588.7
214	1823.9	3456.9	2609.9	2623.4
215	1856.7	3480.1	2644.8	2657.9
216	1892.3	3499.3	2683.4	2692.9
217	1919.8	3522.2	2718.7	2727.3
218	1949.5	3544.2	2754.6	2762.3
219	1971.9	3571.9	2792	2797
220	1997.6	3600.4	2829.1	2831
221	2019.9	3625.8	2866.9	2865.9
222	2046.7	3655.4	2904.6	2900.7
223	2064.8	3681.1	2944.1	2935
224	2085	3713.6	2983.3	2969.8

225	2100.9	3744.9	3022.7	3004
226	2119.8	3775.6	3060.4	3038.6
227	2138.7	3810.6	3098.6	3073
228	2153.1	3846	3133.3	3106.9
229	2165.9	3885.6	3171.1	3141.6
230	2184.7	3926.5	3207.4	3176.4
231	2197.9	3964.9	3241.4	3210.9
232	2219.2	4008.5	3275.3	3245.1
233	2233.2	4057.4	3311.1	3279.7
234	2248.8	4103.3	3342.6	3314.3
235	2259.5	4154.2	3375.8	3348.1
236	2277	4205.6	3411	3382.5
237	2294.6	4262.6	3444.7	3416.9
238	2311	4322	3477.8	3451.3
239	2325.9	4384.3	3509.9	3485.2
240	2341.6	4452.1	3545.2	3520.2
241	2416.1	4455.5	3578.1	3554.9
242	2484.5	4463.9	3611.3	3589.4
243	2556.7	4468.5	3645.8	3623.9
244	2625	4472.7	3680.2	3658.8
245	2697.4	4482.6	3715.1	3693.9
246	2770	4491.4	3747.7	3728.8
247	2839.4	4497.6	3780.8	3763.7
248	2913.5	4504	3815.2	3798.4
249	2987.1	4512	3848.4	3833.2
250	3059.5	4518	3882.1	3868
251	3134.3	4525.9	3916.6	3902.6
252	3205.3	4535.9	3950.5	3937.8
253	3275.3	4544.4	3983.4	3972.5
254	3345.1	4554.8	4016.9	4007.4
255	3421	4565.6	4050.5	4042.4
256	3497.1	4575.6	4084.3	4077.4
257	3564.9	4584.9	4117.1	4112.1

258	3633.5	4596.6	4151.1	4147.1
259	3700.4	4606.4	4183.9	4181.8
260	3767.6	4620	4217.2	4216.6
261	3830.3	4633.3	4251.5	4252.1
262	3893.3	4647.8	4286.3	4287.3
263	3952.4	4662.8	4321.8	4322.7
264	4011.2	4677.8	4356	4357.9
265	4065.9	4694.8	4391.8	4392.9
266	4118.3	4715.2	4427.3	4428.1
267	4165.8	4741.4	4462	4463
268	4204.3	4769.3	4497.9	4498.1
269	4240.8	4801.3	4533.4	4533.5
270	4271.2	4838.8	4568.8	4568.7
271	4314.5	4845.8	4588	4590.5
272	4357.1	4855.7	4606.3	4612.2
273	4399.6	4865.3	4625.4	4634
274	4439.8	4875.7	4644.5	4655.8
275	4476.7	4886.5	4664.1	4677.5
276	4509	4899.8	4685.2	4699.1
277	4535.4	4916.3	4706.8	4720.8
278	4553.4	4939.5	4729.7	4742.5
279	4566.3	4965	4752.4	4764.1
280	4578.8	4994.4	4775.6	4785.9
281	4591.2	5025.8	4798.4	4807.1
282	4600.8	5061.7	4820.3	4828.4
283	4611.8	5100	4841.7	4849.6
284	4622	5140.1	4863.2	4870.9
285	4631.1	5183.4	4884.3	4892.1
286	4638.8	5225.9	4903.9	4913.1
287	4646.1	5272.9	4924.8	4934.5
288	4653.3	5316.8	4944.1	4955.8
289	4659.4	5363	4962.7	4976.8
290	4663.6	5412.2	4981	4998

291	4668.2	5457.8	4999.8	5019.1
292	4674.5	5509.8	5018.2	5040.5
293	4677.3	5556.6	5036.9	5061.4
294	4685	5608	5054.7	5083
295	4688.8	5657.8	5074.7	5104.1
296	4691.3	5707.9	5091.9	5125.2
297	4697.9	5755.8	5110.3	5146.5
298	4702.7	5807.1	5129.1	5167.5
299	4706.7	5858.3	5146.9	5188.9
300	4713	5909.6	5164.7	5210
301	4728.6	5918.6	5180.5	5224.2
302	4746.4	5930.2	5194.2	5238.6
303	4761.5	5941.6	5209.1	5253.2
304	4774.9	5947.4	5225.6	5267.3
305	4786.7	5959.6	5241	5281.6
306	4798.8	5969.9	5256.4	5296.1
307	4811.6	5979.4	5273.4	5310.2
308	4824.4	5992.7	5289.7	5325
309	4835.3	6006.1	5306.5	5339.3
310	4844.9	6020.8	5322.8	5354
311	4855.7	6032.9	5338.7	5368.7
312	4866.2	6049.2	5355.1	5383.5
313	4872	6061.6	5370.6	5397.9
314	4880.3	6074.9	5385.8	5412.1
315	4888.8	6091.4	5400.8	5426.3
316	4896.7	6104.6	5416.6	5441
317	4903.9	6124.4	5431.5	5455.4
318	4911.4	6144	5447.5	5470.3
319	4918.8	6161.6	5462.3	5484.9
320	4924.4	6179.1	5478.1	5499.3
321	4930.3	6196.6	5491.6	5514
322	4937.4	6219.7	5506.4	5528.4
323	4945	6240.9	5520.6	5542.8

324	4949.5	6260.4	5534.1	5557.4
325	4954.3	6285.3	5548.3	5572.1
326	4961.4	6310.8	5562.4	5587.1
327	4968.1	6336	5576.9	5601.6
328	4974.5	6363.2	5591.1	5616
329	4979.3	6383.7	5605.8	5630.9
330	4985.7	6406.5	5619.5	5645.4
331	5002.9	6414.8	5631.9	5658.6
332	5020.2	6428.6	5645.4	5671.9
333	5037.3	6441.3	5659.5	5685.2
334	5054.3	6448.7	5674	5698.9
335	5069.1	6458.6	5689	5712.3
336	5078.2	6468.5	5703	5725.9
337	5094.7	6479.7	5716.2	5739
338	5108.3	6489.6	5731.1	5752.2
339	5121.9	6501.7	5744.7	5765.9
340	5132.4	6510	5757.2	5779.4
341	5145.5	6528.8	5770.6	5792.8
342	5154	6540.4	5783.8	5806.3
343	5165.2	6551.6	5797.3	5819.3
344	5175.7	6558	5810.4	5832.6
345	5186.6	6575.4	5824.8	5846.3
346	5194.2	6590.8	5837.9	5859.5
347	5202.7	6603.2	5851.6	5872.7
348	5212.4	6617.3	5863.6	5886.1
349	5220.9	6637.6	5876.4	5899.8
350	5229.5	6658.6	5888.6	5913.1
351	5236.6	6679.2	5901.3	5926.4
352	5241.2	6698.4	5915	5939.6
353	5249.6	6714.9	5927.4	5953.1
354	5256	6742.6	5940.4	5966.4
355	5261.3	6767.3	5952.5	5979.2
356	5270	6786	5965	5992.8

357	5275.2	6806.5	5978.6	6006.3
358	5282.2	6833	5990.8	6019.3
359	5288.5	6858.2	6003.4	6032.6
360	5295.7	6884.1	6016.5	6045.9
361	5316.1	6892.4	6029.3	6059.7
362	5331.7	6903.9	6042.3	6073.2
363	5350.6	6909.1	6054.2	6086.7
364	5367.8	6918.2	6068.7	6100.1
365	5389.8	6926.2	6083.2	6113.9
366	5401.9	6932.7	6099	6127.7
367	5416.7	6947.3	6112.6	6141.4
368	5434.5	6963.2	6127	6155.1
369	5448	6973.5	6139.3	6168.7
370	5459.7	6981.7	6155.1	6182.3
371	5473.2	6995.6	6169.5	6195.7
372	5485	7008.6	6182.2	6209.8
373	5497.3	7023.5	6198.1	6223.7
374	5506.6	7038.1	6212.4	6237
375	5520.8	7050.4	6228.5	6250.6
376	5530.9	7057.4	6242.3	6264.7
377	5542.6	7074	6257.4	6278.3
378	5556.1	7093.5	6272.2	6292
379	5567.2	7112.3	6286.7	6305.4
380	5576.9	7130.3	6300.7	6319.1
381	5590.2	7147.3	6313.8	6333.4
382	5602.3	7164.5	6326.8	6346.6
383	5615.6	7184.2	6341	6360
384	5623.3	7202.6	6355.1	6373.7
385	5631.5	7223.7	6370.3	6387.6
386	5641.5	7241.9	6383.8	6401.4
387	5649.5	7264.5	6397	6415.1
388	5656	7282.3	6410.4	6428.5
389	5662.1	7304.8	6425	6442.5

390	5670.7	7325.7	6437.9	6456
391	5693.2	7337	6453.8	6471.9
392	5712.9	7349.9	6470.2	6487.7
393	5731.4	7361.7	6485.6	6503
394	5752.5	7371.5	6501.4	6519.1
395	5769.2	7382.7	6517.8	6534.7
396	5785.8	7401	6532.8	6550.4
397	5806.1	7411.6	6548.4	6566.4
398	5820.7	7421.7	6564.2	6582
399	5834.2	7433.7	6579.8	6597.7
400	5847.9	7443.5	6595.5	6613
401	5864.2	7460.9	6612.8	6628.4
402	5878.3	7479.8	6628.7	6644.4
403	5888.3	7496.5	6643	6659.9
404	5900.9	7507.4	6658	6675.6
405	5913.2	7527.9	6673.5	6691.2
406	5924.9	7543.2	6689.8	6707.3
407	5931.6	7560.1	6705.8	6722.9
408	5941.8	7581.4	6719.4	6738.4
409	5952.3	7598.6	6736.2	6754.1
410	5965.4	7623	6751.1	6770.2
411	5972.8	7646.6	6765.6	6785.9
412	5980.6	7673.4	6779.6	6800.7
413	5992.9	7696	6794.7	6816.1
414	6000.1	7735.8	6810.4	6832
415	6009.9	7764.5	6824.6	6847.6
416	6018	7793.8	6838.6	6863.1
417	6026.3	7826.4	6853.5	6878.5
418	6030.1	7860	6868.2	6894.2
419	6037	7885.7	6882	6909.1
420	6047.3	7914.6	6896.3	6924.5
421	6064.2	7925.6	6911	6938.7
422	6076.2	7939.3	6926.6	6953.6

423	6093.1	7949.8	6939.2	6967.7
424	6106.2	7963.5	6955	6982.4
425	6119.4	7978	6970.1	6996.8
426	6129.9	7986.9	6985.3	7011.5
427	6142.3	8002.7	7001.3	7026.4
428	6154.4	8019.3	7013.7	7039.7
429	6169.4	8038.8	7027.4	7054.4
430	6178.7	8056.2	7043.4	7068.9
431	6191	8073.5	7057.5	7083.7
432	6204.1	8088.8	7071.6	7098.3
433	6213.6	8114.7	7086.6	7112.4
434	6227.2	8135.7	7100.3	7125.7
435	6235.3	8150.5	7113.8	7140.2
436	6246.3	8171.9	7128.1	7154.9
437	6256.1	8185.9	7141.6	7169.2
438	6268.1	8206.1	7155.9	7183.6
439	6276	8230.6	7169.4	7198.2
440	6286	8247.3	7183.6	7212.9
441	6296.5	8268.3	7196.8	7227.4
442	6301.7	8293.2	7209.8	7242.2
443	6308.9	8309.6	7223.7	7256.4
444	6319.3	8334.1	7236.7	7270.1
445	6327.7	8356.9	7248.7	7284
446	6338.4	8385.9	7260.9	7299.5
447	6344.9	8406.1	7272.6	7314.2
448	6352.2	8429.5	7285.4	7327.9
449	6360.2	8462.1	7299.3	7342.5
450	6363	8492.8	7312.6	7356.8
451	6382.6	8508.2	7325.3	7372.4
452	6401.4	8523	7340.1	7388.6
453	6418.3	8544.5	7359.5	7404.5
454	6433.9	8558	7374.2	7420
455	6451.4	8578.9	7389.7	7436.2

456	6464.3	8596.6	7405	7452.1
457	6478.7	8620.3	7420.7	7468.1
458	6488.8	8641	7437.1	7483.4
459	6499.7	8661.8	7452	7499.2
460	6516.9	8678.9	7467.4	7515.4
461	6531.4	8704.2	7484.9	7531.6
462	6543.2	8722.7	7502.2	7547.4
463	6555.8	8752.7	7518.7	7563.6
464	6564.5	8770.7	7534.3	7579.9
465	6573.8	8796.9	7548.9	7595.7
466	6581.5	8828.3	7565.9	7611.5
467	6591.8	8858.4	7581.2	7626.8
468	6602.1	8886	7594.6	7642.9
469	6612.9	8917.6	7608.2	7658.9
470	6627	8948.1	7620.9	7674.6

Appendix H: Data Sheets

+	Reddy 2017	0	10	20	30	50	60	80	90	110	120	130	140	160	170	180	190	200	210	220	230	240	250	260	270	280	290	300	310	320	330	340	410	420	430	440	450	460	470
SPIKE,	SPIKE	282	437	882	285	474	438	154	122	125	116	59	182	444	426	263	500	296	895	232	362	255	457	639	151	493	893	800	1176	736	246	681	1072	1668	840	752	654	759	824
ACANTHACEAE undiff.	COASTAL GRASSLAND THICKET MOSAIC	6	4				3	42	11	25		49	17		8	11		7				5		1															
ASTERACEAE Ambrosia	COASTAL GRASSLAND THICKET MOSAIC		4							5					1																							
ASTERACEAE Artemisia	COASTAL GRASSLAND THICKET MOSAIC							7																															
ASTERACEAE Crassocephalum	COASTAL GRASSLAND THICKET MOSAIC														1																								
ASTERACEAE Tubuliflorae	COASTAL GRASSLAND THICKET MOSAIC	12	1	3	3	3	4	35	30		7				2	5		3	3	15	7	13	19	6	16	3	3	3				4	5	6			16	20	14
ASTERACEAE Vernonia	COASTAL GRASSLAND THICKET MOSAIC	1											7	4															7	2	4								
CHENO-AM-type	COASTAL GRASSLAND THICKET MOSAIC	11	7	30	14	5	10	17			1					7		2	3	1				1	1	5	8			3	3		2		2		4	9	3
COMMELINACEAE undiff.	COASTAL GRASSLAND THICKET MOSAIC					2								10												2													
ERICACEAE undiff.	COASTAL GRASSLAND THICKET MOSAIC															11						2								3									
EUPHORBIACEAE undiff.	COASTAL GRASSLAND THICKET MOSAIC				15			1	2			1					1	5	2	4	6		14	4	4			3		2			2		2	6	16	19	
GERANIACEAE undiff.	COASTAL GRASSLAND THICKET MOSAIC						1							4			1					2																	
NYCTAGINACEAE	COASTAL GRASSLAND THICKET MOSAIC			1																							1		1									
PALMAE Hyphaene	COASTAL GRASSLAND THICKET MOSAIC		1	4		4	1	35	6		1				2	6	4	6		4	21	16	25	19	4	4	1											
POACEAE undiff.	COASTAL GRASSLAND THICKET MOSAIC	71	101	67	48	40	51	250	75	19	41	58	62	80	66	47	25	43	67	65	100	96	84	42	37	96	70	72	48	96	38	50	91	104	156	54	109	118	128
SAPINDACEAE undiff.	COASTAL GRASSLAND THICKET																																						

	MOSAIC																																					
THYMELEACEAE Passerina	COASTAL GRASSLAND THICKET MOSAIC																					1																
THYMELEACEAE undiff.	COASTAL GRASSLAND THICKET MOSAIC																	1																				
ANACARDIACEAE Rhus	COASTAL FOREST																					6																
AQUIFOLIACEAE Ilex	COASTAL FOREST			3	5	6					2			15			3									6	3											
CELASTRACEAE Maytenus	COASTAL FOREST	1			1			4																													
COMBRETACEAE Combretum	COASTAL FOREST				2																	1															
EBENACEAE Euclea	COASTAL FOREST																1	2																			
EUPHORBIACEAE Acalypha	COASTAL FOREST																																				
EUPHORBIACEAE Alcornea	COASTAL FOREST		4						8													7					1										
EUPHORBIACEAE Bridelia	COASTAL FOREST						5																														
EUPHORBIACEAE Cleistanthus	COASTAL FOREST								7																												
EUPHORBIACEAE Sapium	COASTAL FOREST								10		6								1																		
FABACEAE undiff.	COASTAL FOREST	2	2		12	3	4		1		8						1		5			1	2		2	21		3	2	3	6		1				
LYCOPODIACEAE Lycopodium jussiae	COASTAL FOREST		4																																	
MIMOSACEAE Acacia	COASTAL FOREST	2		3							1	3					5	1	1																	
MYRSINACEAE undiff.	COASTAL FOREST				14													3																			
OLEACEAE Olea	COASTAL FOREST																											10									
PODOCARPACEAE Podocarpus	COASTAL FOREST	21	10	22	4	7	6	3	5					1	4	7		7		3	18	20	15	1	7	3	21	15	4	3	3		7	4	6		4	6	9
RUBIACEAE undiff.	COASTAL FOREST																										11	1	2								
STERCULIACEAE Dombeya	COASTAL FOREST							1																													
ULMACEAE Celtis	COASTAL FOREST	10	4	6	3				9			6			8		7	2	8	4	21	29		7	54	9	6	5	17	24	3	21	5	2		4	15	12	21
ULMACEAE Trema	COASTAL FOREST																					14	20									3						
APOCYNACEAE Rauvolfia	SWAMP FOREST		4																		3			5										6			
EUPHORBIACEAEMacaranga	SWAMP FOREST		7		1				45	5	7		22	6		12	9	8	8	7	15	21	9	12	3			1	2								
LECYTHIDACEAE Barringtonia	SWAMP FOREST		6	5							1	1			3			2	3		5	3	3	10			5	2								
HIBISCUS undiff.	SWAMP FOREST	2	1	3									1													3	3										
MORACEAE Ficus	SWAMP FOREST		2			1		10			1	3					14		8	2	11	14	40		7	1										
MYRICACEAE Morella	SWAMP FOREST					1			25									48						19		11			2			1			6		
MYRTACEAE Syzygium	SWAMP FOREST				20										4						6	3	7			35		5	5	4		9					
PTERIDOPHYTA Monoletes	SWAMP FOREST	1	26	81	20	48	168	375	350	250	306	214	275	406	175	128	139	49	31	257	71	32	188	66	76	125	39	25	119	28	50	60	71	84	40	50	58	64	59
PTERIDOPHYTA Triletes	SWAMP FOREST	10	1	8	3	12	19		21	20	2	42	23	27	33	7	7	5	2		2	6	16	1	9	2	8			7			1		2				
CYPERACEAE undiff.	REED SEDGE	285	151	246	68	204	468	725	458	125	485	68	136	228	203	200	236	66	108	197	132	143	268	125	107	232	264	176	181	141	203	126	146	234	192	116	129	140	200

	WETLAND																																						
GUNNERACEAE Gunnera	REED SEDGE WETLAND																					7									2			8	2	8	4	6	8
HALORAGACEAE undiff.	REED SEDGE WETLAND																2	3		3					5													
IRIDACEAE undiff.	REED SEDGE WETLAND			7	3	11	7				5						4	11	7	8		45	2		3	11	7											
LILIACEAE undiff.	REED SEDGE WETLAND	3			2												5	15	17	9	23		6	6	4													
NYMPHAEACEAE	REED SEDGE WETLAND																3	16	12	7	14	8							5					4				
TYPHACEAE Typha	REED SEDGE WETLAND	12	25			14	15	74	116	50	18	4		49	27	3	22	17	27	8	41	25	19	16	5	9			4		13	23	7	6	6				
POLYGONUM	REED SEDGE WETLAND	2	11	13	3		2	19	4		5		2	40	40	9		4	7						1	4				1								
UNDETERMINED,	UNDETERMINED	147	150	178	61	91	120	107	191	61	109	60	142	59	162	150	97	94	150	57	54	103	170	95	49	73	178	109	50	73	141	70	41	60	80	102	104	94	87
COASTAL GRASSLAND THICKET MOSAIC,		101	118	105	80	54	70	387	124	49	50	108	86	98	80	87	31	66	76	89	134	135	142	73	62	110	83	78	56	106	45	54	100	110	160	60	145	166	145
COASTAL FOREST,		36	24	34	41	16	15	8	40	0	17	9	0	16	12	7	17	15	15	7	39	78	37	8	63	39	30	35	34	32	12	24	13	6	6	4	19	18	30
SWAMP FOREST,		13	47	97	44	62	187	385	441	275	317	260	321	439	215	147	169	112	52	266	113	79	263	113	95	177	55	33	128	39	50	70	72	84	48	56	58	64	59
REED SEDGE WETLAND,		302	187	266	76	229	492	818	578	175	513	72	138	317	270	212	270	131	181	229	213	228	295	147	120	261	271	176	190	142	218	149	153	248	204	124	133	146	208
*Main Sum		599	526	680	302	452	884	1705	1374	560	1006	509	687	929	739	603	584	406	474	632	553	623	907	436	389	660	617	431	458	392	466	367	379	508	498	346	459	488	529
		599	526	680	302	452	884	1705	1374	560	1006	509	687	929	739	603	584	418	474	648	553	623	907	436	389	660	617	431	458	392	466	367	379	508	498	346	459	488	529